

Non-destructive γ -ray Spectrometry and Analysis
on Spent Fuel Assemblies of the JPDR-I

July 1985

日本原子力研究所

Japan Atomic Energy Research Institute

日本原子力研究所研究成果編集委員会

委員長 森 茂（理事）

委 員

飯泉 仁（物理部）	鈴木 伸武（研究部）
石川 迪夫（動力試験炉部）	鈴木 康夫（臨界プラズマ研究部）
伊藤 彰彦（環境安全研究部）	田中 正俊（核融合研究部）
梅沢 弘一（企画室）	田村 和行（原子力船技術部）
岡下 宏（化学部）	沼宮内綱雄（保健物理部）
小幡 行雄（技術情報部）	萩原 幸（開発部）
金子 義彦（原子炉工学部）	半田 宗男（燃料工学部）
川崎 了（燃料安全工学部）	二村 嘉明（研究炉管理部）
河村 洋（高温工学部）	幕内 恵三（開発部）
工藤 博司（アイソotope部）	村尾 良夫（原子炉安全工学部）
小森 卓二（化学部）	安野 武彦（動力炉開発・安全性研究管理部）
佐藤 雅幸（材料試験炉部）	横田 光雄（動力試験炉部）
鹿園 直基（物理部）	

Japan Atomic Energy Research Institute

Board of Editors

Sigeru Mori (Chief Editor)

Yoshiaki Futamura	Miyuki Hagiwara	Muneo Handa
Masashi Iizumi	Michio Ishikawa	Akihiko Ito
Yoshihiko Kaneko	Hiroshi Kawamura	Satoru Kawasaki
Takuji Komori	Hiroshi Kudo	Keizo Makuuchi
Yoshio Murao	Takao Numakunai	Yukio Obata
Hiroshi Okashita	Masayuki Sato	Naomoto Shikazono
Nobutake Suzuki	Yasuo Suzuki	Kazuyuki Tamura
Masatoshi Tanaka	Hirokazu Umezawa	Takehiko Yasuno
Mitsuo Yokota		

JAERI レポートは、日本原子力研究所が研究成果編集委員会の審査を経て不定期に公刊している研究報告書です。

入手の問合わせは、日本原子力研究所技術情報部情報資料課（〒319-11茨城県那珂郡東海村）あて、お申しつけください。なお、このほかに財団法人原子力弘済会資料センター（〒319-11 茨城県那珂郡東海村日本原子力研究所内）で複写による実費頒布をおこなっております。

JAERI reports are reviewed by the Board of Editors and issued irregularly.

Inquiries about availability of the reports should be addressed to Information Division Department of Technical Information, Japan Atomic Energy Research Institute, Tokai-mura, Naka-gun, Ibaraki-ken 319-11, Japan.

©Japan Atomic Energy Research Institute, 1985

編集兼発行 日本原子力研究所
印 刷 いばらき印刷株

Non-destructive γ -ray Spectrometry and Analysis
on Spent Fuel Assemblies of the JPDR-I

Takenori SUZAKI, Harumichi TSURUTA⁺ and Shojiro MATSUURA⁺⁺

Department of Fuel Safety Research,
Tokai Research Establishment,
Japan Atomic Energy Research Institute
Tokai-mura, Naka-gun, Ibaraki-ken

Received February 4, 1985

Abstract

Non-destructive gamma-ray spectrometry was carried out on the spent fuel assemblies of the whole core of JPDR-I which was a BWR. These data were analyzed by considering power distribution, spatial variation of neutron spectrum, and history of reactor operation. The burnup and the Pu/U atom ratio in each assembly were derived from the non-destructively measured distributions of ^{137}Cs activity and $^{134}\text{Cs}/^{137}\text{Cs}$ activity ratio, respectively, by using calibration curves established for fuel specimens of a standard assembly of the core. The results were compared with calculational ones based on the operational data, and good correlations were found between them. The total amount of plutonium build-up in the core estimated from the non-destructive measurements agreed quite well with the amount obtained from reprocessing.

Keywords: Non-destructive Measurement, Gamma-ray Spectrometry, JPDR, BWR, Cesium-137, Cesium-134, Whole Core, Burnup, Plutonium Build-up, Burnup Calculation, Reprocessing, Fuel assembly

+ Department of Research Reactor Operation

++ Department of Reactor Engineering

JPDR-I 使用済燃料集合体の非破壊 γ 線スペクトロメトリおよび解析

日本原子力研究所東海研究所燃料安全工学部

須崎 武則・鶴田 晴通⁺・松浦祥次郎⁺⁺

(1985年2月4日受理)

要 旨

JPDR-I 全炉心の使用済燃料集合体について、再処理工場への輸送に先立ち、非破壊 γ 線スペクトロメトリを行った。その測定値を、出力分布、中性子スペクトルの空間変化、炉の運転履歴を考慮して解析した。この炉の 1 体の標準的な集合体に関して見出された較正曲線を利用して、非破壊測定による ^{137}Cs の γ 線強度分布および $^{134}\text{Cs} / ^{137}\text{Cs}$ の γ 線強度比分布から、それぞれ、集合体平均の燃焼度および Pu/U 原子数比を求めた。これらの結果と運転データに基づく燃焼計算結果は互に良く一致した。非破壊測定から推定した炉心内の全 Pu 蓄積量は再処理結果ときわめて良い一致を示した。

⁺ 研究炉管理部

⁺⁺ 原子炉工学部

CONTENTS

1. Introduction	1
2. Core and Fuel	2
3. Experimental Apparatus and Measurements	5
4. Analysis of Measured Data	8
4.1 Corrections for Measured Gamma-Ray Intensities	8
4.2 Derivation of Average Gamma-Ray Intensity and Intensity Ratio in an Assembly	9
4.3 Estimation of Errors in Average Gamma-Ray Intensity and Intensity Ratio	13
4.4 Effect of Averaging Method on Determination of Pu/U Atom Ratio in an Assembly	16
5. Results and Discussion	17
5.1 Distributions of FP Intensity and Intensity Ratio in the Core	17
5.2 Correlation between ^{137}Cs Intensity and $^{134}\text{Cs}/^{137}\text{Cs}$ Intensity Ratio	18
5.3 Derivation of Assembly-Averaged Burnup and Pu/U Atom Ratio from NDA	20
5.4 Comparison between Burnup Calculation and NDA	22
6. Conclusions	25
Acknowledgment	26
References	26
Appendix 1 Non-Destructively Measured Gamma-Ray Intensities and Intensity Ratios on the JPDR-I Fuel Assemblies	27
Appendix 2 Axial and Radial Distributions of Gamma-Ray Intensities and Intensity Ratios in the JPDR-I Fuel Assemblies	41
Appendix 3 Measurement of Penetration Rates of Gamma-Rays in a Fuel Assembly	54

目 次

1. 序	1
2. 炉心および燃料	2
3. 実験装置および測定	5
4. 測定値の解析	8
4.1 γ 線強度の測定値に対する補正	8
4.2 γ 線強度および強度比の集合体平均値の導出	9
4.3 γ 線強度および強度比の集合体平均値に含まれる誤差の推定	13
4.4 集合体内 Pu/U 原子数比の決定に対する平均化手法の影響	16
5. 実験結果および検討	17
5.1 FP 強度および強度比の炉心内分布	17
5.2 ^{137}Cs 強度と $^{134}\text{Cs}/^{137}\text{Cs}$ 強度比の間の相関	18
5.3 NDA に基づく集合体平均燃焼度および Pu/U 原子数比の導出	20
5.4 燃焼計算と NDA の比較	22
6. 結 論	25
謝 辞	26
参照文献	26
付録 1 JPDR-I 燃料集合体に関する γ 線強度および強度比の非破壊測定値	27
付録 2 γ 線強度および強度比の JPDR-I 燃料集合体内軸方向および径方向分布	41
付録 3 燃料集合体の γ 線透過率の測定	54

1. Introduction

Sufficiently accurate and rapid methods for determining the amount of plutonium accumulated in spent fuels are indispensable for safeguarding of nuclear materials at reprocessing plants and reactor sites. Burnup is also interesting from the viewpoint of reactor fuel management. Measurements of these parameters are usually performed by chemical analysis. Such destructive assay (DA) techniques, however, are practically inapplicable to the measurement of burnup distribution over a reactor core or to following the burnup history of a specified fuel element.

Techniques usable for the purpose are limited¹⁾. Among several non-destructive assay (NDA) techniques applicable to the purpose, the spectrometry of gamma-rays from fission products (FP) is so far the most experienced and reliable, and the accent will remain on the use of gamma-ray spectrometry for the immediate future. Efforts to demonstrate the effectiveness have been continued on fuels irradiated in various types of reactors²⁾. In many experiments with spent fuels from light water reactors, ^{137}Cs activities and $^{134}\text{Cs}/^{137}\text{Cs}$ activity ratios are often correlated with either burnups or Pu/U atom ratios. The correlations are generally superior in the cases of PWR fuels^{3,4)} to those in the cases of BWR fuels^{5,6)} which may be attributed to the fact that the spatial distributions of power and neutron spectrum in PWR cores are simpler than those in BWR cores.

In a previous study, gamma-ray spectrometry were carried out on 8 separate fuel rods from one selected assembly (A20) of the Japan Power Demonstration Reactor (JPDR-I) which is a BWR^{7,8)}. Chemical analysis was performed on 24 representative points of the rods measured by the NDA for heavy nuclides and fission products⁸⁾. The conclusions are as follows.

The $^{134}\text{Cs}/^{137}\text{Cs}$ or $^{154}\text{Eu}/^{137}\text{Cs}$ activity ratio corresponding to a given burnup varies with the position in the assembly. This is understood in connection with spatial variations of neutron spectrum. The same understanding applies to the correspondence between the Pu/U atom ratio and the burnup. The non-destructively measurable ratios of FPs can be used as a better indicator of Pu/U atom ratio than the burnup.

Gamma-ray spectra of spent fuel assemblies of the JPDR-I were measured prior to shipment to the Tokai Reprocessing Plant of Power Reactor and Nuclear Fuel Development Corporation (PNC). This article deals with the results of measurement and the analysis. It is tried to obtain average values of FP activity and activity ratio in each assembly from a set of data of point-wise measurements on the assembly. The burnup and the Pu/U atom ratio derived from the assembly-averaged FP activity and activity ratio are compared with a calculational result based on the operational data of the reactor. The correlation between the FP activity and the activity ratio is also discussed in consideration of the spatial variation of neutron energy spectrum in the core. In addition, more than seven hundred data of gamma-ray spectrometry are supplied in the appendix for convenience of further investigation of the non-destructive gamma-ray spectrometry on fuel assembly.

2. Core and Fuel

The reactor was a natural circulation BWR of 45 MW thermal output, loaded with 2.6 wt.% enriched UO_2 fuels. The core consisted of 72 fuel assemblies, 16 cruciform control rods and 24 burnable poison curtains. The plan of the core and the identification numbers of assemblies are shown in Fig. 1. An assembly consisted of 36 fuel rods arrayed in 6×6 square lattice in a channel box with a lattice pitch of 19.56 mm. Each rod was formed of two segments – upper and lower – having the same active length of 721 mm. The fuel pellet was 12.5 mm in diameter and clad in Zircaloy-2 sheath of 0.76 mm thick.

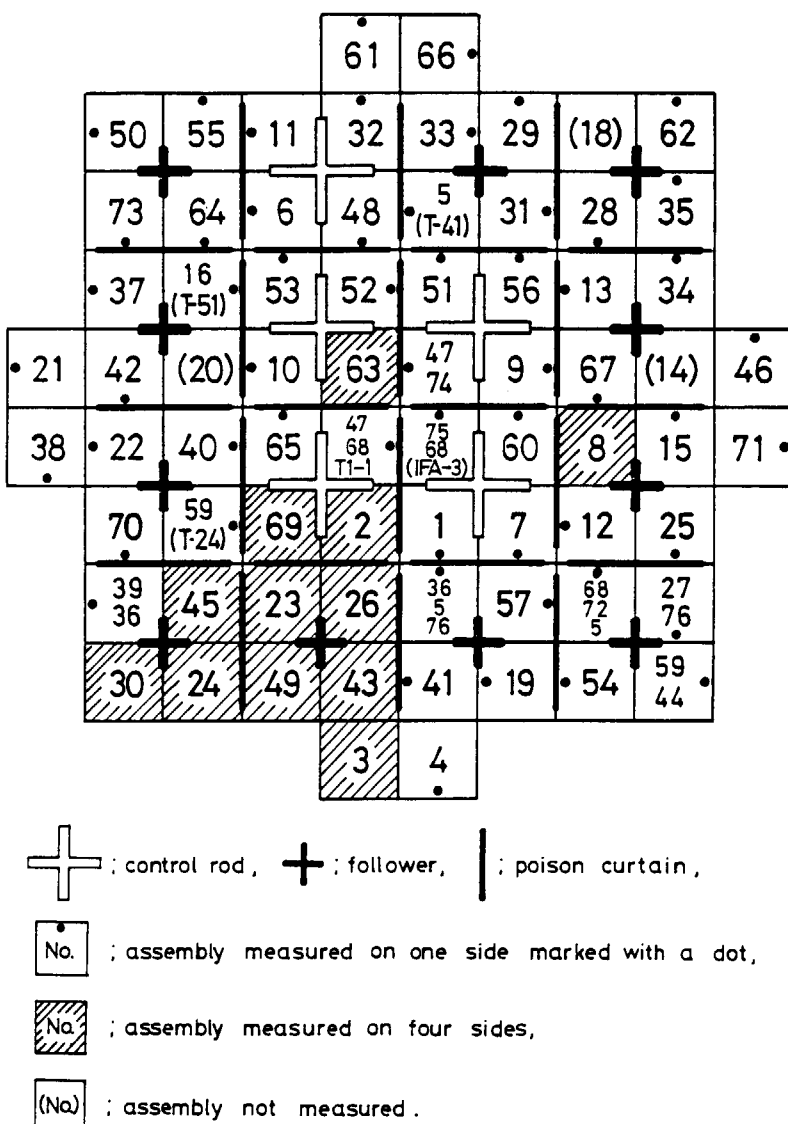


Fig. 1 Plan of JRDR-I core and identification numbers of assemblies.

The assemblies were named as Axx, where xx denotes the identification number, except those named as T-xx, Tx-x and IFA-x which were loaded for special purposes. More than one numbers in one box imply that plural assemblies had occupied the same position during the total operational history.

The core was operated from October 1963 to August 1969, but there was a long shutdown from June 1968 to June 1969. The operation history of the core is illustrated in **Fig. 2**. Most assemblies were kept at the positions where they were loaded initially. The burnups of individual assemblies ranged from 110 to 5640 MWd/t which were calculated using operation data⁹⁾. The cooling times were in the range of 8 to 13 years.

The reactor power was regulated with the four control rods located at the inner region of the core, while the peripheral control rods except one control rod were fully withdrawn. The one peripheral control rod had been fully withdrawn before September 1965, but the position had been kept at a height of about 40% of full insertion since then.

The fuel specifications and the reactor characteristics are summarized in **Table 1** and **Table 2**.

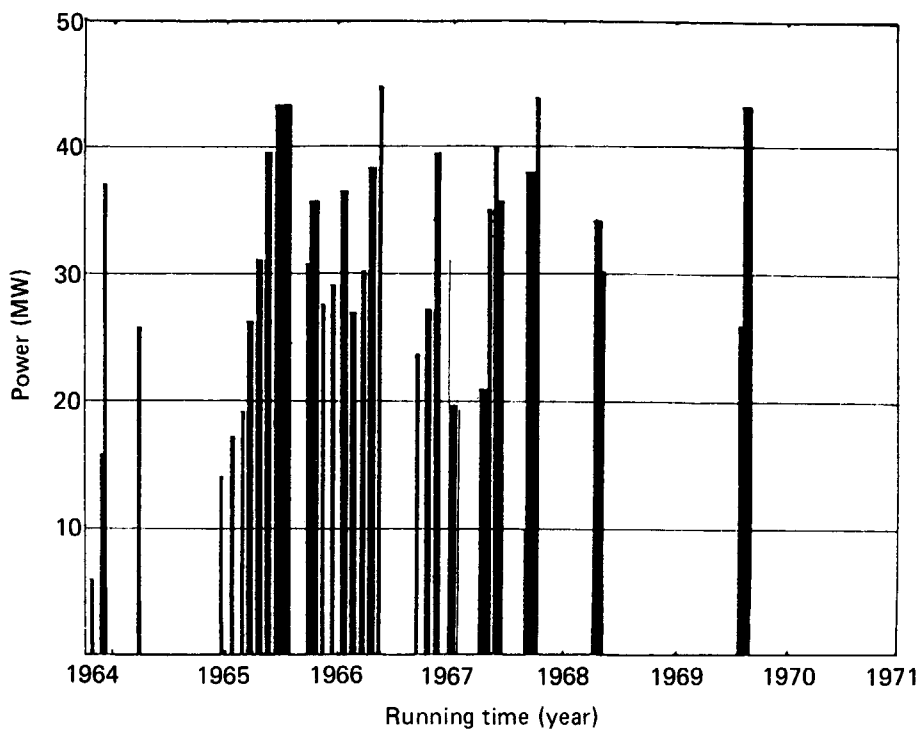


Fig. 2 Operational history of JPDR-I reactor.

Table 1 Specifications of fuel rod and assembly

Fuel material	UO ₂ sintered pellet
²³⁵ U enrichment	2.60 w/o
Pellet diameter	12.5 mm
Pellet height	12.7 mm
Pellet density	10.4 g/cm ³
Cladding material	Zircaloy-2
Cladding thickness	0.76 mm
Cladding outer diameter	14.12 mm
Active fuel length in a segment	721 ± 3 mm
Weight of UO ₂ in a segment	921 ± 25 g
Number of rods in an assembly	36 (= 6 × 6) in square
Lattice pitch	19.56 mm
Volume ratio of moderator to fuel in lattice	1.84
Channel box material	Zircaloy-4

Table 2 Reactor characteristics and operating condition
of the JPDR-I

Reactor type	Naturally circulated BWR
Thermal power	45 MW
Equivalent diameter	127 cm
Effective height	147 cm
Number of fuel assemblies	72
Core-averaged volume ratio of moderator to fuel	2.7
Operating pressure	6.03 MPa
Temperature of coolant	277 °C
Maximum temperature of fuel center	1,610 °C
Average power density	22.5 kW/l
Radial power peaking factor	1.4
Axial power peaking factor	1.5
Average thermal neutron flux	$1.42 \times 10^{13} \text{ n/cm}^2 \cdot \text{s}$
Maximum heat flux	823,000 kcal/m ² ·h
Average heat flux	226,100 kcal/m ² ·h
Average void fraction	19 %
Core-exit steam quality	4.7 %

3. Experimental Apparatus and Measurements

Gamma-ray spectra of 72 assemblies were measured with a gamma-scanning apparatus which was installed temporarily at a spent fuel pool of the JPDR. The apparatus consisted of a reclining fuel bed, a collimator set, a two-dimensional scanning mechanism, and a gamma-ray spectrometer. The arrangement is depicted in **Fig. 3**.

An assembly was held horizontally on the bed. Gamma-rays were collimated by a vertical beam guide of 20 mm in inner diameter and 5.5 m long, and measured with a co-axial type Ge(Li) detector (88 cm^3). The gamma-rays were measured over an energy range from 200 to 2200 keV. The gamma-ray spectra obtained were recorded on cassette magnetic tapes and analyzed with the computer code BOB-73¹⁰⁾. Overall energy resolution was 2.1 keV in FWHM for the 662 keV gamma-ray. Counting rate was less than 13,000 cps and spectrum distortion was negligible. A typical gamma-ray spectrum is shown in **Fig. 4**. Photopeaks of ^{137}Cs (662 keV), ^{134}Cs (sum of 796 keV and 802 keV peaks) and ^{154}Eu (1,275 keV) were identified with sufficient statistics by 400 s counting. But, those of $^{106}\text{Ru-Rh}$ and $^{144}\text{Ce-Pr}$ were too small for use except for a small number of cases of 40,000 s counting. The migration of cesium was neglected because no anomaly was observed among the axial distributions of ^{134}Cs , ^{137}Cs and

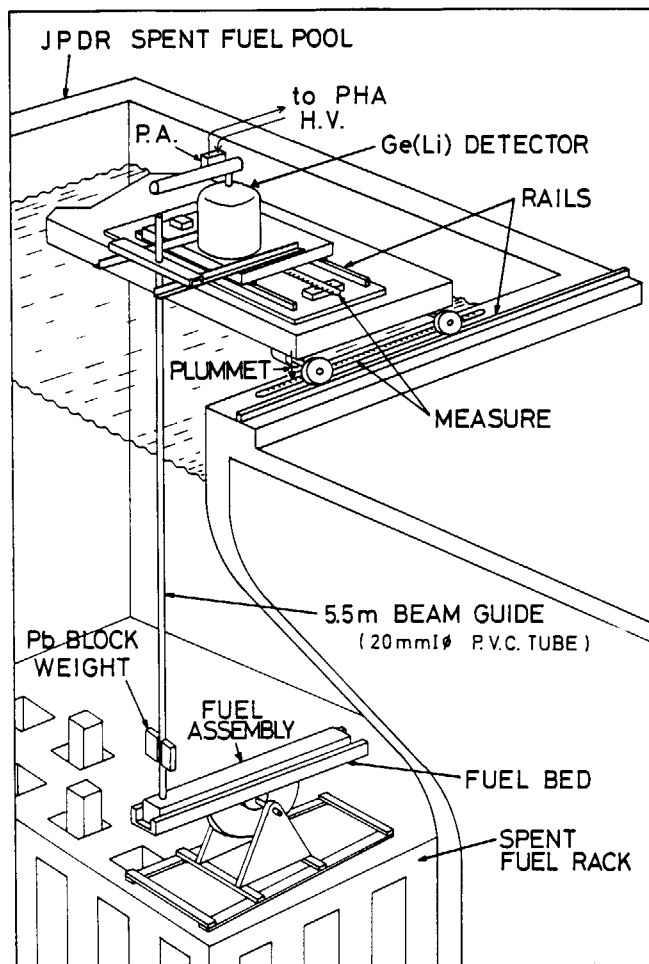


Fig. 3 Arrangement of gamma-scanning apparatus at JPDR spent fuel storage pool.

^{154}Eu .

Measurement positions are shown in **Fig. 5**. Twelve assemblies were measured at ten positions on every side, while the rest were at four positions (No. 2, 3, 4 and 5 in **Fig. 5**) on one side only as specified in **Fig. 1**. Among the twelve assemblies, eleven were selected from one octant of the core and the rest one, A8, was the reference assembly. The assembly A8 had the same irradiation history as A20 which was previously examined by destructive and non-destructive measurements.

Fuel rods in an assembly were covered with a channel box and not visible from the outside. Therefore, the positions of the fuel rods were determined from the distributions of gamma-ray intensities. Both axial and radial distributions of gamma-ray intensities were

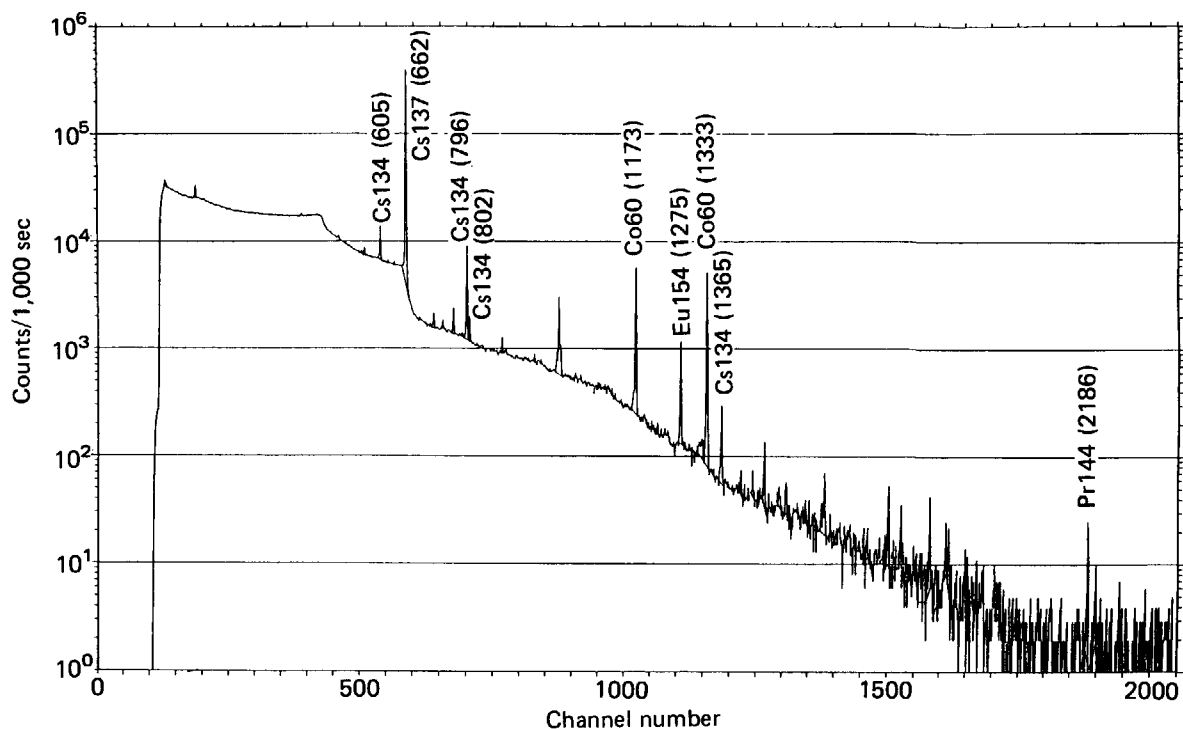


Fig. 4 Typical gamma-ray spectrum of JPDR-I fuel cooled for 8 years.

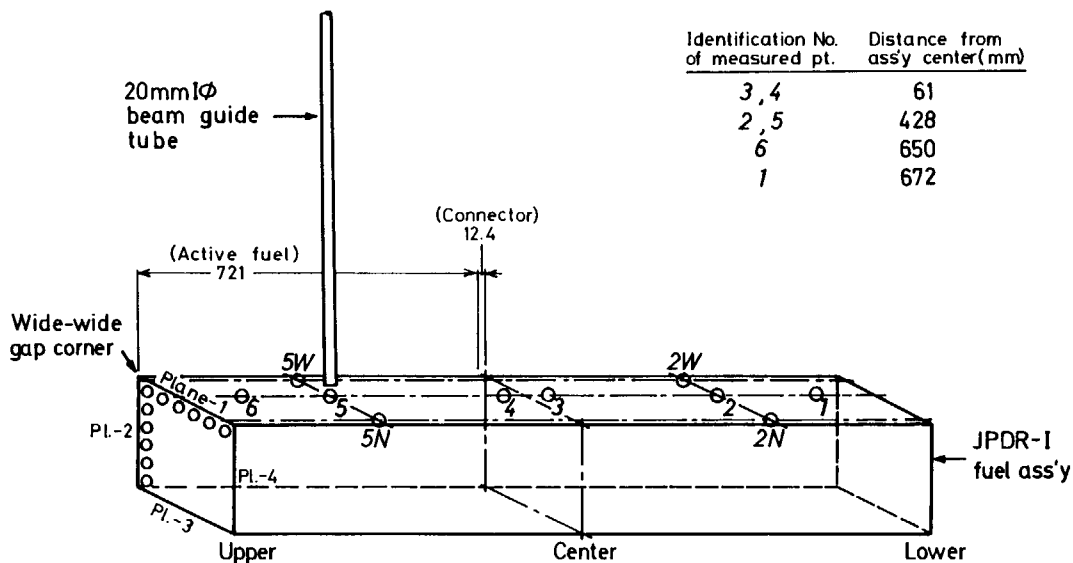


Fig. 5 Measurement positions for gamma spectrometry.

obtained by scanning the fuel assembly. Some examples of the distribution are shown in Figs. 6 and 7. The axial center was determined by a sharp dip due to a fuel vacancy at the connector of a fuel rod and the radial positions were determined as referring to the leading edges of the distribution at the both ends of the fuel assembly.

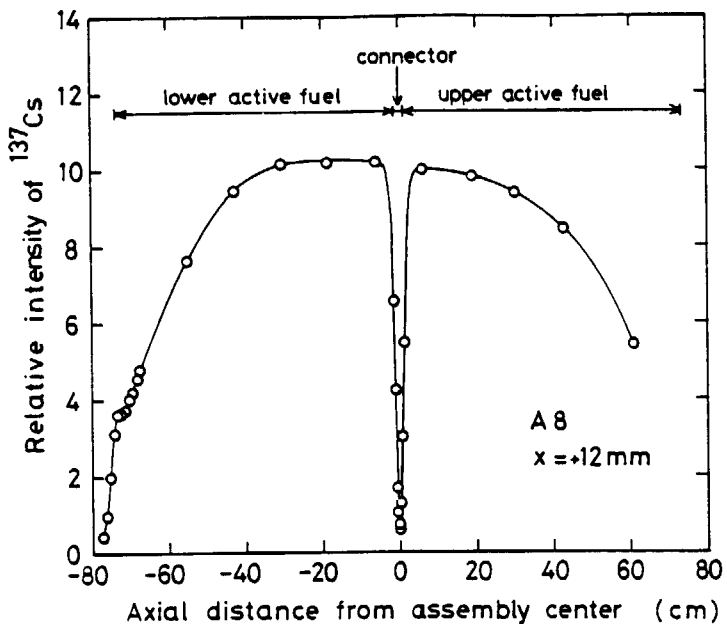


Fig. 6 Axial distribution of gamma-ray intensity of fuel assembly A8.

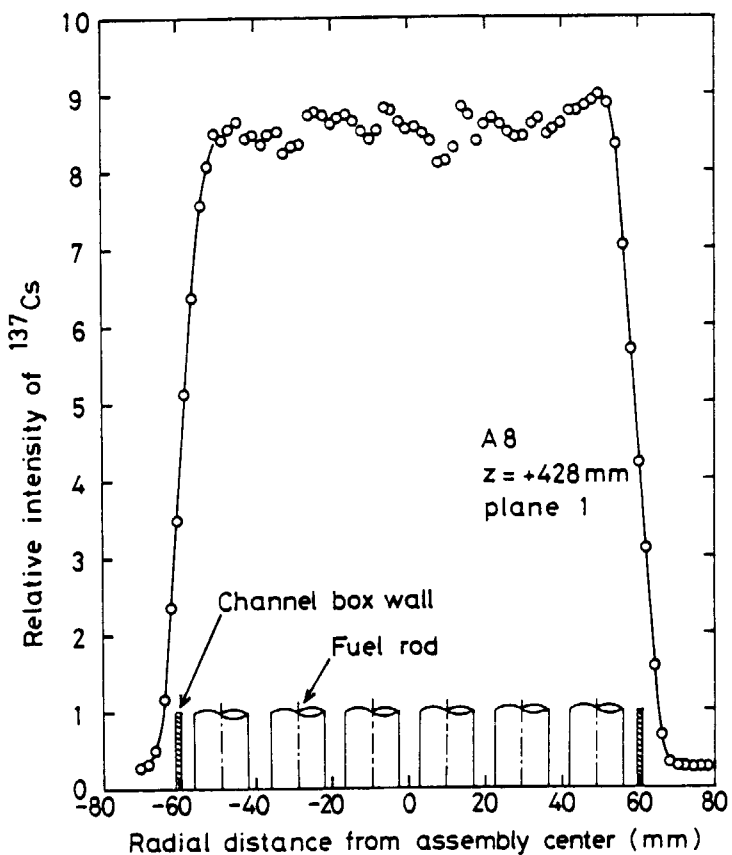


Fig. 7 Radial distribution of gamma-ray intensity of fuel assembly A8 measured at axial position of +428 mm. The right hand side faced to the wide water gap.

4. Analysis of Measured Data

Several corrections were applied to the measured pointwise gamma-ray intensities of the fission products concerning gamma-ray shielding, counting loss, cooling time, and background activities in pool water. The corrected data were used to obtain the pointwise intensity ratios of $^{134}\text{Cs}/^{137}\text{Cs}$ and $^{154}\text{Eu}/^{137}\text{Cs}$.

For the purpose of making comparisons among results of NDA, calculation, and destructive assay, it was required to derive the averaged value over each assembly from the point-wise data. A method was examined to obtain properly the assembly-averaged FP activity and activity ratio.

4.1 Corrections for Measured Gamma-Ray Intensities

(1) There existed a water layer between the end of beam guide tube and the surface of channel box of the fuel assembly. The thickness of the water layer varied from 1 to 36 mm for the measurement positions from No.1 to 6 in Fig. 5, because the fuel assembly was slightly out of the horizontal when it was reclined on the fuel bed. The correction was made for the gamma-ray absorption in the water layer of different thickness by using the linear absorption coefficient of water¹¹⁾.

(2) The intensity of gamma-ray beam was rather high in this experiment. Similar experimental condition is inevitable in cases requiring a large number of measurements in a limited period. The counting loss mainly due to pile-up effect was corrected by

$$\overset{\circ}{A} = \frac{A}{1 - \tau_1 A_t} , \quad (1)$$

where

$A, \overset{\circ}{A}$; measured and corrected count rates of specified gamma-ray,

τ_1 ; loss time due to pile-up effect. This was determined by means of the two-source method using ^{137}Cs sources and found to be $6.75 \pm 0.75 \mu\text{s}$ for this counting system,

A_t ; total count rate of the whole energy range. This was evaluated by using the relation,

$$A_t = \left(\frac{T_t}{T_1} - 1 \right) / \tau_r ,$$

with

T_1, T_t ; live and true counting time of PHA,

τ_r ; average resolution time of PHA. This was found as $20.0 \pm 0.5 \mu\text{s}$ for the present gamma-ray spectra.

(3) The cooling time of each assembly was different because of the variety of period between the unloaded date from the core and the measurement date. The count rate of each assembly was normalized so as to have the same cooling time, from September 1, 1969 to June 1, 1977, that is, the correction on radioactive decay was made for a difference in period between the real and the normalized cooling times.

(4) The gamma-rays of ^{137}Cs were observed in the background activity of the pool water. The count rate, 1.6 cps, was subtracted from those of fuel assemblies. No other back-

ground gamma-rays disturbed the measured spectrum on fuel.

The corrected intensities of ^{137}Cs , ^{134}Cs , ^{154}Eu and $^{144}\text{Ce-Pr}$ at each measurement position are listed in table of Appendix 1, accompanying the intensity ratios of $^{134}\text{Cs}/^{137}\text{Cs}$, $^{154}\text{Eu}/^{137}\text{Cs}$, $(^{134}\text{Cs}/^{137}\text{Cs})/^{137}\text{Cs}$, and $(^{154}\text{Eu}/^{137}\text{Cs})/^{137}\text{Cs}$. The axial and radial distributions of ^{137}Cs , ^{134}Cs , ^{154}Eu , $^{134}\text{Cs}/^{137}\text{Cs}$, and $^{154}\text{Eu}/^{137}\text{Cs}$ are shown in figures in Appendix 2 for the twelve assemblies measured in detail.

4.2 Derivation of Average Gamma-Ray Intensity and Intensity Ratio in an Assembly

Forty count rate and count-rate ratio data were obtained for each of the twelve assemblies. Ten data measured on a side of an assembly are illustrated in **Fig. 8**. An average of the count rate or the count-rate ratio in each assembly, $\langle A \rangle$, was defined by the following equation using the forty data.

$$\langle A \rangle = \frac{1}{8} \sum_{l=1}^4 \{\bar{A}_l(2)/P_l(2) + \bar{A}_l(5)/P_l(5)\} = \frac{1}{2} \sum_{k=2,5} \bar{A}(k)/\bar{P}(k), \quad (2)$$

where $\bar{A}_l(k)$ and $P_l(k)$ are the radial average of three data and the axial peaking factor at k -th axial position on l -th side, respectively. $\bar{A}(k)$ and $\bar{P}(k)$ are their averages on four sides. They are given as

$$\bar{A}_l(k) = w_1 A_l(1, k) + w_2 A_l(3, k) + w_3 A_l(6, k), \quad (3)$$

$$\begin{aligned} P_l(k) &= A_l(3, k) / \{W_1 A_l(3, 3) + W_2 A_l(3, 2) + W_3 A_l(3, 1)\} (k \leq 3) \\ &= A_l(3, k) / \{W'_1 A_l(3, 4) + W'_2 A_l(3, 5) + W'_3 A_l(3, 6)\} (k \geq 4), \end{aligned} \quad (4)$$

$$\bar{A}(k) = \frac{1}{4} \sum_{l=1}^4 \bar{A}_l(k), \quad (5)$$

$$\bar{P}(k) = \bar{A}(k) / \frac{1}{4} \sum_{l=1}^4 \bar{A}_l(k) / P_l(k), \quad (6)$$

where

$A_l(m, k)$; count rate or count-rate ratio of specified gamma-ray obtained at the position on l -th side ($l=1 \sim 4$), at k -th axial position ($k=1 \sim 6$), assigned to m -th row of fuel rods from wide-gap side of assembly ($m=1 \sim 6$), as shown in **Fig. 8**,

w ; weight for radial average,

W, W' ; weights for axial average.

The values of weights were determined so that the distribution of $A_l(m, k) (= y)$ was expressed by a quadratic function as $y = ax^2 + bx + c$, in the radial direction, and by a trigonometric function as

$$y = a' \cos Bx + b' \cos 2Bx + c' \sin 2Bx \quad (B = 0.022 \text{ cm}^{-1}), \quad (7)$$

in the axial direction with three unknowns, where x denotes a distance from an origin in each direction, and B the square root of axial geometric buckling of the core. The resultant values of weights are as follows.

$$\begin{aligned} w_1 &= 0.17500, & w_2 &= 0.54167, & w_3 &= 0.28333, \\ W_1 &= 0.27483, & W_2 &= 0.55745, & W_3 &= 0.13898, \\ W'_1 &= 0.27696, & W'_2 &= 0.53991, & W'_3 &= 0.14997. \end{aligned}$$

In order to examine the availability of the function (7), it was applied to the axial distribution of calculated burnup⁹⁾ on some typical assemblies. As shown in **Fig. 9**, the fitted

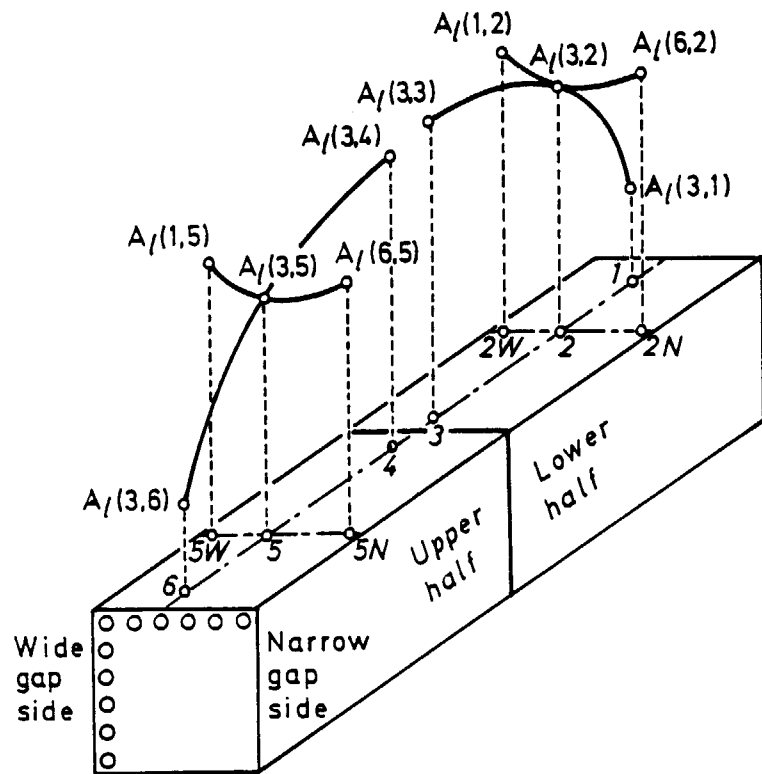


Fig. 8 Gamma-ray intensities or intensity ratios measured at ten positions on l -th side.

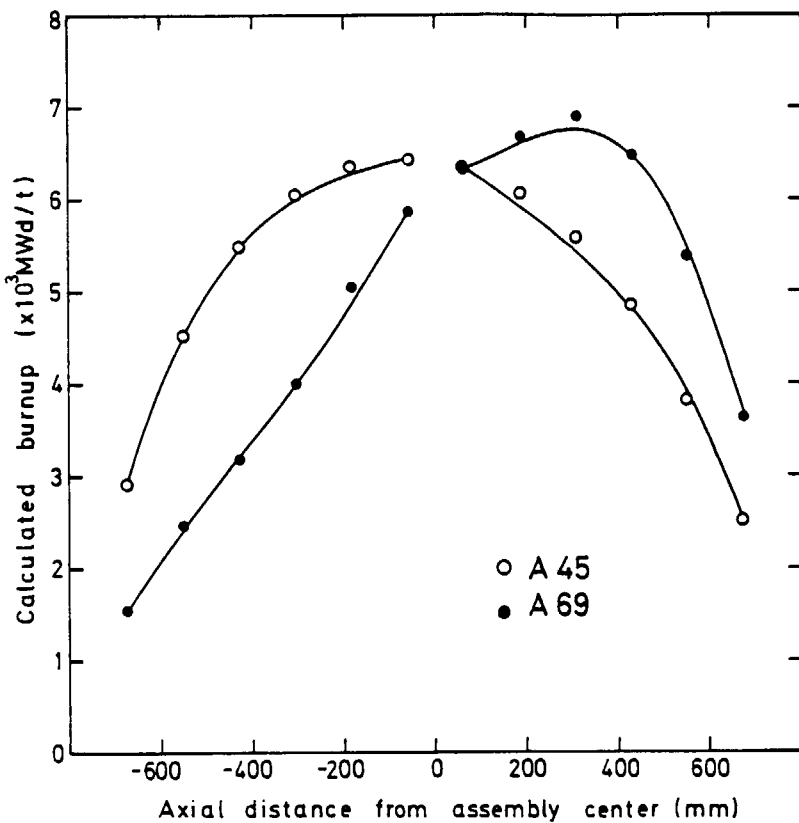


Fig. 9 Axial distribution of calculated burnup in assemblies A69 and A45. Solid lines represent the fitted functions expressed by Eq. (7), which pass through the three data at 61, 428, and 672 mm from the assembly center.

function reproduced the distribution fairly well and consequently the axial averages of calculated and fitted functions agreed within 1% for all of the examined assemblies. The fitted functions to the measured data of ^{137}Cs , $^{134}\text{Cs}/^{137}\text{Cs}$, and $^{154}\text{Eu}/^{137}\text{Cs}$ are also shown in Appendix 2 for the twelve assemblies.

For the assemblies which were measured at four axial positions on one side only, the assembly-average $\langle A \rangle$ was defined as

$$\langle A \rangle = \langle A \rangle_g \sum_{k=2}^5 A_l(3, k) / \sum_{k=2}^5 A_l^g(3, k), \quad (8)$$

where the value suffixed by g corresponds to the assembly which was measured at the forty positions and belonged to the same (g -th) group of location in the core as the assembly of concern. The group numbers assigned to eleven locations in the core are shown in **Fig. 10**.

Thus obtained assembly-averages of count rates of ^{137}Cs ($\langle A^{137} \rangle$) and ^{134}Cs ($\langle A^{134} \rangle$), and count-rate ratios of $^{134}\text{Cs}/^{137}\text{Cs}$ ($\langle A^{134/137} \rangle$) and $^{154}\text{Eu}/^{137}\text{Cs}$ ($\langle A^{154/137} \rangle$) are shown in **Table 3**. They are the values at the date on June 1, 1977, and the correction on different irradiation history is not made.

Table 3 Summary of calculational and experimental burnup and Pu build-up on the JPDR-I fuel assemblies

Ass'y Name	Pos. in Core* ¹	Date of Load./Unload. (Year-Month)	Initial Wt. of U (g)	FLARE Calculation		NDA Assembly Averages* ²				Estimated from NDA				Repr. Batch No.
				Integral BU (MWd/tU)	Pu/U* ³ ($\times 10^{-3}$)	137 (cps)	134 (cps)	$\frac{134}{137}$ ($\times 10^{-2}$)	$\frac{154}{137}$ ($\times 10^{-3}$)	BU (%)	Pu/U* ³ ($\times 10^{-3}$)	Pu* ³ (g)	U (g)	
A74	1	63-9 / 64-1	58048	133	0.072	20.0	—	—	—	0.011	—	—	58042	1
A75	1	63-9 / 64-1	57999	110	0.060	18.3	—	—	—	0.010	—	—	57993	1
A16	5	63-9 / 65-9	58155	1282	0.690	214.1	0.52	0.225	0.52	0.113	0.32	19	58070	2
A59	5	63-6 / 65-9	58117	1240	0.760	260.6	1.03	0.363	0.56	0.138	0.51	30	58007	2
A59	10	69-6 / 69-9	58117	1469	0.760	260.6	1.03	0.363	0.56	0.138	0.51	30	58007	2
A72	6	66-8 / 67-7	58049	1274	0.744	313.1	1.83	0.539	0.84	0.166	0.74	43	57910	2
A72	6	68-1 / 69-6	58049	1567	0.744	313.1	1.83	0.539	0.84	0.166	0.74	43	57910	2
A76	9	64-1 / 65-9	56364	802	0.553	200.4	0.79	0.366	0.57	0.106	0.51	29	56275	2
A76	4	68-1 / 69-6	56364	1130	0.553	200.4	0.79	0.366	0.57	0.106	0.51	29	56275	2
A50	10	63-9 / 69-9	58061	2526	1.083	586.2	5.24	0.785	1.19	0.310	1.06	61	57820	3
A62	10	"	58116	2660	1.140	651.7	5.86	0.800	1.17	0.345	1.08	62	57853	3
A30	10	"	57976	2784	1.187	619.7	5.81	0.831	1.17	0.328	1.11	65	57721	3
A55	9	"	57997	3433	1.514	670.6	8.03	1.084	1.53	0.355	1.42	82	57709	3
A61	11	63-9 / 69-9	57970	2769	1.144	650.0	6.75	0.903	1.30	0.344	1.20	70	57701	4
A66	11	"	57985	2872	1.185	678.0	7.38	0.956	1.42	0.359	1.27	73	57704	4
A 4	11	"	58166	3231	1.334	693.1	8.15	1.047	1.45	0.367	1.37	80	57873	4
A 3	11	"	57933	3249	1.336	741.2	8.72	1.051	1.45	0.392	1.38	80	57626	4
A44	10	63-9 / 69-6	57888	2460	1.060	580.5	3.99	0.609	1.04	0.307	0.83	48	57662	5
A27	9	63-9 / 64-1	58015	104	1.350	626.2	7.08	1.040	1.31	0.331	1.37	79	57744	5
A39	9	65-9 / 69-9	2957	1.350	626.2	7.08	1.040	1.31	0.331	1.37	79	57744	5	
A39	9	63-9 / 68-1	57861	3379	1.513	681.9	6.18	0.834	1.34	0.361	1.12	65	57588	5
T1-1	5	65-9 / 68-1	58494	3175	1.792	743.3	12.25	1.477	1.92	0.393	1.86	109	58155	5
A46	11	68-1 / 69-9	3811	1.792	743.3	12.25	1.477	1.92	0.393	1.86	109	58155	5	
A73	9	63-9 / 69-9	58058	3181	1.313	823.7	9.56	1.036	1.49	0.436	1.36	79	57726	6
A71	11	"	58041	3188	1.315	743.9	8.44	1.013	1.38	0.394	1.33	77	57735	6
A21	11	"	57977	3223	1.326	755.3	8.88	1.047	1.47	0.400	1.37	80	57666	6
A73	9	63-9 / 69-9	58080	3643	1.608	817.9	10.82	1.213	1.68	0.433	1.57	91	57738	7
A35	9	"	57870	3769	1.659	782.1	10.06	1.183	1.62	0.414	1.53	89	57542	7
A54	9	"	58330	3789	1.679	831.6	11.19	1.240	1.72	0.440	1.60	93	57980	7
A24	9	"	58108	3898	1.718	826.3	11.06	1.235	1.71	0.437	1.59	92	57761	7
A47	1	63-9 / 66-8	57998	4252	1.878	855.7	17.44	1.679	2.26	0.453	2.07	120	57615	8
A63	1	66-8 / 69-9	4328	1.952	886.7	18.43	1.708	2.31	0.469	2.10	122	57679	8	
A51	2	"	58004	4424	1.958	864.5	17.69	1.746	2.30	0.458	2.14	124	57615	8
A 9	2	"	58066	4505	2.008	867.0	17.59	1.764	2.33	0.459	2.16	125	57674	8

Table 3 continued

Ass'y Name	Pos. in Core* ¹	Date of Load./Unload.	Initial Wt. of U (Year-Month)	FLARE Calculation		NDA Assembly Averages* ²				Estimated from NDA				Repr. Batch No.				
				Integral BU (MWd/tU)	Pu/U* ³ ($\times 10^{-3}$)	137 (cps)	134 (cps)	$\frac{134}{137}$ ($\times 10^{-2}$)	$\frac{154}{137}$ ($\times 10^{-3}$)	BU (%)	Pu/U* ³ ($\times 10^{-3}$)	Pu* ³ (g)	U (g)					
A11	8	63-9 / 69-9	58095	3831	1.650	848.6	12.87	1.328	1.86	0.449	1.70	98	57736	9				
A29	8	"	58208	4390	1.893	971.2	15.80	1.475	2.04	0.514	1.86	108	57801	9				
A37	8	"	57918	4569	1.960	977.9	15.94	1.482	2.02	0.518	1.86	108	57510	9				
A34	8	"	57851	4599	1.971	964.1	16.17	1.533	1.99	0.510	1.92	111	57445	9				
A65	2	63-9 / 69-9	58039	4611	2.047	952.6	20.17	1.839	2.36	0.504	2.23	129	57617	10				
A 2	2	"	57934	4616	2.050	887.7	18.04	1.769	2.40	0.470	2.16	125	57537	10				
A10	2	"	58067	4625	2.074	938.8	20.05	1.838	2.37	0.497	2.23	129	57649	10				
A60	2	"	58035	4633	2.090	913.3	19.34	1.837	2.29	0.483	2.23	129	57625	10				
A32	7	63-9 / 69-9	58168	4208	1.801	932.2	15.41	1.459	2.04	0.493	1.84	107	57774	11				
A33	7	"	57821	4616	1.960	1008.5	18.21	1.643	2.20	0.534	2.03	117	57395	11				
A15	7	"	57937	5045	2.161	1051.2	19.41	1.697	2.30	0.556	2.09	121	57494	11				
A48	4	"	57933	4815	2.122	1053.8	21.30	1.782	2.32	0.558	2.18	126	57484	11				
A64	6	63-9 / 69-9	58093	4619	2.101	942.1	16.87	1.647	2.22	0.499	2.04	118	57685	12				
A 6	5	"	58133	4649	2.067	977.3	18.48	1.681	2.16	0.517	2.07	120	57712	12				
A28	6	"	58096	4856	2.209	966.4	16.88	1.615	2.18	0.512	2.00	116	57682	12				
A45	6	"	58221	5074	2.306	972.3	17.61	1.679	2.33	0.515	2.07	120	57801	12				
A42	7	63-9 / 69-9	57819	5085	2.159	1035.1	19.93	1.772	2.43	0.548	2.17	125	57377	13				
A22	7	"	57986	5133	2.180	1059.3	19.45	1.691	2.55	0.561	2.08	120	57540	13				
A41	7	"	58029	5109	2.180	1052.0	19.40	1.699	2.33	0.557	2.09	121	57585	13				
A43	7	"	57875	5154	2.184	1048.3	19.52	1.711	2.36	0.555	2.10	121	57432	13				
A13	5	63-9 / 69-9	57953	5314	2.367	1078.7	20.85	1.781	2.45	0.571	2.18	126	57496	14				
A12	5	"	57982	5403	2.414	1067.9	21.43	1.849	2.54	0.565	2.24	130	57524	14				
A57	5	"	58140	5418	2.426	1045.8	20.47	1.801	2.54	0.554	2.20	127	57691	14				
A31	5	"	58132	5173	2.307	1047.0	20.37	1.777	2.46	0.554	2.17	126	57684	14				
A23	5	63-9 / 69-9	58096	5486	2.442	1077.5	21.70	1.857	2.56	0.570	2.25	130	57634	15				
A67	4	"	57922	5519	2.451	1069.8	22.04	1.892	2.75	0.566	2.29	132	57462	15				
A26	4	"	57993	5639	2.500	1105.4	23.43	1.951	2.71	0.585	2.34	135	57518	15				
A40	4	"	58043	5641	2.500	1175.7	25.98	2.030	2.74	0.622	2.42	140	57541	15				
A56	3	63-9 / 69-9	57806	4604	2.049	961.3	18.14	1.660	2.13	0.509	2.05	118	57393	16				
A53	3	"	58315	4600	2.073	921.2	18.39	1.711	2.37	0.488	2.10	122	57908	16				
A 7	3	"	58141	4804	2.180	911.8	18.45	1.791	2.49	0.483	2.19	127	57733	16				
A69	3	"	57861	4786	2.130	927.4	18.58	1.777	2.46	0.491	2.17	125	57451	16				
A25	8	63-9 / 69-9	57804	4628	1.986	987.8	16.66	1.539	2.13	0.523	1.92	111	57391	17				
A19	8	"	58147	4655	2.007	952.0	14.95	1.434	1.91	0.504	1.81	105	57749	17				
A49	8	"	57964	4736	2.025	959.4	15.82	1.501	2.04	0.508	1.88	109	57561	17				
A70	8	"	57801	4765	2.032	1014.3	17.81	1.604	2.12	0.537	1.99	115	57376	17				
				6	63-9 / 66-8	2587												
A68	1	67-3 / 67-7	57811	2880														
	1	67-7 / 68-1		3453	1.852	831.9	11.93	1.323	1.69	0.440	1.69	97	57459	18				
				6	69-6 / 69-9	3888												
				4	63-9 / 67-7	3818												
A 5	6	67-7 / 68-1	58098	4392	2.204	969.5	18.04	1.691	2.47	0.513	2.08	121	57679	18				
	4	69-6 / 69-9		4882														
				A36	4	63-9 / 68-1	4822											
				9	68-1 / 69-9	5354	2.377	1048.4	19.50	1.719	2.35	0.555	2.11	122	57473	18		
				A52	2	63-9 / 69-9	58282	4427	1.981	916.7	18.80	1.739	2.26	0.485	2.13	124	57875	19
				A38	11	"	57878	3224	1.332	827.9	10.05	1.085	1.59	0.438	1.42	82	57542	19
				A 1	2	"	57820	4680	2.101	927.2	20.01	1.880	2.45	0.491	2.27	131	57405	19
				A 8	4	63-9 / 69-9	58150	5551	2.478	1098.2	23.41	1.961	2.70	0.581	2.35	136	57675	—
				A20	4	63-9 / 69-9	58067	5573	2.475	—	—	—	—	—	—	—	—	

*1) Group No. shown in Fig. 10.

*2) as of June 1, 1977.

*3) as of March 1, 1973.

Symbols of ^{137}Cs , ^{134}Cs , $^{134}/^{137}\text{Cs}$, $^{154}/^{137}\text{Cs}$, Pu/U, Pu, and U represent gamma-ray intensities of ^{137}Cs and ^{134}Cs , intensity ratios of $^{134}\text{Cs}/^{137}\text{Cs}$ and $^{154}\text{Eu}/^{137}\text{Cs}$, atom ratio of Pu/U, and final weights of Pu and U, respectively.

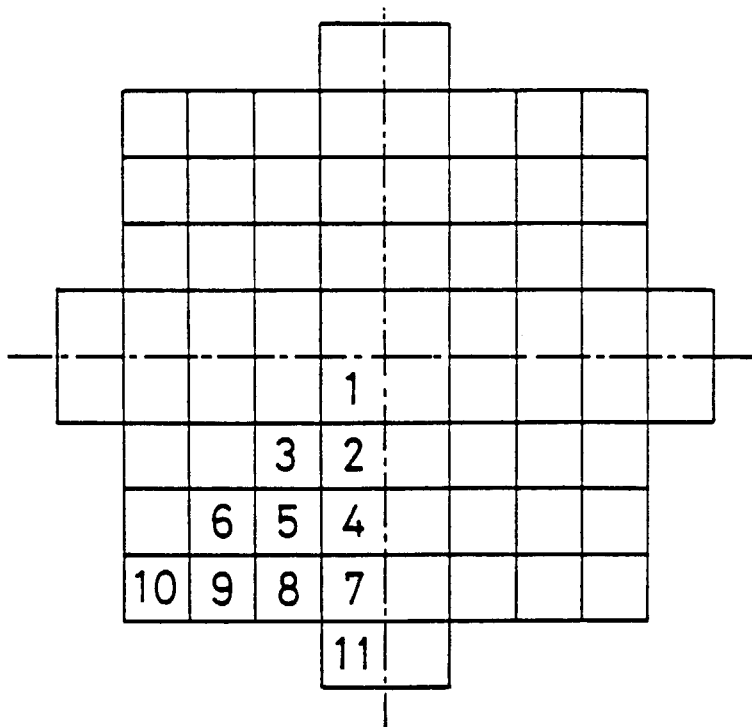


Fig. 10 Group number assigned to representative location of assembly in JPDR-I core.

4.3 Estimation of Errors in Average Gamma-Ray Intensity and Intensity Ratio

Since fuel rods have large absorption coefficients for gamma-rays, most of the measured gamma-ray intensity comes from the outer rods of an assembly. The assembly-averaged count rate and count-rate ratio derived in the last section (which are called apparent assembly-averages, hereafter) are not always proportional to the real assembly-averages of the FP activity and the activity ratio. The apparent average should be compared to the real one by taking into account the three-dimensional distribution of gamma-ray sources inside an assembly. Let $S(i, j, k)$ be the source distribution function where i and j denote the position in the radial plane of k -th axial position, as shown in **Fig. 11**. Then the measured count rate $A_i(m, k)$ is expressed as

$$\begin{aligned} A_1(m, k) &= K \sum_{i=1}^6 r_i S(i, m, k), \\ A_2(m, k) &= K \sum_{j=1}^6 r_j S(m, j, k), \\ A_3(m, k) &= K \sum_{i=1}^6 r_i S(7-i, m, k), \\ A_4(m, k) &= K \sum_{j=1}^6 r_j S(m, 7-j, k), \end{aligned} \quad (9)$$

where K is the detecting efficiency and r_i is the penetration rate of gamma-rays which are emitted in the direction to the detector from the fuel rod located at the i -th position from an assembly surface and finally arrive at the surface. The r_i was calculated by the following equation assuming the flat distribution of gamma-ray source in a fuel rod.

$$r_i = \frac{2}{\pi \rho \mu_f} e^{-\mu_m((i-1)a+h)} \{q_i^- - q_i^+\}, \quad (10)$$

where

$$q_i^{\pm} = \int_0^1 dt e^{-((2i-1)(\mu_f - \mu_m) \pm \mu_f) \rho \sqrt{j-t^2}},$$

μ_f, μ_m ; linear absorption coefficients¹¹⁾ of fuel meat and medium,
 ρ ; radius of fuel meat,
 a ; interval between fuel rods,
 h ; distance from an assembly surface to the center of the peripheral rod.

The calculated results for gamma-rays from ^{137}Cs (662 keV), ^{134}Cs (796 and 802 keV) and ^{154}Eu (1275 keV) are shown in **Table 4**. The availability of Eq.(10) was examined through comparing the calculated penetration rates with measured ones as described in Appendix 3.

Now, assuming the separation of variables, $S(i, j, k)$ is written as

$$S(i, j, k) = N p_x(i) p_y(j) p_z(k), \quad (11)$$

where

N ; normalization factor,
 p ; real peaking factor in the form as $p=1+\Delta$.

It is clear that the assembly-average of S , $\langle S \rangle$, is equal to N , since $\langle p \rangle=1$ or $\langle \Delta \rangle=0$ in each direction. Using the expressions of Eqs.(9) and (11), the axial peaking factors of

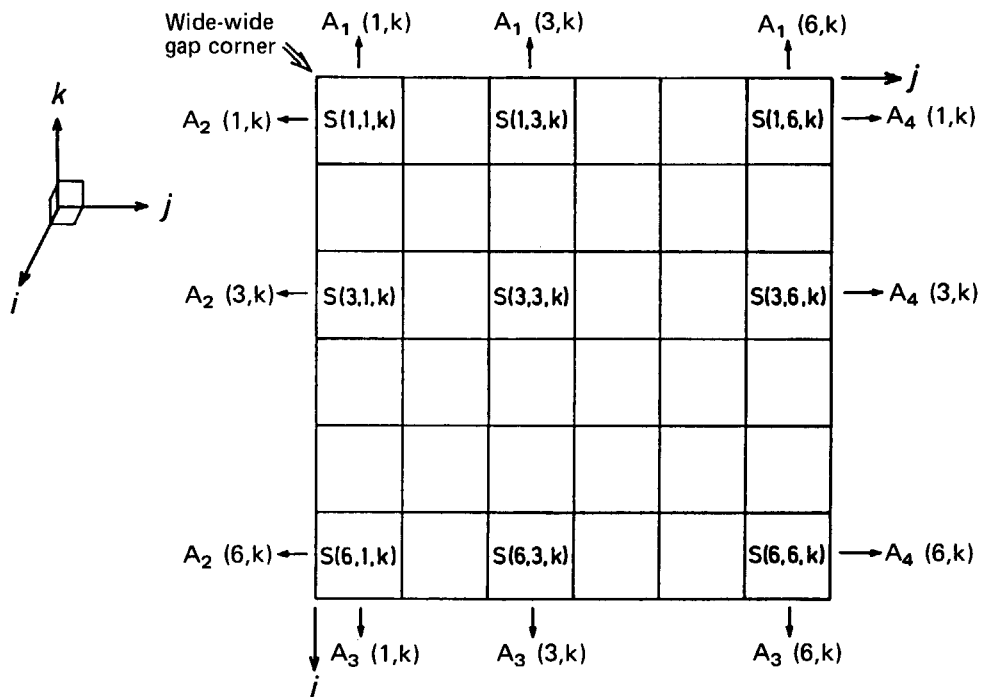


Fig. 11 Relation between measured count rate A_l (m, k) and internal gamma-ray source distribution S (i, j, k).

Table 4 Calculated γ_i and f_i

i	γ_i^{137}	γ_i^{134}	γ_i^{154}	$f_i^{134/137}$	$f_i^{154/137}$
1	0.515	0.569	0.673	0.702	0.570
2	0.149	0.199	0.329	0.297	0.530
3	0.046	0.073	0.167	0.123	0.342
4	0.016	0.029	0.084	0.052	0.189
5	0.006	0.012	0.046	0.023	0.111
6	0.003	0.006	0.024	0.011	0.058

measured data defined by Eq.(4) are expressed as

$$P_l(k) = p_z(k) / \bar{p}_z, \quad (12)$$

where

$$\bar{p}_z = W_1 p_z(3) + W_2 p_z(2) + W_3 p_z(1), \text{ in the lower half,}$$

$$= W'_1 p_z(4) + W'_2 p_z(5) + W'_3 p_z(6), \text{ in the upper half.}$$

Equation (12) shows that $P_l(k)$ is independent of l under the assumption of separation of variables, and therefore, $\bar{P}(k)$ in Eq.(6) is equal to the real peaking factors of source distribution in the axial direction of an assembly, because W and W' are chosen sufficiently correctly as discussed previously.

As for the apparent assembly-average of measured count rate, the following equation is obtained by neglecting multiple products of A .

$$\frac{\langle A \rangle}{N} \approx K \frac{1 + \bar{p}_r}{2} (1 + \bar{A}_r) \sum_{i=1}^6 r_i, \quad (13)$$

where

$$\bar{p}_r = w_1 p_x(1) p_y(1) + w_2 p_x(3) p_y(3) + w_3 p_x(6) p_y(6),$$

$$\bar{A}_r = \sum_{i=1}^6 r_i \{ p_x(i) p_y(i) + p_x(7-i) p_y(7-i) - 2 \} / 2(1 + \bar{p}_r) \sum_{i=1}^6 r_i.$$

In the case that $A_l(m, k)$ is the measured count-rate ratio of $^{134}\text{Cs}/^{137}\text{Cs}$ on the first side, for example, it is expressed as follows by utilizing the fact that S^{134} is approximately proportional to the square of S^{137} and $|A| \ll 1$ in radial directions.

$$A_l^{134/137}(m, k) = \frac{K^{134} \sum_{i=1}^6 r_i^{134} S^{134}(i, m, k)}{K^{137} \sum_{i=1}^6 r_i^{137} S^{137}(i, m, k)} \\ \approx K^{134/137} \sum_{i=1}^6 f_i^{134/137} S^{134/137}(i, m, k), \quad (14)$$

where

$$K^{134/137} = K^{134} / K^{137},$$

$$S^{134/137}(i, j, k) = S^{134}(i, j, k) / S^{137}(i, j, k),$$

$$f_i^{134/137} = \frac{\sum_{j=1}^6 r_j^{134}}{\sum_{j=1}^6 r_j^{137}} \left(\frac{2 r_i^{134}}{\sum_{j=1}^6 r_j^{134}} - \frac{r_i^{137}}{\sum_{j=1}^6 r_j^{137}} \right). \quad (15)$$

The value of f_i given by Eq.(15) is shown in **Table 4** for $^{134}\text{Cs}/^{137}\text{Cs}$ and $^{154}\text{Eu}/^{137}\text{Cs}$. The approximate value of Eq.(14) with f_i given by Eq.(15) agrees with the correct one within a few percent in both cases of $^{134}\text{Cs}/^{137}\text{Cs}$ and $^{154}\text{Eu}/^{137}\text{Cs}$, if maximum values of $|A|$ are less than 0.3 in the radial distribution of ^{137}Cs . Since Eq.(14) and the other equations for $l = 2, 3$, and 4 have the similar form to Eq.(9), the similar result to Eq.(13) can be derived for the apparent assembly-average of measured count-rate ratio.

In order to estimate the difference between $\langle A \rangle$ and $\langle S \rangle$, the applicability of separation of variables and the constancy of \bar{p}_r and \bar{A}_r in Eq.(13) were examined as follows.

The variation of P_l in Eq.(4) among four sides of the same assembly is considered to be

one of the measures of separability of variables. The calculated standard deviation of P_l was less than 1.5% for the assemblies not adjacent to the control rod, while it amounted to 10% for those adjacent to the control rod. This fact shows that the assumption is acceptable for the most assemblies not adjacent to the control rod.

The values of \bar{p}_r and \bar{A}_r were examined by using measured results of radial power distributions in the JPDR-I type fuel assemblies loaded in a critical facility¹²⁾. The results showed that the values of \bar{p}_r were 1.009 and 1.005 corresponding to the cases with and without the control rod, respectively, and the difference between the two cases was negligibly small. The value of \bar{A}_r is affected by r or f as seen in the defining equation. The largest difference between the two cases was found for the gamma-rays of ^{137}Cs , that is, \bar{A}_r in the case without the control rod was 0.05, while that in the case with the control rod was -0.01. This difference in \bar{A}_r was caused by the marked change in shape of the radial power distribution from concave to convex according to the insertion of the control rod. It may be worthy to point out that these results were obtained for fresh fuels in the small critical facility, and the power distributions were considerably steep compared with those in power reactors.

After all, $\langle A \rangle$ derived from the data measured at the forty positions is considered to be proportional to the real assembly-average within the error of 6%, which is attributed to the change in \bar{A}_r between the two extreme cases with and without the control rod surrounding the assembly. It is difficult to clarify the difference between $\langle A \rangle$ and $\langle S \rangle$ for the assemblies adjacent to the control rod, because the simple assumption of separation of variables adopted here hardly holds in such assemblies. In the evaluation of $\langle A \rangle$, however, the change in axial peaking factors on four sides was taken into account as seen in Eq.(6). Therefore, the above conclusion may not fail widely for the assemblies including those adjacent to the control rod.

4.4 Effect of Averaging Method on Determination of Pu/U Atom Ratio in an Assembly

The gamma-ray intensity ratio of $^{134}\text{Cs}/^{137}\text{Cs}$ or $^{154}\text{Eu}/^{137}\text{Cs}$ from NDA is often used to correlate with the Pu/U atom ratio. In order to correlate with the assembly-averaged value $\langle \text{Pu}/\text{U} \rangle$, two kinds of the measured intensity ratios of $^{134}\text{Cs}/^{137}\text{Cs}$ were investigated. They were $\langle A^{134} \rangle / \langle A^{137} \rangle$ and $\langle A^{134/137} \rangle$, which were approximately proportional to $\langle S^{134} \rangle / \langle S^{137} \rangle$ and $\langle S^{134/137} \rangle$, respectively, as discussed in the last section. The results of our measurement showed that $\langle A^{134} \rangle / \langle A^{137} \rangle$ was larger than $\langle A^{134/137} \rangle$ by about 9% for the assembly not adjacent to the control rod and the reflector, and by about 12~20% for the rest. This fact is understood by utilizing the following relations as

$$\langle S^{134/137} \rangle = \frac{\langle \phi \rangle^2 \langle S^{134} \rangle}{\langle \phi^2 \rangle \langle S^{137} \rangle} = C \left\langle \frac{P_u}{U} \right\rangle, \quad (16)$$

where C is a constant, and ϕ is the distribution of thermal neutron flux under which the assembly was irradiated. The factor $\langle \phi \rangle^2 / \langle \phi^2 \rangle$ is considerably sensitive to the change of the flux-distribution mode. The factor decreases from unity as the distribution becomes steeper compared to the flat distribution. This is the reason why $\langle A^{134} \rangle / \langle A^{137} \rangle$ was larger than $\langle A^{134/137} \rangle$ especially for the assembly which was irradiated in the steeper flux-distribution near the control rod and the reflector.

It is concluded that $\langle A^{134/137} \rangle$ is a better indicator of $\langle \text{Pu}/\text{U} \rangle$ than $\langle A^{134} \rangle / \langle A^{137} \rangle$ when the distributions of thermal neutron flux are significantly different among assemblies for measurement. Particular attention should be required for the measurement with a wide collimator, through which a whole assembly could be viewed, because the intensity ratio of $^{134}\text{Cs}/^{137}\text{Cs}$ obtained in such measurements corresponds to $\langle A^{134} \rangle / \langle A^{137} \rangle$.

5. Results and Discussion

5.1 Distributions of FP Intensity and Intensity Ratio in the Core

Figure 12 shows the distributions of A^{137} , $A^{134/137}$, and $A^{154/137}$ in fuel assemblies A69 and A45. The fuel assembly A69 had been adjacent to a control rod inserted partially. On the contrary, the control rod adjacent to the fuel assembly A45 had been fully withdrawn during the reactor operation. The distributions of A^{137} , $A^{134/137}$, and $A^{154/137}$ in A69 have maxima in the upper part of fuel assembly, while those in A45 have rather symmetrical shape. These differences in the distributions were mainly caused by the different insertion of control rods which were adjacent to those fuel assemblies. Another point to be noted is the difference in axial distribution between A^{137} and $A^{134/137}$ or $A^{154/137}$. This point will be discussed in detail in the next section.

Figure 13 and **14** show the radial distributions of A^{137} in a quarter of the core at two different axial heights, 428 mm above and below the mid-plane of the core. They are indicated as +428 mm and -428 mm, respectively. The central four control rods were gradually withdrawn downwards in order to compensate the reactivity loss due to burnup of fissile materials. This fact strongly affected the radial distributions of A^{137} . The distribution of A^{137} shows a concial convex as a whole in the upper part, while a sharp depression can be seen near the inserted control rod in the lower part of the core. The repetitions of sharp increases and

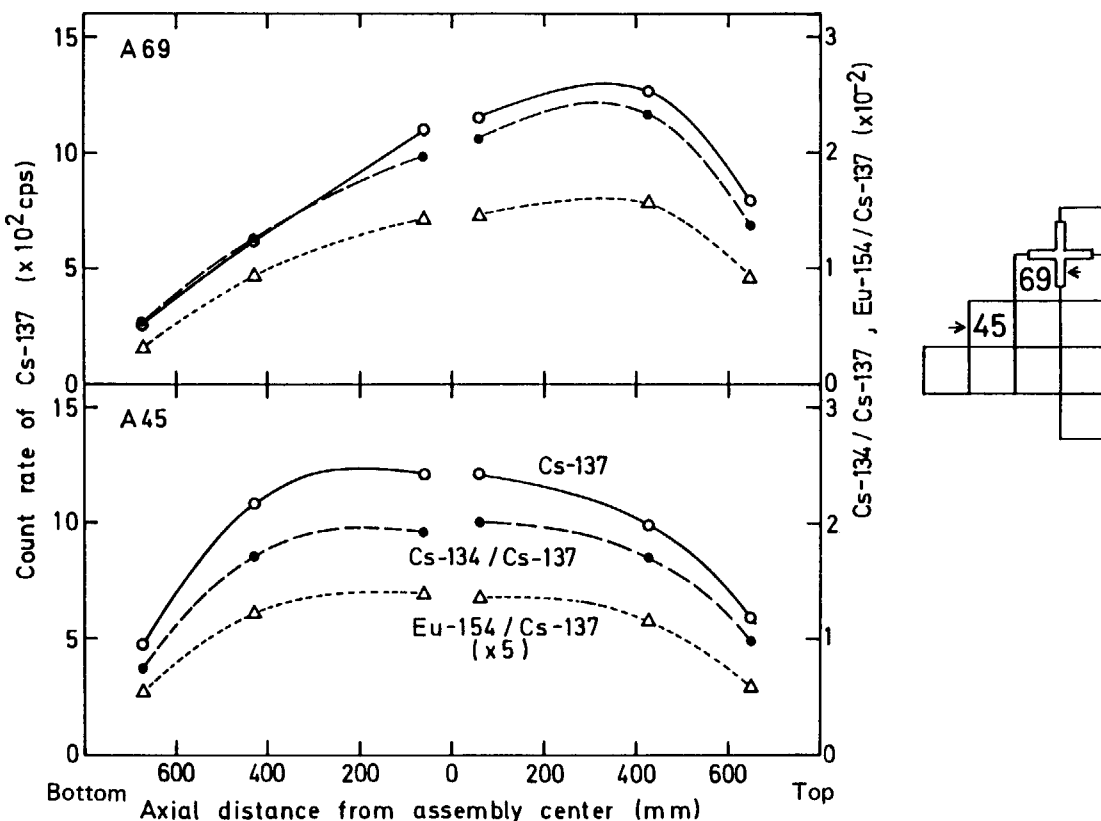


Fig. 12 Axial distributions of Gamma-ray intensity of ^{137}Cs , and intensity ratios of $^{134}\text{Cs}/^{137}\text{Cs}$ and $^{154}\text{Eu}/^{137}\text{Cs}$ in assemblies A45 and A69 measured at radial position indicated by arrows. Solid and broken lines represent the fitted functions.

decreases seen in the radial distributions are understood in accordance with wide water gaps and narrow water gaps with poison curtains existing between fuel assemblies.

As a whole, the measured results revealed that the distributions of fission products in the BWR core are considerably complicated owing to existence of control rods, water gaps, poison curtains, and so on. This fact should be taken into account when assembly-averaged burnups and Pu/U atom ratios are evaluated on fuel assemblies of BWRs from non-destructively measured gamma-ray intensities and intensity ratios at a limited number of points on assembly surfaces.

5.2 Correlation between ^{137}Cs Intensity and $^{134}\text{Cs}/^{137}\text{Cs}$ Intensity Ratio

In the study on fuel rods of the assembly A20, the correlations between the ^{137}Cs intensity and the $^{134}\text{Cs}/^{137}\text{Cs}$ or the $^{154}\text{Eu}/^{137}\text{Cs}$ intensity ratios were examined in connection with the spatial variation of neutron spectrum in the reactor core⁷⁾. The neutron spectrum depends fundamentally on the neutron absorption, leakage, and slowing down in a fuel assembly, and is locally affected by control rods, poison curtains, water gaps, and reflector surrounding the assembly. When the correlation between ^{137}Cs intensity and $^{134}\text{Cs}/^{137}\text{Cs}$ or $^{154}\text{Eu}/^{137}\text{Cs}$ intensity ratio is studied on the measured results of fuel assemblies, the above mentioned effect should be taken into account. **Figure 15** shows the correlation between A^{137} and $A^{134/137}$ which are collected from the measured results on particular sides of fuel assemblies. The assemblies had not been located adjacent to both of partially inserted control rods and reflector. The sides had faced to the poison curtains. As illustrated by open and closed circles, the measured results which belong to the same axial position form a consistent correlation. The change of the correlations with the axial positions corresponds to the change of the steam void fraction in moderator. The gradient of $A^{134/137}$ to A^{137} increases with the axial height,

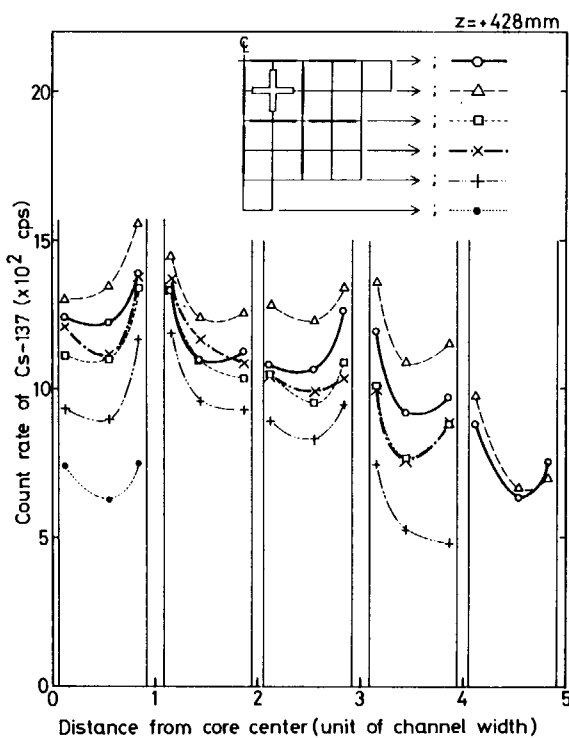


Fig. 13 Radial distributions of gamma-ray intensity of ^{137}Cs in core measured at axial position of +428 mm.

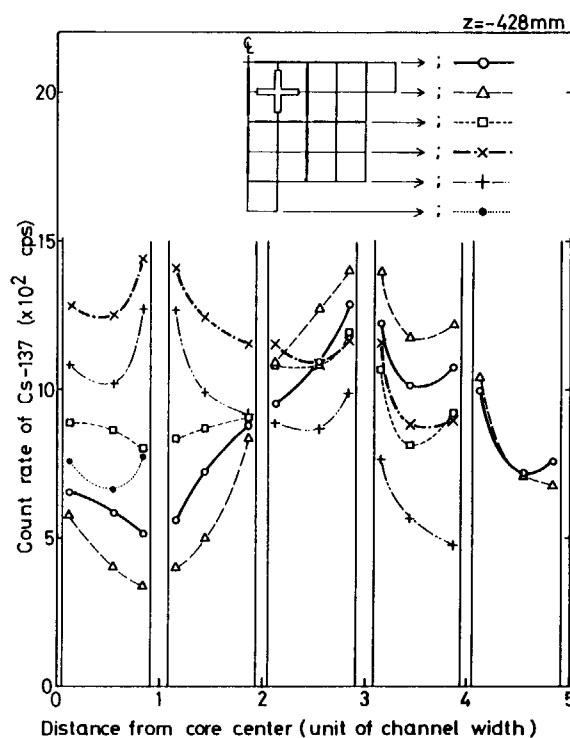


Fig. 14 Radial distributions of gamma-ray intensity of ^{137}Cs in core measured at axial position of -428 mm.

because the neutron spectrum becomes harder at the position of larger void fraction.

The increase of the gradient $A^{134/137}/A^{137}$ with the axial position is not monotonic in general. Some examples of changes of $A^{134/137}/A^{137}$ are indicated with axial positions in **Fig. 16**. The assemblies A45 and A30 had not been adjacent to partially inserted control rods, and the measured data from those assemblies were not affected with control rods. The values of $A^{134/137}/A^{137}$ are higher in the upper part than those in the lower part, and have maximum around the middle position of the upper segment of fuel. The changes of $A^{134/137}/A^{137}$ with axial position should correspond to the change of void fraction which should be largest at the top of fuel assembly. The reason for the decrease of $A^{134/137}/A^{137}$ at the top has not been clearly understood yet. A further investigation is needed on this point. The neutron-spectrum hardening due to void formation can be observed more clearly on narrow gap sides than wide gap sides as shown in curves (1) and (2) of the assembly A45. The lower values of A30 comparing with those of A45 were caused by the lower void fraction and the effect of soft neutron spectrum in reflector.

The assembly A69 had been adjacent to a partially inserted control rod. The larger value of $A^{134/137}/A^{137}$ at the lower part was brought by the control rod. Thermal neutrons around the control rod were strongly absorbed, and the neutron spectrum was apparently hardened by the lack of thermal neutrons. The value of $A^{134/137}/A^{137}$ is maintained rather high at the upper part of A69 because of the void formation. Consequently, the change of $A^{134/137}/A^{137}$ in A69 became quite particular as to have a minimum around the middle height.

The results shown in **Fig. 16** implies that the correlation between the assembly-averages of $A^{134/137}$, $\langle A^{134/137} \rangle$, and those of A^{137} , $\langle A^{137} \rangle$, should be different depending on the location of the fuel assembly. In other words, the correlations should be separated into several

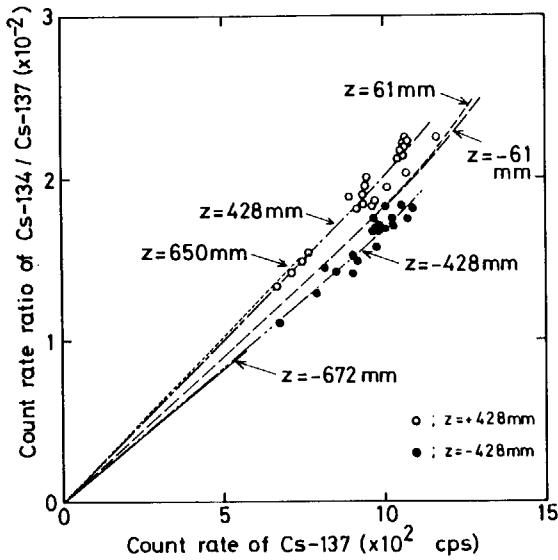


Fig. 15 Correlation between Gamma-ray intensity of ^{137}Cs (A^{137}) and intensity ratio of $^{134}\text{Cs}/^{137}\text{Cs}$ ($A^{134/137}$) measured at positions of Nos. 1 to 6 on narrow gap sides of assemblies remote from control rod and reflector. Open and closed circles belong to the axial positions of +428 mm and -428 mm, respectively. Data at the other axial positions are not presented for simplicity.

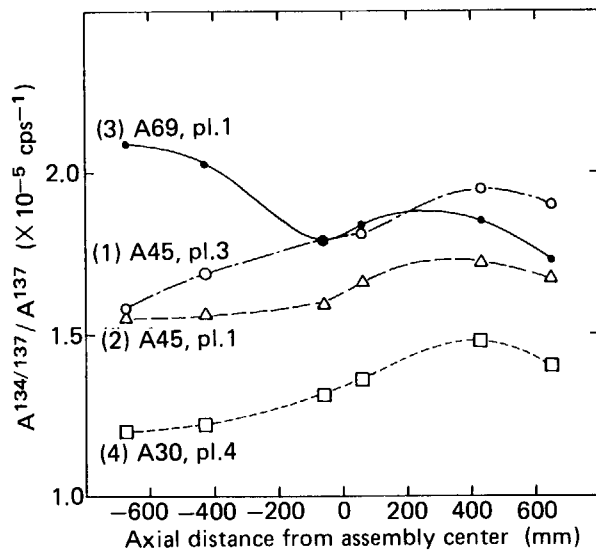


Fig. 16 Change of pointwise $A^{134/137}/A^{137}$ in axial direction. The measured sides of the cases (1), (2), (3), and (4) face to the narrow gap with a poison curtain, the wide gap with a control rod follower, the partially inserted control rod, and the reflector, respectively.

groups in accordance with the locations of fuel assemblies. This is clearly shown in **Fig. 17**. The diverse effects of control rods and reflector are evidently recognized in the figure.

One reason forming the difference in the correlation will be attributed to the difference in average void fraction of each assembly. The correlation between $\langle A^{134/137} \rangle / \langle A^{137} \rangle$ and the calculated void fraction⁹⁾ at the top of assembly is shown in **Fig. 18**. A simple relation is observed among the values of fuel assemblies except only those adjacent control rods.

The correlations between $A^{154/137}$ and A^{137} were similar to those between $A^{134/137}$ and A^{137} , though they are not indicated explicitly here. The values with ^{154}Eu can be used more positively than those with ^{134}Cs , when fuel assemblies have different irradiation histories, because the half-life of ^{154}Eu is much longer than that of ^{134}Cs .

5.3 Derivation of Assembly-Averaged Burnup and Pu/U Atom Ratio from NDA

From the results of the previous measurements on the fuels of the assembly A20⁸⁾, it is concluded that A^{137} and $A^{134/137}$ are good measures of the burnup and the Pu/U atom ratio, respectively, as shown in **Figs. 19** and **20**. The correlations are expressed as

$$\text{burnup} = a_1 \cdot \epsilon \cdot A^{137}, \quad (17)$$

$$\text{Pu/U atom ratio} = a_2 \cdot \epsilon' \cdot A^{134/137} \cdot \exp(-a_3 \cdot \epsilon' \cdot A^{134/137}), \quad (18)$$

where a_1 , a_2 , and a_3 are constants, and ϵ and ϵ' are coefficients which depend on measurement conditions in NDA such as cooling times and detection efficiencies of gamma-rays. The ratio of a_3/a_2 was found as 67.2 ± 11.0 for the JPDR-I fuels at the date on March 1, 1973.

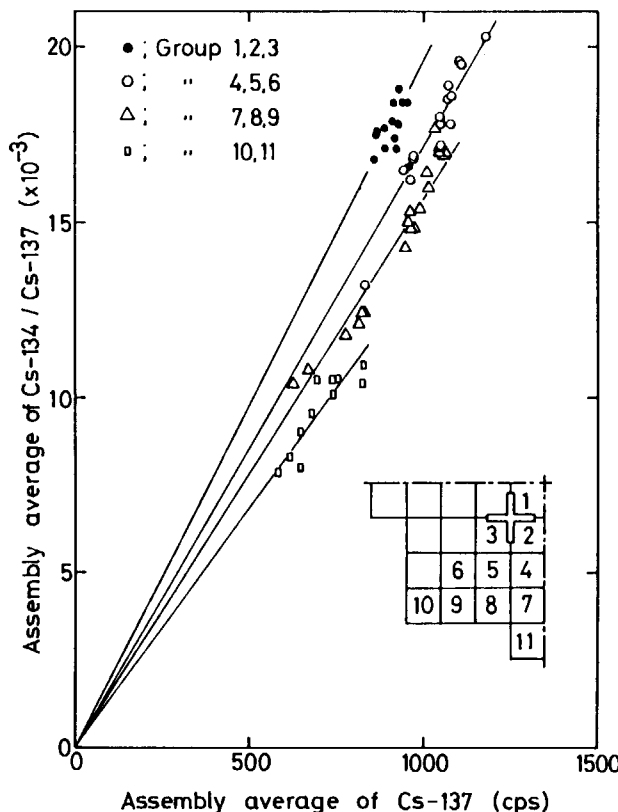


Fig. 17 Correlation between assembly-averages of A^{137} ($\langle A^{137} \rangle$) and $A^{134/137}$ ($\langle A^{134/137} \rangle$).

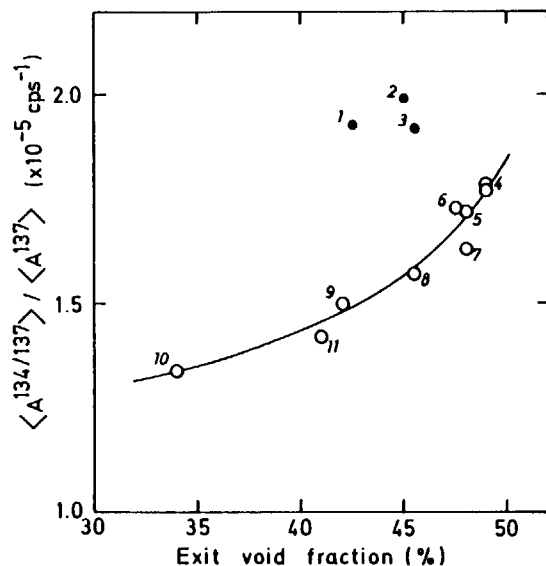


Fig. 18 Change of experimental $\langle A^{134/137} \rangle / \langle A^{137} \rangle$ with calculated void fraction at exit of assembly irradiated under the rated power of the core. Numbers beside the data show the group numbers.

Furthermore, the average burnup and Pu/U atom ratio in the assembly A20 were determined by using the combined data from DA and NDA. The results are shown in Fig. 21. Since the measurements were performed with only 8 rods selected from typical positions in A20, the values of the other rods were interpolated assuming their quadratic distributions and diagonal symmetries in the assembly. The burnups in the unit of atom percent shown in

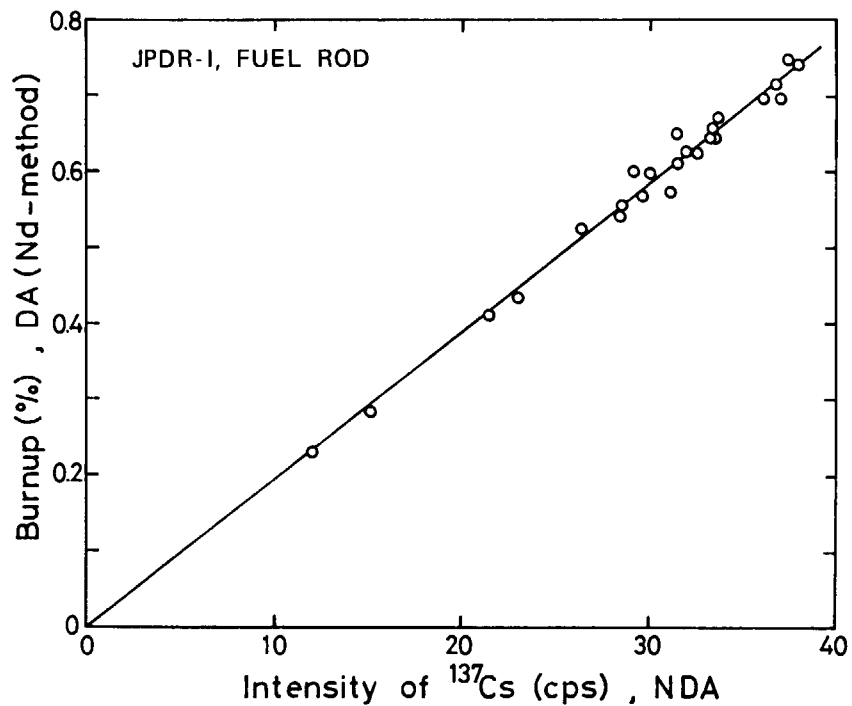


Fig. 19 Correlation between non-destructively measured gamma-ray intensities of ^{137}Cs on fuel rods in assembly A20 and burnups determined by corresponding destructive analysis on heavy elements and ^{148}Nd .

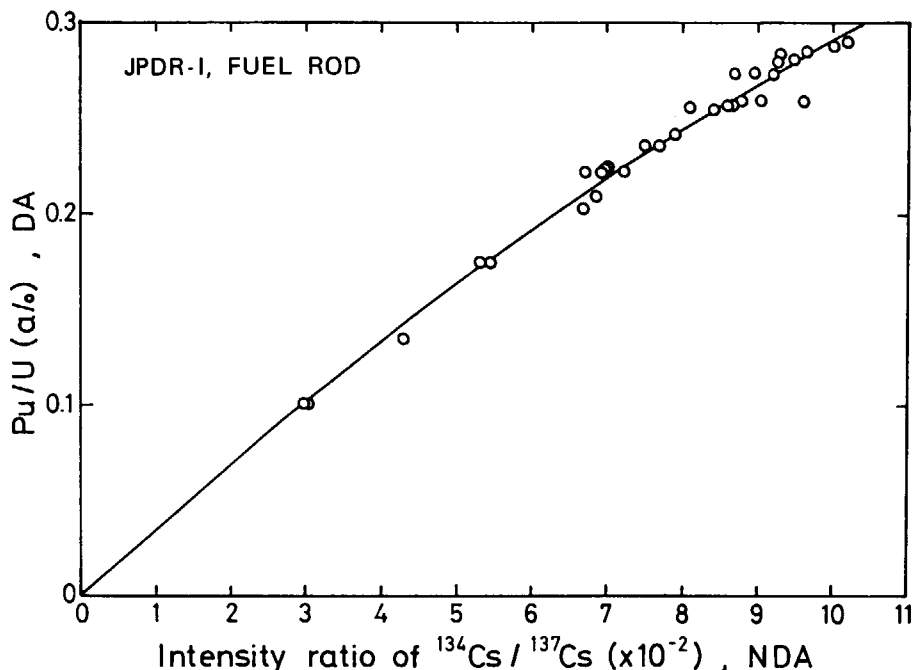


Fig. 20 Correlation between non-destructively measured gamma-ray intensity ratios of $^{134}\text{Cs}/^{137}\text{Cs}$ on fuel rods in assembly A20 and atom ratios of Pu/U determined by corresponding destructive analysis.

Follower Corner	[*] 0.710 2.52	0.671 2.45	0.645 2.41	[*] 0.631 2.40	0.630 2.40	[*] 0.641 2.43	→ BU (%) → Pu/U ($\times 10^{-3}$)
	0.595 2.36	0.573 2.33	0.556 2.31	^{**} 0.566 2.31	0.589 2.36		
		[*] 0.528 2.28	0.511 2.27	0.521 2.28	[*] 0.559 2.33		
Average in Assembly			0.507 2.27	0.509 2.27	0.533 2.33		
	0.581 2.353			0.534 2.33	0.568 2.37		
					[*] 0.607 2.45		

* , ** : Based on DA and NDA. The others are interpolated values.
 ** : Average of two values at the diagonally symmetric positions.

Fig. 21 Distributions of burnup and Pu/U atom ratio in the assembly A20.

the figure were obtained by the Nd-method⁸⁾ in which the cumulative fission yield of ^{148}Nd , 0.01675¹³⁾, was used. The burnup in atom percent can be converted to that in MWd/tU with a conversion factor 9500 MWd/tU/%, which corresponds to the fission energy of 200 MeV.

The average burnup and Pu/U atom ratio in each assembly were derived from the $\langle A^{137} \rangle$ and $\langle A^{134/137} \rangle$, respectively, by using the following equations.

$$\langle BU \rangle (\text{atom \%}) = 5.29 \times 10^{-4} \langle A^{137} \rangle (\text{cps}), \quad (19)$$

$$\langle Pu/U \rangle = 0.1453 \langle A^{134/137} \rangle \exp(-9.77 \langle A^{134/137} \rangle), \quad (20)$$

in which the three constants were determined by using the above ratio of a_3/a_2 and assuming that $\langle BU \rangle$ and $\langle Pu/U \rangle$ in the reference assembly A8 were the same as those in A20. The results are listed in **Table 3**. Masses of Pu and U in each irradiated fuel assembly evaluated by the following equations are also listed in the table.

$$\text{Mass of U} = (1 - \langle BU \rangle - \langle Pu/U \rangle) \times \text{Initial mass of U}, \quad (21)$$

$$\text{Mass of Pu} = \langle Pu/U \rangle \times 239/238 \times \text{Mass of U}, \quad (22)$$

where 239/238 is a factor used to convert the atom ratio to the mass ratio of Pu/U.

5.4 Comparison between Burnup Calculation and NDA

The burnup and the nuclear material balance of the JPDR core has been calculated by a combined code which consisted of FLARE and TERA⁹⁾. The FLARE code¹⁴⁾ and a few subordinate codes were used to calculate the thermo-hydraulic and neutronic situation of the operated reactor through the irradiation history in a three-dimensional model with coarse meshes. The TERA code estimated the depletion and the production of fuel material by solving the simultaneous equations for nuclear transmutations. The neutron flux distribution and the flux level for TERA were supplied from the results of FLARE. The variation of the nuclear constants were taken into account according to the changes of irradiation, void dis-

tribution, and power distribution. The calculated results of assembly-averaged burnup and Pu/U atom ratio are presented in **Table 3**.

The calculated results were compared with the measured ones from NDA as shown in **Figs. 22** and **23**. As a whole, reasonable correlations are observed in the figures. However, small systematic deviations remain among different groups of fuel assemblies. The burnups calculated for assemblies located in the core periphery are consistently smaller than those from the NDA as seen in **Fig. 22**. The calculated atom ratios of Pu/U show larger values for assemblies belonging to the groups 4 to 6, while they are smaller for those of the groups 1 and 2, compared with the results from NDA as seen in **Fig. 23**.

In the calculation, the assembly burnup was determined by distributing the thermo-hydraulically measured integral power to each assembly, according to the power peaking factor evaluated by a one-group neutron-balance equation like

$$\nabla^2 \phi + \frac{k_\infty - 1}{M^2} \phi = 0, \quad (23)$$

where

- ϕ ; neutron flux which produces power by multiplying a fission cross-section and a fission energy,
- k_∞ ; neutron multiplication factor in an infinite medium,
- M^2 ; migration area of neutrons.

The effect of reflector on the peripheral assembly was taken into account by using an albedo (or reflection rate of neutrons) of reflector. The amounts of Pu and the other heavy elements were calculated by the transmutation equations with suitable one-group cross-sections of corresponding reactions.

The discrepancies observed in the comparison between the results from calculation and NDA suggest the following explanations to be acceptable.

(1) The fairly good agreement in burnups of almost all assemblies implies that the calculated power peaking factors were reasonable, and therefore, the values of k_∞ and M^2 , and their changes with burnup were properly given in the calculation. However, there remains a place

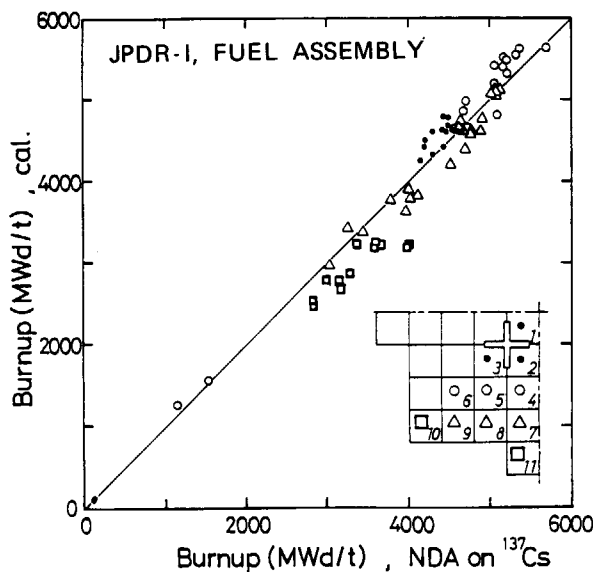


Fig. 22 Comparison on assembly burnups between calculation and NDA.

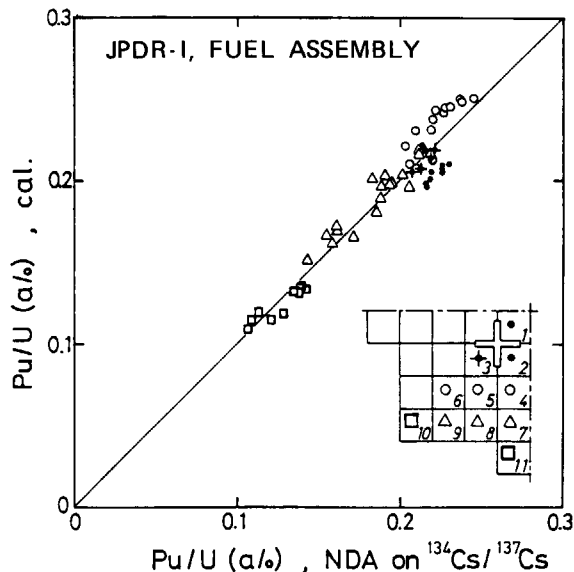


Fig. 23 Comparison on average atom-ratios of Pu/U in an assembly between calculation and NDA.

for further improvement of input values such as the albedo for assemblies faced to the reflector.

(2) Combining the results of comparison on burnups and Pu/U atom ratios, the one-group cross-section for production of Pu might be slightly overestimated for almost all assemblies except for those adjacent to control rods. It is difficult, in general, to evaluate the amount of accumulated Pu with a one-group cross-section, because the reaction concerned depends mostly on neutrons of resonance energy, and the ratio of resonance neutron flux to thermal neutron flux varies with positions in the core and degrees of burnup, especially in a BWR.

The total amount of Pu in the reprocessed assemblies determined by chemical and volumetric measurements on dissolved solutions¹⁵⁾ is considered to be a good reference for the above comparison. Among the 72 assemblies submitted to the NDA, 71 assemblies except A8 were shipped to the Tokai Reprocessing Plant and dissolved into 19 batches which consist of 2 to 4 assemblies of similar irradiation condition. The amount of Pu in each batch was determined at the accountability vessel of input solutions for the following extraction process. Since there were indefinite contaminations among different batches due to tank-heels, only the total amount of Pu in all batches was usable as the reference. The value was 6.98 kg, while the corresponding values from NDA and calculation were 7.11 kg and 7.25 kg, respectively. It should be taken into consideration that a small amount of Pu is accompanied by hulls in the dissolving process, and not accounted in the measurement at the accountability vessel. The amount is, usually, less than 1% of the total amount. Therefore, it could be concluded that the NDA made better estimation of Pu-build-up compared to the calculation. Thus the non-destructive gamma-ray spectrometry is usable to assure an accuracy of burnup calculation, in a good combination with destructive analyses.

Other than the measurement at the accountability vessel, solution samples were taken out of the dissolver vessel for the individual batches and submitted to precise chemical analyses. As the contaminations among different batches hardly occur in the dissolver vessel, the results from chemical analyses will provide the best reference for further examination on the accuracies of NDA and burnup calculation. The results on dissolver samples will be reported elsewhere in near future.

6. Conclusions

Non-destructive gamma-ray spectrometry was carried out on the whole-core assemblies of the JPDR-I, a BWR, using the gamma-scanning apparatus installed temporarily in the fuel storage pool. Gamma-ray intensities of fission-product nuclides such as ^{137}Cs , ^{134}Cs , and ^{154}Eu were identified in the measured spectrum at several points on each assembly surface, and average values of the intensity of ^{137}Cs and the intensity ratios of $^{134}\text{Cs}/^{137}\text{Cs}$ and $^{154}\text{Eu}/^{137}\text{Cs}$ were obtained for individual assemblies.

The effect of gamma-ray shielding inside an assembly upon the assembly-averages of the intensity and the intensity ratio was investigated in consideration of the difference in radial power distributions. It was found that the four-sides measurement for each assembly gave a difference of only about 6% in the assembly-averages between the cases with and without the control rod surrounding the assembly, in which the radial power distribution changed from concave to convex owing to the control rod insertion.

The point-wise $^{134}\text{Cs}/^{137}\text{Cs}$ intensity ratio was correlated with the ^{137}Cs intensity. The correlation showed a marked dependence on the neutron spectrum, that is, the gradient of the correlated line increased at the position of harder neutron spectrum owing to the effects of steam void and control rod, while it decreased near the reflector where the neutron spectrum was softened by the reflecting-back of well-thermalized neutrons.

The average burnup and Pu/U atom ratio in each assembly were derived from the assembly-averages of ^{137}Cs intensity and the $^{134}\text{Cs}/^{137}\text{Cs}$ intensity ratio, respectively, utilizing the correlations established in the previous experiment on a standard assembly of the JPDR-I. The non-destructively determined burnup and Pu/U atom ratio were compared with the calculational results. Although some discrepancies were pointed out for further investigations, good agreements were found between the experimental and the calculational results.

The amount of Pu build-up in each assembly was calculated by using the initial weight of U and the experimental burnup and Pu/U atom ratio. The calculated amount of total Pu for the assemblies subjected to reprocessing agreed quite well with the amount reported from the reprocessing plant.

Thus, the non-destructive gamma-ray spectrometry technique was satisfactorily applied to the spent fuel assemblies from the BWR, in which the spatial variations of power and neutron spectrum were considerably complicated owing to the effects of control rods, water gaps, steam void formation and reflector. The effects were minimized by averaging the measured data on every four sides, and by taking correlations between the values of the same dependence on neutron spectrum.

Measurement capability of burnup and fissile contents of irradiated fuels is one of the most important measures in accomplishing the effectiveness of nuclear safeguards and the performance of nuclear facilities. A good combination of NDA and DA provides substantial information on burnup and Pu build-up with a relatively little experimental effort. It is recommended that each facility concerning nuclear material accounting of irradiated fuels should be equipped with a built-in apparatus for NDA measurements with a sufficient precision in order to accumulate the further information and to demonstrate the applicability of NDA to various fuels.

Acknowledgment

The authors are grateful to Messrs. I. Kobayashi, A. Ohno, and K. Murakami for help with the experiment. Thanks are also due to Messrs. T. Hidaka and M. Ishizuka for unfailing support and encouragement to this work.

They are much indebted to Mr. H. Ezure for helpful comments in utilizing the results of burnup calculation on the JPDR-I core.

References

- 1) Hsue, S.T., et al. : LA-6923 (1978).
- 2) Tsuruta, H. : Proceedings of the Fifth International Conference on Nondestructive Evaluation in the Nuclear Industry, San Diego, U.S.A., 10-13 May 1982.
- 3) Bresesti, A.M., et al. : EUR-5334e (1975).
- 4) Gualandi, M.P., et al. : IAEA-SM-201/3, p.613-624 (1976).
- 5) Brand, P., et al. : EUR-5141e (1974).
- 6) Adiletta, G., et al. : EUR-5289e (1974).
- 7) Matsuura, S., et al. : J. Nucl. Sci. Technol., 12 (1), p.24 (1975).
- 8) Natsume, H., et al. : J. Nucl. Sci. Technol., 14 (10), p.745 (1977).
- 9) Ezure, H., et al. : JAERI-memo (published) 4083 (1970) [in Japanese].
- 10) Baba, H., et al. : JAERI-1227 (1973).
- 11) Storm, E. and Israel, H.I. : LA-3753 (1967).
- 12) Matsuura, S., et al. : JAERI-memo (published) 2871 (1967) [in Japanese].
- 13) Rider, B.F. : NEDO-12154-3(C) (1981).
- 14) Delp, D.L., et al. : GEAP-4598 (1964).
- 15) Power Reactor and Nuclear Fuel Development Corporation : Business Reports on Reprocessed Results of JPDR Spent Fuels (1978, 1981).

Appendix 1 Non-Destructively Measured Gamma-Ray Intensities and Intensity Ratios on the JPDR-I Fuel Assemblies

The measured gamma-ray intensities of ^{137}Cs (662 keV), ^{134}Cs (796+802 keV), ^{154}Eu (1275 keV), and $^{144}\text{Ce-Pr}$ (2186 keV) were corrected for several items described in Section 4.1. The corrected data were used to obtain the intensity ratios of $^{134}\text{Cs}/^{137}\text{Cs}$, $^{154}\text{Eu}/^{137}\text{Cs}$, $(^{134}\text{Cs}/^{137}\text{Cs})/^{137}\text{Cs}$, and $(^{154}\text{Eu}/^{137}\text{Cs})/^{137}\text{Cs}$. These data are listed in the following table. The measurement position is expressed by three parameters explained below.

PLANE ; measured side of an assembly shown in **Fig. 5**.

Z ; axial distance from the assembly center.

X ; radial position. X = 0, 1, and 2 correspond to the center axes of fuel rods located at the positions of i (or j) = 3, 6, and 1 in **Fig. 11**, respectively.

Symbols of 134/137 and 154/137 denotes the intensity ratios of $^{134}\text{Cs}/^{137}\text{Cs}$ and $^{154}\text{Eu}/^{137}\text{Cs}$, and those of 134/137/137 and 154/137/137 the ratios of 134/137 and 154/137 to the intensity of ^{137}Cs (cps), respectively.

ASSEMBLY	PLANE	Z(MM)	X	RUN NO.	CS137(CPS)	CS134(CPS)	EU154(CPS)	PH144(CPS)	134/137	154/137	134/137/137	154/137/137
A74	3	-428.0	0	18	0.20202E+02							
		-61.0	0	19	0.29441E+02							
		61.0	0	20	0.29922E+02							
		428.0	0	21	0.23232E+02							
A75	3	-428.0	0	23	0.20583E+02							
		-61.0	0	24	0.26456E+02							
		61.0	0	25	0.26137E+02							
		428.0	0	26	0.20411E+02							
A16	3	-428.0	0	27	0.24928E+03	0.2122E+01	0.1971E+00		0.8514E-02	0.7907E-03	0.3416E-04	0.3172E-05
		-61.0	0	28	0.27267E+03	0.2504E+01	0.2240E+00		0.9163E-02	0.8215E-03	0.3368E-04	0.3013E-05
		61.0	0	29	0.26007E+03	0.2502E+01	0.2130E+00		0.9621E-02	0.8192E-03	0.3700E-04	0.3150E-05
		428.0	0	30	0.19453E+03	0.1688E+01	0.1076E+00		0.8677E-02	0.5529E-03	0.4461E-04	0.2842E-05
A59	4	-428.0	0	32	0.27570E+03	0.9842E+00	0.1805E+00		0.3570E-02	0.6548E-03	0.1295E-04	0.2375E-05
		-61.0	0	34	0.29722E+03	0.1372E+01	0.2070E+00		0.4616E-02	0.6966E-03	0.1553E-04	0.2344E-05
		61.0	0	35	0.28831E+03	0.1393E+01	0.1822E+00		0.4831E-02	0.6319E-03	0.1676E-04	0.2192E-05
		428.0	0	36	0.22279E+03	0.7943E+00	0.1354E+00		0.3565E-02	0.6078E-03	0.1600E-04	0.2728E-05
A72	3	-428.0	0	37	0.30566E+03	0.1771E+01	0.2351E+00		0.5795E-02	0.7691E-03	0.1896E-04	0.2516E-05
		-61.0	0	38	0.36331E+03	0.2837E+01	0.3952E+00		0.7810E-02	0.1088E-02	0.2150E-04	0.2994E-05
		61.0	0	39	0.36456E+03	0.2530E+01	0.3515E+00		0.6941E-02	0.9642E-03	0.1904E-04	0.2643E-05
		428.0	0	40	0.36746E+03	0.1692E+01	0.3487E+00		0.5503E-02	0.1134E-02	0.1790E-04	0.3689E-05
A76	3	-428.0	0	41	0.22176E+03	0.8871E+00	0.1157E+00		0.4000E-02	0.5217E-03	0.1804E-04	0.2353E-05
		-61.0	0	42	0.24765E+03	0.9179E+00	0.1644E+00		0.3703E-02	0.6635E-03	0.1494E-04	0.2677E-05
		61.0	0	43	0.23926E+03	0.9461E+00	0.1394E+00		0.3954E-02	0.5825E-03	0.1653E-04	0.2435E-05
		428.0	0	44	0.18656E+03	0.5919E+00	0.9192E-01		0.3173E-02	0.4927E-03	0.1701E-04	0.2641E-05
A50	4	-428.0	0	50	0.46488E+03	0.2681E+01	0.4015E+00		0.5767E-02	0.8638E-03	0.1241E-04	0.1858E-05
		-61.0	0	51	0.60330E+03	0.5108E+01	0.7261E+00		0.8467E-02	0.1204E-02	0.1403E-04	0.1999E-05
		61.0	0	52	0.63000E+03	0.5089E+01	0.8812E+00		0.8079E-02	0.1399E-02	0.1282E-04	0.2220E-05
		428.0	0	53	0.53554E+03	0.4072E+01	0.6178E+00		0.7604E-02	0.11154E-02	0.1420E-04	0.2154E-05
A62	4	-428.0	0	57	0.64567E+03	0.4078E+01	0.5951E+00	0.2534E-01	0.6316E-02	0.9217E-03	0.9782E-05	0.1427E-05
		-61.0	0	56	0.64326E+03	0.5387E+01	0.8572E+00		0.8370E-02	0.1333E-02	0.1302E-04	0.2072E-05
		61.0	0	55	0.63850E+03	0.5588E+01	0.8060E+00		0.8752E-02	0.1262E-02	0.1371E-04	0.1977E-05
		428.0	0	54	0.55607E+03	0.3905E+01	0.5526E+00		0.7023E-02	0.9937E-03	0.1263E-04	0.1787E-05

ASSEMBLY PLANE	Z(MM)	X	RUN NO.	C5137(CPS)	C5134(CPS)	EU154(CPS)	PR144(CPS)	134/137	154/137	134/137/137	154/137/137
A30	1 -672.0	0	69	0.32798E+03	0.1706E+01	0.2222E+00		0.5200E-02	0.6775E-03	0.1585E-04	0.2066E-05
	1 -428.0	0	70	0.73817E+03	0.7616E+01	0.1005E+01		0.1032E-01	0.1362E-02	0.1398E-04	0.1845E-05
	1 -428.0	1	72	0.77590E+03	0.6836E+01	0.9012E+00		0.8811E-02	0.1161E-02	0.1136E-04	0.1497E-05
	1 -428.0	2	71	0.93025E+03	0.1257E+02	0.1858E+01		0.1352E-01	0.1997E-02	0.1453E-04	0.2147E-05
	1 -61.0	0	73	0.82452E+03	0.9850E+01	0.1300E+01		0.1195E-01	0.1577E-02	0.1449E-04	0.1913E-05
	1 61.0	0	74	0.80448E+03	0.1022E+02	0.1314E+01		0.1270E-01	0.1633E-02	0.1578E-04	0.2030E-05
	1 428.0	0	75	0.63505E+03	0.6928E+01	0.8557E+00		0.1091E-01	0.1348E-02	0.1718E-04	0.2122E-05
	1 428.0	1	77	0.75014E+03	0.6594E+01	0.8623E+00		0.8790E-02	0.1149E-02	0.1172E-04	0.1532E-05
	1 428.0	2	76	0.81794E+03	0.1094E+02	0.1273E+01		0.1338E-01	0.1556E-02	0.1635E-04	0.1903E-05
	1 650.0	0	78	0.36925E+03	0.2026E+01	0.2292E+00		0.5486E-02	0.6207E-03	0.1486E-04	0.1681E-05
	2 -672.0	0	87	0.34529E+03	0.1697E+01	0.2449E+00		0.4916E-02	0.7091E-03	0.1424E-04	0.2054E-05
	2 -428.0	0	88	0.75991E+03	0.7931E+01	0.1033E+01	0.3205E-01	0.1044E-01	0.1359E-02	0.1373E-04	0.1788E-05
	2 -428.0	1	86	0.77886E+03	0.6558E+01	0.9754E+00		0.8420E-02	0.1252E-02	0.1081E-04	0.1608E-05
	2 -428.0	2	85	0.97160E+03	0.1275E+02	0.1791E+01		0.1312E-01	0.1844E-02	0.1350E-04	0.1897E-05
	2 -61.0	0	84	0.83556E+03	0.1013E+02	0.1424E+01		0.1212E-01	0.1704E-02	0.1451E-04	0.2039E-05
	2 61.0	0	83	0.82283E+03	0.1032E+02	0.1343E+01		0.1254E-01	0.1632E-02	0.1524E-04	0.1984E-05
	2 428.0	0	80	0.65753E+03	0.6819E+01	0.7492E+00		0.1037E-01	0.1139E-02	0.1577E-04	0.1733E-05
	2 428.0	1	82	0.70509E+03	0.5845E+01	0.9021E+00		0.8289E-02	0.1279E-02	0.1176E-04	0.1815E-05
	2 428.0	2	81	0.83700E+03	0.1097E+02	0.1360E+01		0.1310E-01	0.1623E-02	0.1565E-04	0.1941E-05
	2 650.0	0	79	0.37961E+03	0.1961E+01	0.2370E+00		0.5166E-02	0.6243E-03	0.1361E-04	0.1645E-05
	3 -672.0	0	89	0.25265E+03	0.7385E+00	0.9322E-01		0.2923E-02	0.3690E-03	0.1157E-04	0.1460E-05
	3 -428.0	0	90	0.57740E+03	0.4096E+01	0.5795E+00		0.7049E-02	0.1004E-02	0.1228E-04	0.1738E-05
	3 -428.0	1	92	0.46495E+03	0.2263E+01	0.4116E+00		0.4868E-02	0.8852E-03	0.1047E-04	0.1904E-05
	3 -428.0	2	91	0.81568E+03	0.1957E+01	0.1177E+01		0.9755E-02	0.1443E-02	0.1196E-04	0.1769E-05
	3 -61.0	0	93	0.64292E+03	0.5493E+01	0.8802E+00		0.8543E-02	0.1369E-02	0.1329E-04	0.2129E-05
	3 61.0	0	94	0.64851E+03	0.5379E+01	0.7350E+00		0.8294E-02	0.1133E-02	0.1279E-04	0.1748E-05
	3 428.0	0	95	0.51336E+03	0.3619E+01	0.5664E+00		0.7050E-02	0.1103E-02	0.1373E-04	0.2149E-05
	3 428.0	1	97	0.45672E+03	0.2859E+01	0.4612E+00		0.6260E-02	0.1010E-02	0.1371E-04	0.2211E-05
	3 428.0	2	96	0.73309E+03	0.6815E+01	0.1146E+01		0.9296E-02	0.1563E-02	0.1268E-04	0.2132E-05
	3 650.0	0	98	0.28890E+03	0.1066E+01	0.1596E+00		0.3689E-02	0.5525E-03	0.1277E-04	0.1912E-05
	4 -672.0	0	107	0.24798E+03	0.7352E+00	0.1085E+00		0.2965E-02	0.4377E-03	0.1196E-04	0.1765E-05
	4 -428.0	0	108	0.56396E+03	0.3865E+01	0.5849E+00	0.2496E-01	0.6853E-02	0.1037E-02	0.1215E-04	0.1839E-05
	4 -428.0	1	105	0.47482E+03	0.2613E+01	0.4577E+00		0.5502E-02	0.9640E-03	0.1159E-04	0.2030E-05
	4 -428.0	2	106	0.76337E+03	0.6993E+01	0.1137E+01		0.9160E-02	0.1489E-02	0.1200E-04	0.1950E-05
	4 -61.0	0	104	0.63781E+03	0.5338E+01	0.7549E+00		0.6370E-02	0.1184E-02	0.1312E-04	0.1856E-05
	4 61.0	0	103	0.63674E+03	0.5528E+01	0.8419E+00		0.8681E-02	0.1322E-02	0.1363E-04	0.2077E-05
	4 428.0	0	100	0.52300E+03	0.4060E+01	0.5213E+00		0.7763E-02	0.9967E-03	0.1484E-04	0.1906E-05
	4 428.0	1	102	0.48045E+03	0.3146E+01	0.4736E+00		0.6548E-02	0.9856E-03	0.1363E-04	0.2051E-05
	4 428.0	2	101	0.74322E+03	0.7076E+01	0.9784E+00		0.9521E-02	0.1316E-02	0.1281E-04	0.1771E-05
	4 650.0	0	99	0.28461E+03	0.1131E+01	0.1481E+00		0.3972E-02	0.5202E-03	0.1396E-04	0.1828E-05
A55	4 -428.0	0	110	0.57953E+03	0.4078E+01	0.6552E+00		0.7036E-02	0.1131E-02	0.1214E-04	0.1951E-05
	4 -61.0	0	111	0.78864E+03	0.8523E+01	0.1215E+01		0.1081E-01	0.1540E-02	0.1370E-04	0.1933E-05
	4 61.0	0	112	0.85744E+03	0.1035E+02	0.1406E+01		0.1207E-01	0.1640E-02	0.1407E-04	0.1912E-05
	4 428.0	0	113	0.75316E+03	0.8116E+01	0.1246E+01		0.1078E-01	0.1654E-02	0.1431E-04	0.2196E-05
A61	1 -428.0	0	118	0.45351E+03	0.2302E+01	0.3617E+00	0.1816E-01	0.5077E-02	0.7975E-03	0.1119E-04	0.1759E-05
	1 -61.0	0	116	0.65928E+03	0.5426E+01	0.8492E+00		0.8231E-02	0.1288E-02	0.1248E-04	0.1934E-05
	1 61.0	0	115	0.71018E+03	0.6791E+01	0.9494E+00		0.9563E-02	0.1337E-02	0.1347E-04	0.1882E-05
	1 428.0	0	114	0.64278E+03	0.5862E+01	0.9667E+00		0.9120E-02	0.1504E-02	0.1419E-04	0.2340E-05
A66	1 -428.0	0	119	0.51671E+03	0.3351E+01	0.5150E+00		0.6486E-02	0.9961E-03	0.1255E-04	0.1929E-05
	1 -61.0	0	120	0.74261E+03	0.7021E+01	0.1063E+01		0.9454E-02	0.1431E-02	0.1273E-04	0.1927E-05
	1 61.0	0	121	0.73732E+03	0.8108E+01	0.1146E+01		0.1100E-01	0.1555E-02	0.1491E-04	0.2109E-05
	1 428.0	0	122	0.67876E+03	0.7143E+01	0.1041E+01		0.1052E-01	0.1534E-02	0.1550E-04	0.2260E-05
A 4	1 -428.0	0	128	0.61247E+03	0.5091E+01	0.7651E+00	0.2742E-01	0.8312E-02	0.1249E-02	0.1357E-04	0.2040E-05
	1 -61.0	0	126	0.71470E+03	0.7092E+01	0.1042E+01		0.9923E-02	0.1458E-02	0.1388E-04	0.2040E-05
	1 61.0	0	125	0.71425E+03	0.7531E+01	0.1133E+01		0.1054E-01	0.1586E-02	0.1476E-04	0.2220E-05
	1 428.0	0	123	0.58773E+03	0.4891E+01	0.7144E+00		0.8332E-02	0.1216E-02	0.1418E-04	0.2068E-05

ASSEMBLY PLANE	Z(MM)	X	RUN NO.	CS137(CPS)	CS134(CPS)	Eu154(CPS)	Pb144(CPS)	134/137	154/137	134/137/137	154/137/137
A 3	1 -672.0	0	129	0.32826E+03	0.1390E+01	0.2140E+00		0.4253E-02	0.6518E-03	0.1296E-04	0.1986E-05
	1 -428.0	0	130	0.70728E+03	0.6224E+01	0.9064E+00		0.8800E-02	0.1282E-02	0.1244E-04	0.1812E-05
	1 -428.0	1	132	0.10395E+04	0.1580E+02	0.1949E+01		0.1327E-01	0.1875E-02	0.1276E-04	0.1803E-05
	1 -428.0	2	131	0.67709E+03	0.5623E+01	0.8160E+00		0.8304E-02	0.1205E-02	0.1226E-04	0.1780E-05
	1 -61.0	0	133	0.78085E+03	0.8658E+01	0.1203E+01		0.1109E-01	0.1541E-02	0.1420E-04	0.1973E-05
	1 61.0	0	134	0.77442E+03	0.8666E+01	0.1175E+01		0.1119E-01	0.1517E-02	0.1445E-04	0.1959E-05
	1 428.0	0	135	0.66245E+03	0.6711E+01	0.8687E+00		0.1013E-01	0.1311E-02	0.1529E-04	0.1980E-05
	1 428.0	1	137	0.97214E+03	0.1452E+02	0.2027E+01		0.1493E-01	0.2085E-02	0.1536E-04	0.2145E-05
	1 428.0	2	136	0.69703E+03	0.6074E+01	0.8310E+00		0.8714E-02	0.1192E-02	0.1250E-04	0.1710E-05
	1 650.0	0	138	0.33716E+03	0.1423E+01	0.1958E+00		0.4220E-02	0.5808E-03	0.1252E-04	0.1723E-05
	2 -672.0	0	147	0.31226E+03	0.1163E+01	0.2085E+00		0.3726E-02	0.6678E-03	0.1193E-04	0.2139E-05
	2 -428.0	0	150	0.66288E+03	0.544	0.8215E+00	0.3070E-01	0.8212E-02	0.1239E-02	0.1239E-04	0.1870E-05
	2 -428.0	1	146	0.75407E+03	0.7296E+01	0.1169E+01		0.9676E-02	0.1550E-02	0.1283E-04	0.2035E-05
	2 -428.0	2	145	0.78063E+03	0.6445E+01	0.1007E+01		0.8257E-02	0.1290E-02	0.1058E-04	0.1653E-05
	2 -61.0	0	144	0.75703E+03	0.7232E+01	0.1220E+01		0.9554E-02	0.1611E-02	0.1262E-04	0.2128E-05
	2 61.0	0	143	0.76552E+03	0.7956E+01	0.1134E+01		0.1039E-01	0.1482E-02	0.1358E-04	0.1936E-05
	2 428.0	0	140	0.62640E+03	0.5706E+01	0.7428E+00		0.9109E-02	0.1166E-02	0.1454E-04	0.1893E-05
	2 428.0	1	142	0.73842E+03	0.8016E+01	0.9483E+00		0.1086E-01	0.1284E-02	0.1470E-04	0.1739E-05
	2 428.0	2	141	0.74781E+03	0.7332E+01	0.1060E+01		0.9804E-02	0.1417E-02	0.1311E-04	0.1895E-05
	2 650.0	0	139	0.33683E+03	0.1502E+01	0.2456E+00		0.4460E-02	0.7291E-03	0.1324E-04	0.2164E-05
	3 -672.0	0	151	0.33968E+03	0.1508E+01	0.2338E+00		0.4439E-02	0.6883E-03	0.1307E-04	0.2026E-05
	3 -428.0	0	152	0.71949E+03	0.7255E+01	0.1054E+01		0.1006E-01	0.1465E-02	0.1398E-04	0.2036E-05
	3 -428.0	1	154	0.99991E+03	0.1524E+02	0.2275E+01		0.1524E-01	0.2276E-02	0.1524E-04	0.2276E-05
	3 -428.0	2	153	0.75759E+03	0.6461E+01	0.9770E+00		0.8528E-02	0.1290E-02	0.1126E-04	0.1702E-05
	3 -61.0	0	155	0.77160E+03	0.9117E+01	0.1287E+01		0.1182E-01	0.1668E-02	0.1531E-04	0.2162E-05
	3 61.0	0	156	0.77616E+03	0.9766E+01	0.1364E+01		0.1258E-01	0.1758E-02	0.1621E-04	0.2265E-05
	3 428.0	0	157	0.63471E+03	0.6619E+01	0.9095E+00		0.1043E-01	0.1433E-02	0.1643E-04	0.2257E-05
	3 428.0	1	159	0.87947E+03	0.1296E+02	0.1804E+01		0.1474E-01	0.2051E-02	0.1676E-04	0.2332E-05
	3 428.0	2	158	0.75666E+03	0.7378E+01	0.1004E+01		0.9751E-02	0.1327E-02	0.1289E-04	0.1753E-05
	3 650.0	0	160	0.33373E+03	0.1568E+01	0.2282E+00		0.4698E-02	0.6838E-03	0.1408E-04	0.2049E-05
	4 -672.0	0	169	0.41979E+03	0.2361E+01	0.3219E+00		0.5624E-02	0.7668E-03	0.1340E-04	0.1827E-05
	4 -428.0	0	171	0.91507E+03	0.1120E+02	0.1454E+01	0.3478E-01	0.1222E-01	0.1589E-02	0.1337E-04	0.1737E-05
	4 -428.0	1	168	0.10123E+04	0.1479E+02	0.1829E+01		0.1461E-01	0.1806E-02	0.1444E-04	0.1785E-05
	4 -428.0	2	167	0.10799E+04	0.1464E+02	0.1874E+01		0.1356E-01	0.1735E-02	0.1256E-04	0.1607E-05
	4 -61.0	0	166	0.10012E+04	0.1477E+02	0.1893E+01		0.1476E-01	0.1890E-02	0.1474E-04	0.1888E-05
	4 61.0	0	165	0.98627E+03	0.1510E+02	0.1923E+01		0.1531E-01	0.1949E-02	0.1553E-04	0.1977E-05
	4 428.0	0	162	0.79828E+03	0.9863E+01	0.1385E+01		0.1236E-01	0.1735E-02	0.1548E-04	0.2173E-05
	4 428.0	1	164	0.91732E+03	0.1366E+02	0.1615E+01		0.1511E-01	0.1761E-02	0.1648E-04	0.1919E-05
	4 428.0	2	163	0.10194E+04	0.1458E+02	0.1906E+01		0.1430E-01	0.1870E-02	0.1403E-04	0.1834E-05
	4 650.0	0	161	0.41883E+03	0.3003E+01	0.3894E+00		0.7171E-02	0.9297E-03	0.1712E-04	0.2220E-05
A46	4 -428.0	0	172	0.51871E+03	0.2988E+01	0.4517E+00		0.5761E-02	0.8708E-03	0.1111E-04	0.1679E-05
	4 -61.0	0	173	0.59338E+03	0.4001E+01	0.7348E+00		0.6743E-02	0.1238E-02	0.1136E-04	0.2007E-05
	4 61.0	0	174	0.62115E+03	0.4200E+01	0.6688E+00		0.6762E-02	0.1077E-02	0.1089E-04	0.1733E-05
	4 428.0	0	175	0.49170E+03	0.2857E+01	0.4493E+00		0.5810E-02	0.9137E-03	0.1102E-04	0.1858E-05
A27	2 -428.0	0	180	0.62559E+03	0.6402E+01	0.8442E+00	0.3477E-01	0.1023E-01	0.1349E-02	0.1636E-04	0.2157E-05
	2 -61.0	0	178	0.72284E+03	0.8387E+01	0.1095E+01		0.1160E-01	0.1514E-02	0.1605E-04	0.2095E-05
	2 61.0	0	177	0.72980E+03	0.9054E+01	0.1107E+01		0.1241E-01	0.1517E-02	0.1700E-04	0.2079E-05
	2 428.0	0	176	0.57345E+03	0.5902E+01	0.7362E+00		0.1029E-01	0.1284E-02	0.1795E-04	0.2239E-05
A39	4 -428.0	0	181	0.75741E+03	0.9255E+01	0.1041E+01		0.1222E-01	0.1375E-02	0.1613E-04	0.1813E-05
	4 -61.0	0	182	0.85876E+03	0.1206E+02	0.1361E+01		0.1406E-01	0.1585E-02	0.1638E-04	0.1846E-05
	4 61.0	0	183	0.84920E+03	0.1268E+02	0.1345E+01		0.1493E-01	0.1584E-02	0.1758E-04	0.1865E-05
	4 428.0	0	184	0.68207E+03	0.7890E+01	0.8240E+00		0.1157E-01	0.1208E-02	0.1696E-04	0.1771E-05
T11	3 -428.0	0	189	0.55086E+03	0.5825E+01	0.7704E+00	0.3115E-01	0.1057E-01	0.1399E-02	0.1919E-04	0.2539E-05
	3 -61.0	0	187	0.81401E+03	0.1403E+02	0.1905E+01		0.1724E-01	0.2340E-02	0.2118E-04	0.2875E-05
	3 61.0	0	186	0.87726E+03	0.1729E+02	0.2230E+01		0.1971E-01	0.2542E-02	0.2246E-04	0.2897E-05
	3 428.0	0	185	0.84996E+03	0.1701E+02	0.2160E+01		0.2001E-01	0.2541E-02	0.2354E-04	0.2989E-05
A46	2 -428.0	0	190	0.76717E+03	0.6921E+01	0.1087E+01		0.9021E-02	0.1417E-02	0.1176E-04	0.1847E-05
	2 -61.0	0	191	0.87196E+03	0.9586E+01	0.1359E+01		0.1099E-01	0.1558E-02	0.1261E-04	0.1787E-05
	2 61.0	0	192	0.88349E+03	0.9743E+01	0.1313E+01		0.1103E-01	0.1486E-02	0.1248E-04	0.1682E-05
	2 428.0	0	193	0.72782E+03	0.6941E+01	0.9628E+00		0.9545E-02	0.1323E-02	0.1311E-04	0.1818E-05

ASSEMBLY PLANE	Z(MM)	X	RUN NO.	(S137(CPS)	(S134(CPS)	(U154(CPS)	PR144(CPS)	134/137	154/137	134/137/137	154/137/137	
A71	2	-428.0	0	198	0.66782E+03	0.5284E+01	0.8502E+00	0.2757E+01	0.7912E-02	0.1273E-02	0.1185E-04	0.1906E-05
	2	-61.0	0	196	0.76078E+03	0.7260E+01	0.1091E+01		0.9543E-02	0.1434E-02	0.1254E-04	0.1885E-05
	2	61.0	0	195	0.76241E+03	0.7493E+01	0.1074E+01		0.9828E-02	0.1408E-02	0.1289E-04	0.1847E-05
	2	428.0	0	194	0.63096E+03	0.5448E+01	0.7162E+00		0.8635E-02	0.1135E-02	0.1369E-04	0.1799E-05
A21	2	-428.0	0	199	0.65195E+03	0.5103E+01	0.8116E+00		0.7828E-02	0.1245E-02	0.1201E-04	0.1909E-05
	2	-61.0	0	200	0.78310E+03	0.8092E+01	0.1276E+01		0.1033E-01	0.1629E-02	0.1319E-04	0.2080E-05
	2	61.0	0	201	0.77555E+03	0.7911E+01	0.1122E+01		0.1020E-01	0.1447E-02	0.1315E-04	0.1866E-05
	2	428.0	0	202	0.65464E+03	0.5717E+01	0.8194E+00		0.8733E-02	0.1252E-02	0.1334E-04	0.1912E-05
A38	2	-428.0	0	207	0.79223E+03	0.7425E+01	0.1054E+01	0.3545E+01	0.9372E-02	0.1330E-02	0.1183E-04	0.1679E-05
	2	-61.0	0	205	0.88502E+03	0.1000E+02	0.1552E+01		0.1139E-01	0.1754E-02	0.1287E-04	0.1902E-05
	2	61.0	0	204	0.87794E+03	0.1004E+02	0.1377E+01		0.1144E-01	0.1568E-02	0.1303E-04	0.1786E-05
	2	428.0	0	203	0.71192E+03	0.7351E+01	0.1073E+01		0.1033E-01	0.1507E-02	0.1450E-04	0.2117E-05
A73	4	-428.0	0	208	0.68080E+03	0.7560E+01	0.1073E+01		0.1110E-01	0.1575E-02	0.1631E-04	0.2314E-05
	4	-61.0	0	209	0.84620E+03	0.1267E+02	0.1877E+01		0.1497E-01	0.2210E-02	0.1769E-04	0.2621E-05
	4	61.0	0	210	0.88003E+03	0.1383E+02	0.1938E+01		0.1571E-01	0.2202E-02	0.1785E-04	0.2502E-05
	4	428.0	0	211	0.71192E+03	0.1009E+02	0.1255E+01		0.1411E-01	0.1755E-02	0.1974E-04	0.2455E-05
A35	1	-428.0	0	216	0.77039E+03	0.8440E+01	0.1210E+01	0.3164E+01	0.1096E-01	0.1581E-02	0.1422E-04	0.2052E-05
	1	-61.0	0	214	0.89480E+03	0.1247E+02	0.1639E+01		0.1394E-01	0.1831E-02	0.1558E-04	0.2046E-05
	1	61.0	0	213	0.90795E+03	0.1245E+02	0.1782E+01		0.1371E-01	0.1963E-02	0.1910E-04	0.2162E-05
	1	428.0	0	212	0.73876E+03	0.8968E+01	0.1209E+01		0.1206E-01	0.1636E-02	0.1632E-04	0.2215E-05
A54	3	-428.0	0	218	0.79319E+03	0.1018E+02	0.1436E+01		0.1283E-01	0.1810E-02	0.1618E-04	0.2282E-05
	3	-61.0	0	217	0.86113E+03	0.1335E+02	0.1779E+01		0.1550E-01	0.2066E-02	0.1800E-04	0.2399E-05
	3	61.0	0	219	0.85274E+03	0.1320E+02	0.1977E+01		0.1548E-01	0.2319E-02	0.1815E-04	0.2719E-05
	3	428.0	0	220	0.66700E+03	0.8890E+01	0.1156E+01		0.1333E-01	0.1739E-02	0.1998E-04	0.2599E-05
A24	1	-672.0	0	229	0.42317E+03	0.2820E+01	0.3759E+00		0.6664E-02	0.8883E-03	0.1575E-04	0.2099E-05
	1	-428.0	0	231	0.96633E+03	0.1371E+02	0.1777E+01	0.3824E+01	0.1419E-01	0.1839E-02	0.1469E-04	0.1903E-05
	1	-428.0	1	228	0.98626E+03	0.1550E+02	0.2118E+01		0.1571E-01	0.2148E-02	0.1593E-04	0.2178E-05
	1	-428.0	2	227	0.10490E+04	0.1617E+02	0.2123E+01		0.1541E-01	0.2024E-02	0.1469E-04	0.1929E-05
	1	-61.0	0	226	0.10279E+04	0.1706E+02	0.2325E+01		0.1660E-01	0.2262E-02	0.1615E-04	0.2200E-05
	1	61.0	0	225	0.10322E+04	0.1765E+02	0.2499E+01		0.1710E-01	0.2421E-02	0.1656E-04	0.2345E-05
	1	428.0	0	222	0.82872E+03	0.1196E+02	0.1642E+01		0.1443E-01	0.1982E-02	0.1742E-04	0.2391E-05
	1	428.0	1	224	0.91176E+03	0.1540E+02	0.1987E+01		0.1689E-01	0.2179E-02	0.1852E-04	0.2390E-05
	1	428.0	2	223	0.89424E+03	0.1289E+02	0.1631E+01		0.1442E-01	0.1823E-02	0.1612E-04	0.2039E-05
	1	650.0	0	221	0.49003E+03	0.4417E+01	0.4826E+00		0.9014E-02	0.9848E-03	0.1839E-04	0.2010E-05
	2	-672.0	0	240	0.41394E+03	0.2437E+01	0.3379E+00		0.5888E-02	0.8163E-03	0.1422E-04	0.1972E-05
	2	-428.0	0	242	0.88247E+03	0.1072E+02	0.1500E+01	0.3708E+01	0.1215E-01	0.1700E-02	0.1376E-04	0.1927E-05
	2	-428.0	1	239	0.89831E+03	0.9403E+01	0.1300E+01		0.1047E-01	0.1448E-02	0.1165E-04	0.1611E-05
	2	-428.0	2	238	0.11600E+04	0.1821E+02	0.2534E+01		0.1569E-01	0.2185E-02	0.1953E-04	0.1883E-05
	2	-61.0	0	237	0.92298E+03	0.1296E+02	0.1833E+01		0.1404E-01	0.1986E-02	0.1522E-04	0.2151E-05
	2	61.0	0	236	0.93526E+03	0.1346E+02	0.1823E+01		0.1439E-01	0.1949E-02	0.1539E-04	0.2084E-05
	2	428.0	0	233	0.75817E+03	0.9339E+01	0.1325E+01		0.1232E-01	0.1747E-02	0.1625E-04	0.2305E-05
	2	428.0	1	235	0.88524E+03	0.9537E+01	0.1411E+01		0.1077E-01	0.1594E-02	0.1217E-04	0.1800E-05
	2	428.0	2	234	0.99675E+03	0.1582E+02	0.2204E+01		0.1588E-01	0.2211E-02	0.1593E-04	0.2218E-05
	2	650.0	0	232	0.44443E+03	0.3305E+01	0.4312E+00		0.7436E-02	0.9702E-03	0.1673E-04	0.2183E-05
	3	-672.0	0	248	0.40689E+03	0.1874E+01	0.3133E+00		0.4606E-02	0.7701E-03	0.1132E-04	0.1893E-05
	3	-428.0	0	247	0.86770E+03	0.8986E+01	0.1294E+01		0.1036E-01	0.1492E-02	0.1194E-04	0.1719E-05
	3	-428.0	1	246	0.88839E+03	0.1027E+02	0.1604E+01		0.1156E-01	0.1806E-02	0.1301E-04	0.2033E-05
	3	-428.0	2	245	0.98720E+03	0.1132E+02	0.1686E+01		0.1147E-01	0.1708E-02	0.1162E-04	0.1730E-05
	3	-61.0	0	249	0.98436E+03	0.1234E+02	0.1680E+01		0.1254E-01	0.1707E-02	0.1274E-04	0.1734E-05
	3	61.0	0	250	0.98883E+03	0.1264E+02	0.1886E+01		0.1278E-01	0.1907E-02	0.1293E-04	0.1929E-05
	3	428.0	0	251	0.82947E+03	0.8851E+01	0.1291E+01		0.1067E-01	0.1556E-02	0.1286E-04	0.1876E-05
	3	428.0	1	244	0.88934E+03	0.1096E+02	0.1502E+01		0.1233E-01	0.1689E-02	0.1386E-04	0.1899E-05
	3	428.0	2	243	0.94061E+03	0.1081E+02	0.1423E+01		0.1149E-01	0.1512E-02	0.1221E-04	0.1608E-05
	3	650.0	0	252	0.46373E+03	0.3089E+01	0.3789E+00		0.6661E-02	0.8170E-03	0.1436E-04	0.1762E-05

ASSEMBLY PLANE	Z (MM)	X	RUN NO.	C5137(CPS)	C5134(CPS)	E0154(CPS)	PH144(CPS)	134/137	154/137	134/137/137	154/137/137	
	4	-672.0	0	259	0.34836E+03	0.1999E+01	0.2704E+00	0.5737E-02	0.7762E-03	0.1647E-04	0.2228E-05	
	4	-428.0	0	263	0.77028E+03	0.9910E+01	0.1390E+01	0.3512E-01	0.1287E-01	0.1804E-02	0.1670E-04	0.2342E-05
	4	-428.0	1	261	0.89548E+03	0.1021E+02	0.1381E+01	0.1140E-01	0.1544E-02	0.1274E-04	0.1722E-05	
	4	-428.0	2	260	0.10096E+04	0.1695E+02	0.2533E+01	0.1679E-01	0.2509E-02	0.1663E-04	0.2485E-05	
	4	-61.0	0	258	0.84749E+03	0.1303E+02	0.1856E+01	0.1538E-01	0.2190E-02	0.1815E-04	0.2585E-05	
	4	61.0	0	257	0.84643E+03	0.1303E+02	0.1739E+01	0.1539E-01	0.2054E-02	0.1818E-04	0.2427E-05	
	4	428.0	0	254	0.68972E+03	0.9150E+01	0.1250E+01	0.1327E-01	0.1813E-02	0.1923E-04	0.2629E-05	
	4	428.0	1	256	0.92357E+03	0.1178E+02	0.1477E+01	0.1276E-01	0.1599E-02	0.1382E-04	0.1732E-05	
	4	428.0	2	255	0.91880E+03	0.1645E+02	0.2359E+01	0.1790E-01	0.2568E-02	0.1949E-04	0.2795E-05	
	4	650.0	0	253	0.37489E+03	0.2411E+01	0.3821E+00	0.6430E-02	0.1019E-02	0.1715E-04	0.2719E-05	
A47	3	-428.0	0	264	0.59831E+03	0.6539E+01	0.8753E+00	0.1093E-01	0.1463E-02	0.1827E-04	0.2445E-05	
	3	-61.0	0	265	0.10294E+04	0.2015E+02	0.2648E+01	0.1957E-01	0.2573E-02	0.1901E-04	0.2499E-05	
	3	61.0	0	266	0.11000E+04	0.2474E+02	0.3333E+01	0.2249E-01	0.3030E-02	0.2044E-04	0.2755E-05	
	3	428.0	0	267	0.11308E+04	0.2780E+02	0.3752E+01	0.2458E-01	0.3318E-02	0.2174E-04	0.2934E-05	
A63	1	-672.0	0	276	0.14966E+03	0.5117E+00	0.5848E-01	0.3419E-02	0.3908E-03	0.2284E-04	0.2611E-05	
	1	-428.0	0	278	0.41645E+03	0.3740E+01	0.5395E+00	0.2321E-01	0.8980E-02	0.1295E-02	0.2156E-04	0.3111E-05
	1	-428.0	1	275	0.58088E+03	0.5921E+01	0.9055E+00	0.1019E-01	0.1559E-02	0.1755E-04	0.2684E-05	
	1	-428.0	2	274	0.31091E+03	0.1057E+01	0.3259E+00	0.5974E-02	0.1048E-02	0.1921E-04	0.3371E-05	
	1	-61.0	0	273	0.10558E+04	0.2083E+02	0.2862E+01	0.1973E-01	0.2711E-02	0.1869E-04	0.2567E-05	
	1	61.0	0	272	0.11228E+04	0.2535E+02	0.3389E+01	0.2258E-01	0.3018E-02	0.2011E-04	0.2688E-05	
	1	428.0	0	269	0.13041E+04	0.3300E+02	0.4245E+01	0.2530E-01	0.3255E-02	0.1940E-04	0.2496E-05	
	1	428.0	1	271	0.14616E+04	0.3920E+02	0.5383E+01	0.2682E-01	0.3683E-02	0.1835E-04	0.2520E-05	
	1	428.0	2	270	0.14259E+04	0.3869E+02	0.5182E+01	0.2713E-01	0.3634E-02	0.1903E-04	0.2548E-05	
	1	650.0	0	268	0.78167E+03	0.1140E+02	0.1550E+01	0.1458E-01	0.1982E-02	0.1866E-04	0.2536E-05	
	2	-672.0	0	288	0.15159E+03	0.4230E+00	0.9880E-01	0.2790E-02	0.6318E-03	0.1841E-04	0.4300E-05	
	2	-428.0	0	285	0.40109E+03	0.3963E+01	0.4961E+00	0.9881E-02	0.1237E-02	0.2463E-04	0.3084E-05	
	2	-428.0	1	287	0.57530E+03	0.6133E+01	0.9182E+00	0.1066E-01	0.1596E-02	0.1853E-04	0.2774E-05	
	2	-428.0	2	286	0.33804E+03	0.2912E+01	0.3562E+00	0.8614E-02	0.1054E-02	0.2548E-04	0.3117E-05	
	2	-61.0	0	284	0.10656E+04	0.2059E+02	0.2839E+01	0.1932E-01	0.2664E-02	0.1813E-04	0.2500E-05	
	2	61.0	0	283	0.11519E+04	0.2535E+02	0.3440E+01	0.2201E-01	0.2986E-02	0.1910E-04	0.2593E-05	
	2	428.0	0	280	0.13452E+04	0.3388E+02	0.4343E+01	0.2519E-01	0.3228E-02	0.1872E-04	0.2400E-05	
	2	428.0	1	282	0.13005E+04	0.3360E+02	0.4483E+01	0.2583E-01	0.3720E-02	0.1907E-04	0.2860E-05	
	2	428.0	2	281	0.15542E+04	0.4164E+02	0.5576E+01	0.2679E-01	0.3587E-02	0.1724E-04	0.2308E-05	
	2	650.0	0	279	0.79542E+03	0.1193E+02	0.1382E+01	0.1500E-01	0.1737E-02	0.1886E-04	0.2184E-05	
	3	-672.0	0	289	0.22234E+03	0.8051E+00	0.8468E-01	0.3604E-02	0.3790E-03	0.1613E-04	0.1697E-05	
	3	-428.0	0	290	0.60907E+03	0.6531E+01	0.8633E+00	0.1072E-01	0.1417E-02	0.1761E-04	0.2327E-05	
	3	-428.0	1	292	0.66017E+03	0.7468E+01	0.1008E+01	0.1131E-01	0.1527E-02	0.1714E-04	0.2313E-05	
	3	-428.0	2	291	0.53910E+03	0.5125E+01	0.7377E+00	0.9506E-02	0.1368E-02	0.1763E-04	0.2538E-05	
	3	-61.0	0	293	0.10740E+04	0.2203E+02	0.2768E+01	0.2051E-01	0.2578E-02	0.1910E-04	0.2400E-05	
	3	61.0	0	294	0.11432E+04	0.2630E+02	0.3638E+01	0.2300E-01	0.3183E-02	0.2012E-04	0.2784E-05	
	3	428.0	0	295	0.11724E+04	0.2890E+02	0.3999E+01	0.2465E-01	0.3411E-02	0.2102E-04	0.2910E-05	
	3	428.0	1	297	0.12468E+04	0.3201E+02	0.4100E+01	0.2567E-01	0.3288E-02	0.2059E-04	0.2637E-05	
	3	428.0	2	296	0.13471E+04	0.3585E+02	0.4690E+01	0.2662E-01	0.3482E-02	0.1976E-04	0.2585E-05	
	3	650.0	0	298	0.67048E+03	0.9770E+01	0.1309E+01	0.1457E-01	0.1953E-02	0.2173E-04	0.2913E-05	
	4	-672.0	0	307	0.21567E+03	0.7965E+00	0.1753E+01	0.3692E-02	0.8126E-03	0.1712E-04	0.3768E-05	
	4	-428.0	0	309	0.58336E+03	0.6104E+01	0.8176E+00	0.2475E-01	0.1046E-01	0.1402E-02	0.1794E-04	0.2403E-05
	4	-428.0	1	305	0.65214E+03	0.7921E+01	0.1077E+01	0.1215E-01	0.1652E-02	0.1863E-04	0.2933E-05	
	4	-428.0	2	306	0.51201E+03	0.4912E+01	0.5462E+00	0.9593E-02	0.1067E-02	0.1874E-04	0.2084E-05	
	4	-61.0	0	304	0.10960E+04	0.2307E+02	0.3118E+01	0.2105E-01	0.2845E-02	0.1920E-04	0.2596E-05	
	4	61.0	0	303	0.11869E+04	0.2718E+02	0.3487E+01	0.2290E-01	0.2938E-02	0.1930E-04	0.2475E-05	
	4	428.0	0	300	0.12212E+04	0.3113E+02	0.4164E+01	0.2549E-01	0.3410E-02	0.2087E-04	0.2792E-05	
	4	428.0	1	301	0.12385E+04	0.3196E+02	0.4293E+01	0.2580E-01	0.3466E-02	0.2083E-04	0.2798E-05	
	4	428.0	2	302	0.13844E+04	0.3782E+02	0.5022E+01	0.2732E-01	0.3627E-02	0.1973E-04	0.2620E-05	
	4	650.0	0	299	0.68953E+03	0.1005E+02	0.1299E+01	0.1457E-01	0.1884E-02	0.2113E-04	0.2732E-05	
A51	3	-428.0	0	310	0.72805E+03	0.9335E+01	0.1259E+01	0.1262E-01	0.1729E-02	0.1761E-04	0.2374E-05	
	3	-61.0	0	311	0.11002E+04	0.2378E+02	0.3123E+01	0.2162E-01	0.2838E-02	0.1965E-04	0.2500E-05	
	3	61.0	0	312	0.11859E+04	0.2718E+02	0.3717E+01	0.2292E-01	0.3134E-02	0.1933E-04	0.2643E-05	
	3	428.0	0	313	0.11435E+04	0.2643E+02	0.3618E+01	0.2311E-01	0.3164E-02	0.2021E-04	0.2767E-05	

ASSEMBLY PLANE	Z(MM)	X	RUN NO.	CS137(CPS)	CS134(CPS)	EU154(CPS)	PR144(CPS)	134/137	154/137	134/137/137	154/137/137	
A 9	4	-428.0	0	314	0.84102E+03	0.1251E+02	0.1481E+01	0.1487E-01	0.1761E-02	0.1768E-04	0.2094E-05	
	4	-61.0	0	315	0.11212E+04	0.2346E+02	0.3221E+01	0.2093E-01	0.2873E-02	0.1866E-04	0.2562E-05	
	4	61.0	0	316	0.11471E+04	0.2626E+02	0.3523E+01	0.2290E-01	0.3071E-02	0.1996E-04	0.2677E-05	
	4	428.0	0	317	0.10603E+04	0.2398E+02	0.3522E+01	0.2262E-01	0.3321E-02	0.2133E-04	0.3132E-05	
A11	4	-428.0	0	318	0.51023E+03	0.4159E+01	0.6170E+00	0.6152E-02	0.1209E-02	0.1598E-04	0.2370E-05	
	4	-61.0	0	319	0.81618E+03	0.1173E+02	0.1501E+01	0.1437E-01	0.1839E-02	0.1761E-04	0.2253E-05	
	4	61.0	0	320	0.90958E+03	0.1536E+02	0.2401E+01	0.1689E-01	0.2640E-02	0.1857E-04	0.2902E-05	
	4	428.0	0	321	0.81762E+03	0.1237E+02	0.1805E+01	0.1513E-01	0.2208E-02	0.1850E-04	0.2700E-05	
A29	4	-428.0	0	322	0.92003E+03	0.1058E+02	0.1563E+01	0.1150E-01	0.1699E-02	0.1250E-04	0.1846E-05	
	4	-61.0	0	323	0.11242E+04	0.1667E+02	0.2383E+01	0.1482E-01	0.2119E-02	0.1319E-04	0.1885E-05	
	4	61.0	0	324	0.11512E+04	0.1961E+02	0.2762E+01	0.1703E-01	0.2400E-02	0.1479E-04	0.2084E-05	
	4	428.0	0	325	0.10404E+04	0.1655E+02	0.2260E+01	0.1590E-01	0.2172E-02	0.1529E-04	0.2088E-05	
A37	4	-428.0	0	330	0.97796E+03	0.1227E+02	0.1737E+01	0.4653E-01	0.1254E-01	0.1776E-02	0.1282E-04	0.1816E-05
	4	-61.0	0	328	0.11495E+04	0.1917E+02	0.2692E+01	0.1648E-01	0.2342E-02	0.1451E-04	0.2037E-05	
	4	61.0	0	327	0.11599E+04	0.1848E+02	0.2625E+01	0.1597E-01	0.2269E-02	0.1380E-04	0.1961E-05	
	4	428.0	0	326	0.98098E+03	0.1407E+02	0.1885E+01	0.1434E-01	0.1921E-02	0.1462E-04	0.1958E-05	
A34	4	-428.0	0	331	0.81685E+03	0.1189E+C2	0.1581E+01	0.1456E-01	0.1935E-02	0.1782E-04	0.2369E-05	
	4	-61.0	0	332	0.90992E+03	0.1523E+02	0.1932E+01	0.1673E-01	0.2124E-02	0.1839E-04	0.2334E-05	
	4	61.0	0	333	0.97188E+03	0.1580E+02	0.2291E+01	0.1626E-01	0.2357E-02	0.1673E-04	0.2425E-05	
	4	428.0	0	334	0.77699E+03	0.1188E+02	0.1565E+01	0.1542E-01	0.2032E-02	0.2002E-04	0.2637E-05	
A65	3	-428.0	0	335	0.75615E+03	0.1062E+02	0.1299E+01	0.1405E-01	0.1717E-02	0.1857E-04	0.2271E-05	
	3	-61.0	0	336	0.11582E+04	0.2544E+02	0.3568E+01	0.2197E-01	0.3080E-02	0.1897E-04	0.2660E-05	
	3	61.0	0	337	0.11865E+04	0.2764E+02	0.3669E+01	0.2329E-01	0.3092E-02	0.1963E-04	0.2606E-05	
	3	428.0	0	338	0.12079E+04	0.2882E+02	0.4121E+01	0.2386E-01	0.3412E-02	0.1975E-04	0.2825E-05	
A 2	1	-672.0	0	339	0.19154E+03	0.8914E+00	0.1301E+00	0.4654E-02	0.6790E-03	0.2430E-04	0.3545E-05	
	1	-428.0	0	340	0.51597E+03	0.5732E+01	0.8161E+00	0.1111E-01	0.1582E-02	0.2153E-04	0.3065E-05	
	1	-428.0	1	341	0.67918E+03	0.8833E+01	0.1212E+01	0.1300E-01	0.1784E-02	0.1915E-04	0.2627E-05	
	1	-428.0	2	342	0.34916E+03	0.3531E+01	0.4947E+00	0.1011E-01	0.1417E-02	0.2896E-04	0.4058E-05	
	1	-61.0	0	343	0.77351E+03	0.1527E+02	0.2213E+01	0.1974E-01	0.2861E-02	0.2552E-04	0.3699E-05	
	1	61.0	0	344	0.82786E+03	0.1804E+02	0.2632E+01	0.2179E-01	0.3180E-02	0.2632E-04	0.3841E-05	
	1	428.0	0	345	0.12628E+04	0.3219E+02	0.4132E+01	0.2549E-01	0.3272E-02	0.2019E-04	0.2591E-05	
	1	428.0	1	346	0.13324E+04	0.3379E+02	0.4286E+01	0.2536E-01	0.3217E-02	0.1903E-04	0.2414E-05	
	1	428.0	2	347	0.14164E+04	0.3675E+02	0.4678E+01	0.2595E-01	0.3303E-02	0.1832E-04	0.2332E-05	
	1	650.0	0	348	0.81660E+03	0.1206E+02	0.1382E+01	0.1477E-01	0.1693E-02	0.1809E-04	0.2073E-05	
	2	-672.0	0	355	0.19694E+03	0.9883E+00	0.1063E+00	0.5018E-02	0.5396E-03	0.2548E-04	0.2740E-05	
	2	-428.0	0	359	0.49711E+03	0.5621E+01	0.8533E+00	0.2624E-01	0.1131E-01	0.1717E-02	0.2275E-04	0.3453E-05
	2	-428.0	1	357	0.33528E+03	0.1261E+02	0.1760E+01	0.1510E-01	0.2107E-02	0.1808E-04	0.2522E-05	
	2	-428.0	2	356	0.39730E+03	0.3165E+01	0.5204E+00	0.7968E-02	0.1310E-02	0.2005E-04	0.3297E-05	
	2	-61.0	0	354	0.10287E+04	0.2061E+02	0.2935E+01	0.2004E-01	0.2853E-02	0.1948E-04	0.2773E-05	
	2	61.0	0	353	0.10609E+04	0.2309E+02	0.3263E+01	0.2196E-01	0.3018E-02	0.1976E-04	0.2792E-05	
	2	428.0	0	350	0.12371E+04	0.2949E+02	0.3895E+01	0.2384E-01	0.3148E-02	0.1927E-04	0.2545E-05	
	2	428.0	1	352	0.12524E+04	0.3127E+02	0.3902E+01	0.2497E-01	0.3115E-02	0.1994E-04	0.2488E-05	
	2	428.0	2	351	0.14416E+04	0.3616E+02	0.4685E+01	0.2500E-01	0.3250E-02	0.1740E-04	0.2294E-05	
	2	650.0	0	349	0.76948E+03	0.1104E+02	0.1420E+01	0.1434E-01	0.1845E-02	0.1864E-04	0.2398E-05	
	3	-672.0	0	360	0.36480E+03	0.2398E+01	0.2953E+00	0.6573E-02	0.8095E-03	0.1802E-04	0.2219E-05	
	3	-428.0	0	361	0.86043E+03	0.1288E+02	0.1699E+01	0.1496E-01	0.1975E-02	0.1739E-04	0.2295E-05	
	3	-428.0	1	363	0.87275E+03	0.1387E+02	0.1743E+01	0.1589E-01	0.1997E-02	0.1821E-04	0.2288E-05	
	3	-428.0	2	362	0.79854E+03	0.1076E+02	0.1576E+01	0.1348E-01	0.1973E-02	0.1688E-04	0.2471E-05	
	3	-61.0	0	364	0.11458E+04	0.2428E+02	0.3561E+01	0.2119E-01	0.3108E-02	0.1850E-04	0.2713E-05	
	3	61.0	0	365	0.11653E+04	0.2576E+02	0.3668E+01	0.2210E-01	0.3148E-02	0.1897E-04	0.2701E-05	
	3	428.0	0	366	0.10974E+04	0.2952E+02	0.3422E+01	0.2326E-01	0.3118E-02	0.2120E-04	0.2842E-05	
	3	428.0	1	368	0.11103E+04	0.2707E+02	0.3320E+01	0.2438E-01	0.2990E-02	0.2196E-04	0.2693E-05	
	3	428.0	2	367	0.13339E+04	0.3357E+02	0.4298E+01	0.2516E-01	0.3222E-02	0.1886E-04	0.2415E-05	
	3	650.0	0	369	0.63342E+03	0.8629E+01	0.1007E+01	0.1362E-01	0.1589E-02	0.2151E-04	0.2509E-05	

ASSEMBLY PLANE	Z(MM)	X	RUN NO.	CS137(CPS)	CS134(CPS)	EU154(CPS)	PR144(CPS)	134/137	154/137	134/137/137	154/137/137	
	4	-672.0	0	370	0.29615E+03	0.1742E+01	0.2239E+00	0.5883E-02	0.7560E-03	0.1987E-04	0.2553E-05	
	4	-428.0	0	371	0.72089E+03	0.9701E+01	0.1388E+01	0.1346E-01	0.1925E-02	0.1867E-04	0.2670E-05	
	4	-428.0	1	372	0.87759E+03	0.1399E+02	0.1982E+01	0.1594E-01	0.2259E-02	0.1816E-04	0.2574E-05	
	4	-428.0	2	373	0.56010E+03	0.6467E+01	0.9003E+00	0.1155E-01	0.1607E-02	0.2061E-04	0.2870E-05	
	4	-61.0	0	374	0.10764E+04	0.2199E+02	0.3312E+01	0.2043E-01	0.3077E-02	0.1898E-04	0.2858E-05	
	4	61.0	0	375	0.11253E+04	0.2528E+02	0.3631E+01	0.2247E-01	0.3227E-02	0.1997E-04	0.2867E-05	
	4	428.0	0	376	0.10925E+04	0.2580E+02	0.3564E+01	0.2362E-01	0.3262E-02	0.2162E-04	0.2986E-05	
	4	428.0	1	377	0.11211E+04	0.2657E+02	0.3545E+01	0.2370E-01	0.3162E-02	0.2114E-04	0.2821E-05	
	4	428.0	2	378	0.13250E+04	0.3550E+02	0.4713E+01	0.2680E-01	0.3557E-02	0.2022E-04	0.2685E-05	
	4	650.0	0	379	0.64264E+03	0.9112E+01	0.1117E+01	0.1418E-01	0.1738E-02	0.2206E-04	0.2704E-05	
A10	3	-428.0	0	384	0.84566E+03	0.1214E+02	0.1565E+01	0.3991E-01	0.1435E-01	0.1850E-02	0.1697E-04	0.2188E-05
	3	-61.0	0	382	0.12275E+04	0.2829E+02	0.3634E+01	0.2305E-01	0.2961E-02	0.1877E-04	0.2412E-05	
	3	61.0	0	381	0.12547E+04	0.3036E+02	0.4094E+01	0.2420E-01	0.3263E-02	0.1929E-04	0.2600E-05	
	3	428.0	0	380	0.11871E+04	0.2747E+02	0.3720E+01	0.2314E-01	0.3133E-02	0.1949E-04	0.2639E-05	
A60	4	-428.0	0	385	0.72918E+03	0.9792E+01	0.1325E+01	0.1343E-01	0.1817E-02	0.1842E-04	0.2492E-05	
	4	-61.0	0	386	0.11414E+04	0.2552E+02	0.3295E+01	0.2235E-01	0.2887E-02	0.1958E-04	0.2529E-05	
	4	61.0	0	387	0.11526E+04	0.2691E+02	0.3679E+01	0.2340E-01	0.3192E-02	0.2030E-04	0.2769E-05	
	4	428.0	0	388	0.11081E+04	0.2645E+02	0.3367E+01	0.2387E-01	0.3038E-02	0.2154E-04	0.2742E-05	
A68	3	-428.0	0	389	0.78899E+03	0.9162E+01	0.1327E+01	0.1161E-01	0.1682E-02	0.1472E-04	0.2132E-05	
	3	-61.0	0	390	0.95817E+03	0.1520E+02	0.1987E+01	0.1586E-01	0.2074E-02	0.1656E-04	0.2164E-05	
	3	61.0	0	391	0.96216E+03	0.1593E+02	0.2010E+01	0.1656E-01	0.2089E-02	0.1721E-04	0.2171E-05	
	3	428.0	0	392	0.83336E+03	0.1257E+02	0.1646E+01	0.1509E-01	0.1976E-02	0.1811E-04	0.2371E-05	
A5	3	-428.0	0	393	0.80958E+03	0.1143E+02	0.1686E+01	0.1412E-01	0.2083E-02	0.1744E-04	0.2573E-05	
	3	-61.0	0	394	0.11205E+04	0.2265E+02	0.3331E+01	0.2039E-01	0.2973E-02	0.1820E-04	0.2653E-05	
	3	61.0	0	395	0.11768E+04	0.2515E+02	0.3559E+01	0.2137E-01	0.3025E-02	0.1816E-04	0.2570E-05	
	3	428.0	0	396	0.10187E+04	0.2002E+C2	0.2808E+01	0.1966E-01	0.2757E-02	0.1929E-04	0.2706E-05	
A36	3	-428.0	0	397	0.95092E+03	0.1646E+02	0.2183E+01	0.1731E-01	0.2296E-02	0.1821E-04	0.2414E-05	
	3	-61.0	0	398	0.11311E+04	0.2290E+02	0.3328E+01	0.2025E-01	0.2942E-02	0.1790E-04	0.2601E-05	
	3	61.0	0	399	0.11467E+04	0.2323E+02	0.3350E+01	0.2025E-01	0.2922E-02	0.1766E-04	0.2548E-05	
	3	428.0	0	400	0.98933E+03	0.1847E+02	0.2559E+01	0.1867E-01	0.2586E-02	0.1887E-04	0.2614E-05	
A52	3	-428.0	0	405	0.66710E+03	0.7035E+01	0.9305E+00	0.2983E-01	0.1055E-01	0.1395E-02	0.1581E-04	0.2091E-05
	3	-61.0	0	402	0.11077E+04	0.2216E+02	0.3250E+01	0.2001E-01	0.2934E-02	0.1806E-04	0.2649E-05	
	3	61.0	0	403	0.11798E+04	0.2769E+02	0.3723E+01	0.2347E-01	0.3156E-02	0.1989E-04	0.2675E-05	
	3	428.0	0	404	0.11917E+04	0.2935E+02	0.3960E+01	0.2463E-01	0.3323E-02	0.2067E-04	0.2788E-05	
A32	4	-428.0	0	406	0.64001E+03	0.5447E+01	0.8024E+00	0.8511E-02	0.1254E-02	0.1330E-04	0.1959E-05	
	4	-61.0	0	407	0.98877E+03	0.1592E+02	0.2226E+01	0.1610E-01	0.2251E-02	0.1628E-04	0.2277E-05	
	4	61.0	0	408	0.11078E+04	0.2040E+02	0.2817E+01	0.1842E-01	0.2543E-02	0.1662E-04	0.2295E-05	
	4	428.0	0	409	0.10029E+04	0.1672E+02	0.2500E+01	0.1667E-01	0.2493E-02	0.1663E-04	0.2486E-05	
A33	2	-428.0	0	410	0.98444E+03	0.1341E+02	0.1744E+01	0.1362E-01	0.1772E-02	0.1383E-04	0.1800E-05	
	2	-61.0	0	411	0.12653E+04	0.2525E+02	0.3557E+01	0.1995E-01	0.2811E-02	0.1577E-04	0.2221E-05	
	2	61.0	0	412	0.13431E+04	0.2664E+02	0.3635E+01	0.2132E-01	0.2706E-02	0.1588E-04	0.2015E-05	
	2	428.0	0	413	0.11470E+04	0.2313E+02	0.2981E+01	0.2017E-01	0.2599E-02	0.1758E-04	0.2266E-05	
A15	4	-428.0	0	414	0.10168E+04	0.1701E+02	0.2612E+01	0.1673E-01	0.2569E-02	0.1646E-04	0.2527E-05	
	4	-61.0	0	415	0.11827E+04	0.2409E+02	0.3309E+01	0.2037E-01	0.2798E-02	0.1722E-04	0.2366E-05	
	4	61.0	0	416	0.11472E+04	0.2361E+C2	0.3252E+01	0.2058E-01	0.2835E-02	0.1794E-04	0.2471E-05	
	4	428.0	0	417	0.92536E+03	0.1675E+02	0.2275E+01	0.1810E-01	0.2459E-02	0.1956E-04	0.2657E-05	
A46	3	-428.0	0	418	0.68149E+03	0.7776E+01	0.9827E+00	0.1141E-01	0.1442E-02	0.1674E-04	0.2116E-05	
	3	-61.0	0	419	0.11094E+04	0.2242E+02	0.3075E+01	0.2021E-01	0.2772E-02	0.1822E-04	0.2499E-05	
	3	61.0	0	420	0.12741E+04	0.3044E+02	0.4192E+01	0.2389E-01	0.3290E-02	0.1875E-04	0.2582E-05	
	3	428.0	0	421	0.11746E+04	0.2792E+02	0.3633E+01	0.2377E-01	0.3093E-02	0.2023E-04	0.2633E-05	
A25	3	-428.0	0	426	0.91029E+03	0.1284E+02	0.1898E+01	0.4234E-01	0.1411E-01	0.2085E-02	0.1550E-04	0.2291E-05
	3	-61.0	0	424	0.95564E+03	0.1664E+02	0.2481E+01	0.1742E-01	0.2596E-02	0.1823E-04	0.2716E-05	
	3	61.0	0	423	0.93791E+03	0.1586E+02	0.2273E+01	0.1691E-01	0.2423E-02	0.1803E-04	0.2584E-05	
	3	428.0	0	422	0.75066E+03	0.1110E+02	0.1444E+01	0.1479E-01	0.1924E-02	0.1970E-04	0.2563E-05	
A19	2	-428.0	0	427	0.11152E+04	0.1804E+02	0.2475E+01	0.1617E-01	0.2220E-02	0.1450E-04	0.1990E-05	
	2	-61.0	0	429	0.12138E+04	0.2300E+02	0.3274E+01	0.1895E-01	0.2690E-02	0.1561E-04	0.2222E-05	
	2	61.0	0	430	0.12129E+04	0.2334E+02	0.3099E+01	0.1925E-01	0.2555E-02	0.1587E-04	0.2107E-05	
	2	428.0	0	431	0.99365E+03	0.1716E+02	0.2125E+01	0.1727E-01	0.2138E-02	0.1738E-04	0.2152E-05	

ASSEMBLY PLANE	Z(MM)	X	RUN NO.	CS137(CPS)	CS134(CPS)	EU154(CPS)	PR144(CPS)	134/137	134/137	134/137/137	134/137/137	
A49	1	-672.0	0	432	0.41191E+03	0.2533E+01	0.3056E+00	0.6150E-02	0.7418E-03	0.1493E-04	0.1801E-05	
	1	-428.0	0	433	0.10818E+04	0.1789E+02	0.2479E+01	0.1654E-01	0.2292E-02	0.1529E-04	0.2119E-05	
	1	-428.0	1	434	0.12096E+04	0.1789E+02	0.2417E+01	0.1479E-01	0.1998E-02	0.1223E-04	0.1652E-05	
	1	-428.0	2	435	0.12970E+04	0.2444E+02	0.3594E+01	0.1884E-01	0.2771E-02	0.1453E-04	0.2136E-05	
	1	-61.0	0	436	0.12335E+04	0.2489E+02	0.3471E+01	0.2018E-01	0.2814E-02	0.1636E-04	0.2201E-05	
	1	61.0	0	437	0.12353E+04	0.2548E+02	0.3329E+01	0.2063E-01	0.2695E-02	0.1670E-04	0.2182E-05	
	1	428.0	0	438	0.10203E+04	0.1802E+02	0.2529E+01	0.1766E-01	0.2479E-02	0.1731E-04	0.2429E-05	
	1	428.0	1	439	0.11847E+04	0.1986E+02	0.2520E+01	0.1676E-01	0.2127E-02	0.1415E-04	0.1795E-05	
	1	428.0	2	440	0.12018E+04	0.2549E+02	0.3249E+01	0.2121E-01	0.2704E-02	0.1765E-04	0.2250E-05	
	1	650.0	0	441	0.59080E+03	0.5623E+01	0.7274E+00	0.9517E-02	0.1231E-02	0.1611E-04	0.2084E-05	
	2	-672.0	0	451	0.51010E+03	0.3822E+01	0.5427E+00	0.7492E-02	0.1064E-02	0.1469E-04	0.2086E-05	
	2	-428.0	0	448	0.11318E+04	0.1917E+02	0.2521E+01	0.1693E-01	0.2228E-02	0.1496E-04	0.1968E-05	
	2	-428.0	1	450	0.97960E+03	0.1588E+02	0.2235E+01	0.1621E-01	0.2281E-02	0.1654E-04	0.2329E-05	
	2	-428.0	2	449	0.13339E+04	0.2633E+02	0.3423E+01	0.1974E-01	0.2566E-02	0.1480E-04	0.1924E-05	
	2	-61.0	0	447	0.12649E+04	0.2553E+02	0.3397E+01	0.2019E-01	0.2686E-02	0.1596E-04	0.2123E-05	
	2	61.0	0	446	0.12598E+04	0.2681E+02	0.3379E+01	0.2128E-01	0.2682E-02	0.1689E-04	0.2129E-05	
	2	428.0	0	443	0.10402E+04	0.1885E+02	0.2552E+01	0.1812E-01	0.2454E-02	0.1742E-04	0.2359E-05	
	2	428.0	1	445	0.91518E+03	0.1616E+02	0.1883E+01	0.1765E-01	0.2057E-02	0.1929E-04	0.2248E-05	
	2	428.0	2	444	0.12164E+04	0.2493E+02	0.3169E+01	0.2049E-01	0.2605E-02	0.1685E-04	0.2142E-05	
	2	650.0	0	442	0.60763E+03	0.6300E+01	0.7360E+00	0.1037E-01	0.1211E-02	0.1706E-04	0.1994E-05	
	3	-672.0	0	460	0.34970E+03	0.2282E+01	0.3138E+00	0.6526E-02	0.8973E-03	0.1866E-04	0.2566E-05	
	3	-428.0	0	462	0.81099E+03	0.1122E+02	0.1662E+01	0.3872E-01	0.1383E-01	0.2049E-02	0.1705E-04	0.2527E-05
	3	-428.0	1	459	0.91820E+03	0.1071E+02	0.1534E+01	0.1166E-01	0.1670E-02	0.1270E-04	0.1819E-05	
	3	-428.0	2	458	0.10627E+04	0.1813E+02	0.2769E+01	0.1706E-01	0.2606E-02	0.1605E-04	0.2452E-05	
	3	-61.0	0	457	0.93142E+03	0.1500E+02	0.2241E+01	0.1610E-01	0.2406E-02	0.1729E-04	0.2583E-05	
	3	61.0	0	456	0.94366E+03	0.1641E+02	0.2209E+01	0.1739E-01	0.2341E-02	0.1842E-04	0.2481E-05	
	3	428.0	0	453	0.76637E+03	0.1099E+02	0.1425E+01	0.1434E-01	0.1859E-02	0.1471E-04	0.2426E-05	
	3	428.0	1	455	0.87679E+03	0.1238E+02	0.1731E+01	0.1412E-01	0.1974E-02	0.1611E-04	0.2252E-05	
	3	428.0	2	454	0.10089E+04	0.1812E+02	0.2585E+01	0.1796E-01	0.2564E-02	0.1781E-04	0.2542E-05	
	3	650.0	0	452	0.40111E+03	0.3290E+01	0.4715E+00	0.8203E-02	0.1175E-02	0.2045E-04	0.2930E-05	
	4	-672.0	0	463	0.45136E+03	0.2831E+01	0.3960E+00	0.6273E-02	0.8773E-03	0.1390E-04	0.1944E-05	
	4	-428.0	0	464	0.98753E+03	0.1273E+02	0.2066E+01	0.1289E-01	0.2092E-02	0.1305E-04	0.2118E-05	
	4	-428.0	1	465	0.91523E+03	0.1103E+02	0.1609E+01	0.1205E-01	0.1758E-02	0.1316E-04	0.1921E-05	
	4	-428.0	2	466	0.12673E+04	0.1982E+02	0.2858E+01	0.1564E-01	0.2256E-02	0.1234E-04	0.1780E-05	
	4	-61.0	0	467	0.11427E+04	0.1871E+02	0.2410E+01	0.1638E-01	0.2109E-02	0.1433E-04	0.1845E-05	
	4	61.0	0	468	0.11007E+04	0.1800E+02	0.2473E+01	0.1643E-01	0.2246E-02	0.1492E-04	0.2041E-05	
	4	428.0	0	469	0.95383E+03	0.1394E+02	0.1834E+01	0.1462E-01	0.1923E-02	0.1533E-04	0.2016E-05	
	4	428.0	1	470	0.92791E+03	0.1243E+02	0.1618E+01	0.1346E-01	0.1744E-02	0.1444E-04	0.1880E-05	
	4	428.0	2	471	0.11869E+04	0.2082E+02	0.2871E+01	0.1754E-01	0.2419E-02	0.1478E-04	0.2038E-05	
	4	650.0	0	472	0.49416E+03	0.3372E+01	0.5149E+00	0.6823E-02	0.1042E-02	0.1381E-04	0.2109E-05	
A70	4	-428.0	0	473	0.87762E+03	0.1356E+02	0.1816E+01	0.1545E-01	0.2069E-02	0.1761E-04	0.2357E-05	
	4	-61.0	0	474	0.98734E+03	0.1645E+02	0.2477E+01	0.1666E-01	0.2509E-02	0.1687E-04	0.2541E-05	
	4	61.0	0	475	0.98655E+03	0.1775E+02	0.2404E+01	0.1800E-01	0.2437E-02	0.1824E-04	0.2470E-05	
	4	428.0	0	476	0.79834E+03	0.1259E+02	0.1593E+01	0.1578E-01	0.1995E-02	0.1976E-04	0.2499E-05	
A5b	4	-428.0	0	477	0.80174E+03	0.1101E+02	0.1357E+01	0.1374E-01	0.1692E-02	0.1713E-04	0.2111E-05	
	4	-61.0	0	478	0.10953E+04	0.2184E+02	0.2958E+01	0.1994E-01	0.2701E-02	0.1821E-04	0.2466E-05	
	4	61.0	0	479	0.11613E+04	0.2486E+02	0.3550E+01	0.2141E-01	0.3056E-02	0.1843E-04	0.2632E-05	
	4	428.0	0	480	0.11159E+04	0.2440E+02	0.3081E+01	0.2186E-01	0.2761E-02	0.1959E-04	0.2474E-05	
A53	3	-428.0	0	485	0.69594E+03	0.7900E+01	0.1081E+01	0.3035E-01	0.1135E-01	0.1553E-02	0.1631E-04	0.2232E-05
	3	-61.0	0	483	0.11111E+04	0.2426E+02	0.3156E+01	0.2184E-01	0.2840E-02	0.1965E-04	0.2536E-05	
	3	61.0	0	482	0.12040E+04	0.2797E+02	0.3912E+01	0.2323E-01	0.3249E-02	0.1930E-04	0.2699E-05	
	3	428.0	0	481	0.117795E+04	0.2691E+02	0.3659E+01	0.2222E-01	0.3102E-02	0.1934E-04	0.2630E-05	
A 7	3	-428.0	0	489	0.83740E+03	0.1352E+02	0.1774E+01	0.1614E-01	0.2119E-02	0.1927E-04	0.2531E-05	
	3	-61.0	0	488	0.11253E+04	0.2482E+02	0.3365E+01	0.2206E-01	0.2990E-02	0.1960E-04	0.2657E-05	
	3	61.0	0	487	0.11492E+04	0.2676E+02	0.3767E+01	0.2328E-01	0.3278E-02	0.2026E-04	0.2852E-05	
	3	428.0	0	486	0.10362E+04	0.2224E+02	0.3013E+01	0.2147E-01	0.2907E-02	0.2072E-04	0.2806E-05	

ASSEMBLY	PLANE	Z(MM)	X	RUN NO.	CS137(CPS)	CS134(CPS)	EU154(CPS)	PR144(CPS)	134/137	154/137	134/137/137	154/137/137
A69	1	-672.0	0	499	0.25403E+03	0.1347E+01	0.1558E+00		0.5302E+02	0.6133E-03	0.2087E-04	0.2414E-05
	1	-428.0	0	496	0.61435E+03	0.7646E+01	0.1129E+01		0.1245E+01	0.1838E-02	0.2026E-04	0.2992E-05
	1	-428.0	1	497	0.93290E+03	0.1437E+02	0.1912E+01		0.1540E+01	0.2049E-02	0.1651E-04	0.2196E-05
	1	-428.0	2	498	0.45067E+03	0.5148E+01	0.7747E+00		0.1142E+01	0.1719E-02	0.2534E-04	0.3814E-05
	1	-61.0	0	495	0.10939E+04	0.2140E+02	0.3092E+01		0.1957E+01	0.2826E-02	0.1789E-04	0.2584E-05
	1	61.0	0	494	0.11518E+04	0.2443E+02	0.3336E+01		0.2121E+01	0.2896E-02	0.1841E-04	0.2514E-05
	1	428.0	0	491	0.12583E+04	0.2927E+02	0.3845E+01		0.2326E+01	0.3055E-02	0.1849E-04	0.2428E-05
	1	428.0	1	492	0.13691E+04	0.3316E+02	0.4304E+01		0.2422E+01	0.3144E-02	0.1769E-04	0.2296E-05
	1	428.0	2	493	0.14222E+04	0.3628E+02	0.4717E+01		0.2551E+01	0.3317E-02	0.1794E-04	0.2332E-05
	1	650.0	0	490	0.79026E+03	0.1080E+02	0.1444E+01		0.1367E+01	0.1827E-02	0.1729E-04	0.2311E-05
	2	-672.0	0	500	0.21983E+03	0.9472E+00	0.2139E+00		0.4309E+02	0.9730E-03	0.1960E-04	0.4426E-05
	2	-428.0	0	501	0.49390E+03	0.6229E+01	0.9159E+00		0.1261E+01	0.1854E-02	0.2554E-04	0.3755E-05
	2	-428.0	1	503	0.85598E+03	0.1387E+02	0.1965E+01		0.1620E+01	0.2296E-02	0.1892E-04	0.2682E-05
	2	-428.0	2	502	0.39996E+03	0.4044E+01	0.6492E+00		0.1011E+01	0.1623E-02	0.2528E-04	0.4038E-05
	2	-61.0	0	504	0.10359E+04	0.1936E+02	0.2910E+01		0.1869E+01	0.2809E-02	0.1804E-04	0.2712E-05
	2	61.0	0	505	0.10876E+04	0.2203E+02	0.3271E+01		0.2026E+01	0.3008E-02	0.1862E-04	0.2766E-05
	2	428.0	0	506	0.12415E+04	0.3029E+02	0.3667E+01		0.2440E+01	0.2954E-02	0.1965E-04	0.2379E-05
	2	428.0	1	508	0.12706E+04	0.3138E+02	0.4291E+01		0.2470E+01	0.3377E-02	0.1944E-04	0.2657E-05
	2	428.0	2	507	0.14092E+04	0.3452E+02	0.4800E+01		0.2450E+01	0.3406E-02	0.1738E-04	0.2417E-05
	2	650.0	0	509	0.77103E+03	0.1086E+02	0.1302E+01		0.1409E+01	0.1689E-02	0.1827E-04	0.2190E-05
	3	-672.0	0	518	0.38064E+03	0.2578E+01	0.3050E+00		0.6773E+02	0.8012E-03	0.1779E-04	0.2105E-05
	3	-428.0	0	520	0.86570E+03	0.1376E+02	0.1836E+01	0.4056E+01	0.1589E+01	0.2121E-02	0.1835E-04	0.2449E-05
	3	-428.0	1	517	0.90325E+03	0.1592E+02	0.2116E+01		0.1763E+01	0.2343E-02	0.1951E-04	0.2594E-05
	3	-428.0	2	516	0.83180E+03	0.1301E+02	0.1649E+01		0.1564E+01	0.1982E-02	0.1881E-04	0.2383E-05
	3	-61.0	0	515	0.11040E+04	0.2381E+02	0.3278E+01		0.2157E+01	0.2969E-02	0.1954E-04	0.2689E-05
	3	61.0	0	514	0.11592E+04	0.2618E+02	0.3514E+01		0.2258E+01	0.3032E-02	0.1948E-04	0.2615E-05
	3	428.0	0	511	0.10899E+04	0.2423E+02	0.3274E+01		0.2223E+01	0.3004E-02	0.2039E-04	0.2756E-05
	3	428.0	1	512	0.10307E+04	0.2352E+02	0.3396E+01		0.2282E+01	0.3295E-02	0.2214E-04	0.3197E-05
	3	428.0	2	513	0.13299E+04	0.3237E+02	0.4529E+01		0.2434E+01	0.3406E-02	0.1830E-04	0.2561E-05
	3	650.0	0	510	0.64960E+03	0.8363E+01	0.1148E+01		0.1287E+01	0.1767E-02	0.1982E-04	0.2720E-05
	4	-672.0	0	521	0.35644E+03	0.2056E+01	0.3121E+00		0.5767E+02	0.8756E-03	0.1618E-04	0.2457E-05
	4	-428.0	0	522	0.80541E+03	0.1301E+02	0.1764E+01		0.1615E+01	0.2190E-02	0.2006E-04	0.2720E-05
	4	-428.0	1	523	0.91938E+03	0.1605E+02	0.2109E+01		0.1746E+01	0.2294E-02	0.1899E-04	0.2495E-05
	4	-428.0	2	524	0.75207E+03	0.1066E+02	0.1390E+01		0.1417E+01	0.1849E-02	0.1884E-04	0.2458E-05
	4	-61.0	0	525	0.10705E+04	0.2266E+02	0.3351E+01		0.2116E+01	0.3130E-02	0.1977E-04	0.2924E-05
	4	61.0	0	526	0.11112E+04	0.2518E+02	0.3586E+01		0.2266E+01	0.3227E-02	0.2039E-04	0.2904E-05
	4	428.0	0	527	0.10399E+04	0.2326E+02	0.3340E+01		0.2237E+01	0.3212E-02	0.2151E-04	0.3089E-05
	4	428.0	1	528	0.10413E+04	0.2302E+02	0.3162E+01		0.2211E+01	0.3036E-02	0.2123E-04	0.2916E-05
	4	428.0	2	529	0.12698E+04	0.3082E+02	0.4069E+01		0.2427E+01	0.3205E-02	0.1912E-04	0.2524E-05
	4	650.0	0	530	0.61823E+03	0.7870E+01	0.1132E+01		0.1273E+01	0.1832E-02	0.2059E-04	0.2963E-05
A64	3	-428.0	0	531	0.65680E+03	0.1224E+02	0.1732E+01		0.1428E+01	0.2022E-02	0.1667E-04	0.2360E-05
	3	-61.0	0	532	0.10798E+04	0.2160E+02	0.2935E+01		0.2001E+01	0.2718E-02	0.1853E-04	0.2517E-05
	3	61.0	0	533	0.11358E+04	0.2307E+02	0.3414E+01		0.2031E+01	0.3006E-02	0.1788E-04	0.2646E-05
	3	428.0	0	534	0.93927E+03	0.1784E+02	0.2339E+01		0.1899E+01	0.2491E-02	0.2022E-04	0.2652E-05
A6	3	-428.0	0	535	0.70105E+03	0.7777E+01	0.1011E+01		0.1109E+01	0.1442E-02	0.1582E-04	0.2057E-05
	3	-61.0	0	536	0.10630E+04	0.2010E+02	0.2650E+01		0.1891E+01	0.2493E-02	0.1779E-04	0.2345E-05
	3	61.0	0	537	0.11974E+04	0.2623E+02	0.3583E+01		0.2191E+01	0.2993E-02	0.1830E-04	0.2499E-05
	3	428.0	0	538	0.10165E+04	0.2123E+02	0.2627E+01		0.2089E+01	0.2584E-02	0.2055E-04	0.2542E-05
A28	4	-428.0	0	543	0.91751E+03	0.1369E+02	0.1947E+01	0.3956E+01	0.1492E+01	0.2122E-02	0.1626E-04	0.2313E-05
	4	-61.0	0	541	0.10555E+04	0.2108E+02	0.2988E+01		0.1997E+01	0.2831E-02	0.1892E-04	0.2682E-05
	4	61.0	0	540	0.10797E+04	0.2170E+02	0.2776E+01		0.2009E+01	0.2573E-02	0.1861E-04	0.2383E-05
	4	428.0	0	539	0.92223E+03	0.1687E+02	0.2316E+01		0.1830E+01	0.2511E-02	0.1984E-04	0.2723E-05

ASSEMBLY PLANE	Z(MM)	X	RUN NO.	CS137(CPS)	CS134(CPS)	EU154(CPS)	PR144(CPS)	134/137	154/137	134/137/137	154/137/137
A45	1 -672.0	0	544	0.47547E+03	0.3497E+01	0.4970E+00		0.7356E-02	0.1045E-02	0.1547E-04	0.2199E-05
	1 -428.0	0	545	0.10846E+04	0.1839E+02	0.2614E+01		0.1696E-01	0.2410E-02	0.1564E-04	0.2222E-05
	1 -428.0	1	546	0.11533E+04	0.2014E+02	0.2739E+01		0.1746E-01	0.2375E-02	0.1514E-04	0.2059E-05
	1 -428.0	2	547	0.11657E+04	0.1969E+02	0.2807E+01		0.169UE-01	0.2408E-02	0.1449E-04	0.2066E-05
	1 -61.0	0	548	0.12032E+04	0.2302E+02	0.3313E+01		0.1913E-01	0.2754E-02	0.1590E-04	0.2289E-05
	1 61.0	0	549	0.12105E+04	0.2431E+02	0.3267E+01		0.2008E-01	0.2699E-02	0.1659E-04	0.2230E-05
	1 428.0	0	550	0.99070E+03	0.1687E+02	0.2278E+01		0.1703E-01	0.2299E-02	0.1719E-04	0.2321E-05
	1 428.0	1	551	0.10404E+04	0.1982E+02	0.2632E+01		0.1904E-01	0.2528E-02	0.1829E-04	0.2429E-05
	1 428.0	2	552	0.10344E+04	0.1854E+02	0.2472E+01		0.1793E-01	0.2390E-02	0.1733E-04	0.2311E-05
	1 650.0	0	553	0.58661E+03	0.5761E+01	0.6726E+00		0.9821E-02	0.1147E-02	0.1674E-04	0.1955E-05
	2 -672.0	0	554	0.55628E+03	0.4245E+01	0.6487E+00		0.7631E-02	0.1166E-02	0.1372E-04	0.2096E-05
	2 -428.0	0	555	0.11197E+04	0.1820E+02	0.2557E+01		0.1626E-01	0.2283E-02	0.1452E-04	0.2039E-05
	2 -428.0	1	557	0.11478E+04	0.2057E+02	0.2908E+01		0.1792E-01	0.2534E-02	0.1561E-04	0.2208E-05
	2 -428.0	2	556	0.11913E+04	0.1971E+02	0.2941E+01		0.1654E-01	0.2469E-02	0.1389E-04	0.2073E-05
	2 -61.0	0	558	0.12203E+04	0.2370E+02	0.3316E+01		0.1942E-01	0.2718E-02	0.1592E-04	0.2227E-05
	2 61.0	0	559	0.12172E+04	0.2462E+02	0.3548E+01		0.2023E-01	0.2915E-02	0.1662E-04	0.2395E-05
	2 428.0	0	560	0.10337E+04	0.1751E+02	0.2345E+01		0.1694E-01	0.2269E-02	0.1639E-04	0.2195E-05
	2 428.0	1	562	0.10632E+04	0.2098E+02	0.2845E+01		0.1973E-01	0.2674E-02	0.1856E-04	0.2517E-05
	2 428.0	2	561	0.10875E+04	0.1899E+02	0.2463E+01		0.1747E-01	0.2264E-02	0.1606E-04	0.2082E-05
	2 650.0	0	563	0.59258E+03	0.5968E+01	0.7867E+00		0.1007E-01	0.1328E-02	0.1699E-04	0.2240E-05
	3 -672.0	0	570	0.42375E+03	0.2841E+01	0.3853E+00		0.6705E-02	0.9091E-03	0.1582E-04	0.2145E-05
	3 -428.0	0	574	0.99242E+03	0.1665E+02	0.2363E+01	0.4317E-01	0.1677E-01	0.2381E-02	0.1690E-04	0.2399E-05
	3 -428.0	1	572	0.10355E+04	0.1956E+02	0.2923E+01		0.1889E-01	0.2023E-02	0.1824E-04	0.2726E-05
	3 -428.0	2	571	0.12084E+04	0.2208E+02	0.3077E+01		0.1827E-01	0.2547E-02	0.1512E-04	0.2107E-05
	3 -61.0	0	569	0.11016E+04	0.2176E+02	0.3058E+01		0.1976E-01	0.2776E-02	0.1794E-04	0.2520E-05
	3 61.0	0	568	0.11103E+04	0.2237E+02	0.3320E+01		0.2014E-01	0.2991E-02	0.1814E-04	0.2693E-05
	3 428.0	0	565	0.93985E+03	0.1725E+02	0.2465E+01		0.1835E-01	0.2622E-02	0.1953E-04	0.2790E-05
	3 428.0	1	567	0.92140E+03	0.1861E+02	0.2404E+01		0.2019E-01	0.2609E-02	0.2192E-04	0.2831E-05
	3 428.0	2	566	0.11150E+04	0.2009E+02	0.2802E+01		0.1802E-01	0.2513E-02	0.1616E-04	0.2254E-05
	3 650.0	0	564	0.51698E+03	0.5081E+01	0.7353E+00		0.9829E-02	0.1422E-02	0.1901E-04	0.2751E-05
	4 -672.0	0	584	0.42941E+03	0.3263E+01	0.4722E+00		0.7598E-02	0.1100E-02	0.1770E-04	0.2561E-05
	4 -428.0	0	581	0.96487E+03	0.1616E+02	0.2347E+01		0.1675E-01	0.2432E-02	0.1736E-04	0.2521E-05
	4 -428.0	1	582	0.10433E+04	0.1932E+02	0.2580E+01		0.1851E-01	0.2473E-02	0.1774E-04	0.2370E-05
	4 -428.0	2	583	0.11182E+04	0.2042E+02	0.2694E+01		0.1826E-01	0.2409E-02	0.1633E-04	0.2155E-05
	4 -61.0	0	580	0.10663E+04	0.2139E+02	0.3247E+01		0.2006E-01	0.3045E-02	0.1881E-04	0.2855E-05
	4 61.0	0	579	0.10781E+04	0.2218E+02	0.3084E+01		0.2058E-01	0.2860E-02	0.1909E-04	0.2653E-05
	4 428.0	0	576	0.89355E+03	0.1680E+02	0.2127E+01		0.1880E-01	0.2380E-02	0.2104E-04	0.2664E-05
	4 428.0	1	577	0.98490E+03	0.2082E+02	0.2641E+01		0.2114E-01	0.2682E-02	0.2147E-04	0.2723E-05
	4 428.0	2	578	0.10403E+04	0.1949E+02	0.2689E+01		0.1873E-01	0.2585E-02	0.1801E-04	0.2485E-05
	4 650.0	0	575	0.48602E+03	0.4880E+01	0.6768E+00		0.1004E-01	0.1393E-02	0.2066E-04	0.2865E-05
A42	4 -428.0	0	585	0.10028E+04	0.1688E+02	0.2567E+01		0.1684E-01	0.2560E-02	0.1679E-04	0.2553E-05
	4 -61.0	0	586	0.11178E+04	0.2430E+02	0.3391E+01		0.2174E-01	0.3034E-02	0.1945E-04	0.2714E-05
	4 61.0	0	587	0.11410E+04	0.2407E+02	0.3341E+01		0.2110E-01	0.2928E-02	0.1849E-04	0.2566E-05
	4 428.0	0	588	0.94507E+03	0.1838E+02	0.2595E+01		0.1945E-01	0.2746E-02	0.2058E-04	0.2906E-05
A22	4 -428.0	0	589	0.10417E+04	0.1638E+02	0.2576E+01		0.1572E-01	0.2473E-02	0.1509E-04	0.2374E-05
	4 -61.0	0	590	0.11444E+04	0.2061E+02	0.3300E+01		0.1801E-01	0.2884E-02	0.1574E-04	0.2520E-05
	4 61.0	0	591	0.11363E+04	0.2150E+02	0.3436E+01		0.1892E-01	0.3024E-02	0.1665E-04	0.2661E-05
	4 428.0	0	592	0.92700E+03	0.1936E+02	0.2107E+01		0.1657E-01	0.2273E-02	0.1787E-04	0.2452E-05
A41	3 -428.0	0	597	0.10323E+04	0.1769E+02	0.2523E+01	0.4779E-01	0.1714E-01	0.2444E-02	0.1660E-04	0.2368E-05
	3 -61.0	0	595	0.11262E+04	0.2300E+02	0.3412E+01		0.2042E-01	0.3030E-02	0.1814E-04	0.2690E-05
	3 61.0	0	594	0.11470E+04	0.2314E+02	0.3295E+01		0.2018E-01	0.2872E-02	0.1759E-04	0.2504E-05
	3 428.0	0	593	0.97001E+03	0.1759E+02	0.2399E+01		0.1814E-01	0.2473E-02	0.1870E-04	0.2549E-05

ASSEMBLY PLANE	Z(MM)	X	RUN NO.	CS137(CPS)	CS134(CPS)	Lu154(CPS)	Pr144(CPS)	134/137	154/137	134/137/137	154/137/137	
A43	1	-672.0	0	598	0.52545E+03	0.4120E+01	0.5298E+00	0.7842E-02	0.1008E-02	0.1492E-04	0.1919E-05	
	1	-428.0	0	599	0.12396E+04	0.2281E+02	0.3163E+01	0.1840E-01	0.2551E-02	0.1485E-04	0.2059E-05	
	1	-428.0	1	600	0.12040E+04	0.2311E+02	0.3331E+01	0.1920E-01	0.2766E-02	0.1594E-04	0.2299E-05	
	1	-428.0	2	601	0.13073E+04	0.2683E+02	0.3540E+01	0.2052E-01	0.2708E-02	0.1570E-04	0.2071E-05	
	1	-61.0	0	602	0.13530E+04	0.3046E+02	0.4193E+01	0.2252E-01	0.3099E-02	0.1664E-04	0.2290E-05	
	1	61.0	0	603	0.13716E+04	0.3174E+02	0.4249E+01	0.2314E-01	0.3098E-02	0.1687E-04	0.2259E-05	
	1	428.0	0	604	0.11347E+04	0.2158E+02	0.3153E+01	0.1901E-01	0.2778E-02	0.1676E-04	0.2449E-05	
	1	428.0	1	605	0.11377E+04	0.2314E+02	0.3031E+01	0.2034E-01	0.2664E-02	0.1788E-04	0.2342E-05	
	1	428.0	2	606	0.12208E+04	0.2656E+C2	0.3469E+01	0.2176E-01	0.2842E-02	0.1782E-04	0.2328E-05	
	1	650.0	0	607	0.67400E+03	0.7690E+01	0.9593E+00	0.1141E-01	0.1423E-02	0.1693E-04	0.2112E-05	
	2	-672.0	0	608	0.49736E+03	0.3693E+01	0.4288E+00	0.7426E-02	0.8621E-03	0.1493E-04	0.1733E-05	
	2	-428.0	0	618	0.11764E+04	0.2032E+02	0.2821E+01	0.4877E-01	0.1727E-01	0.2398E-02	0.1468E-04	0.2038E-05
	2	-428.0	1	611	0.12170E+04	0.1988E+02	0.2800E+01	0.1634E-01	0.2301E-02	0.1342E-04	0.1891E-05	
	2	-428.0	2	610	0.13944E+04	0.2721E+02	0.4026E+01	0.1951E-01	0.2889E-02	0.1399E-04	0.2072E-05	
	2	-61.0	0	612	0.13244E+04	0.2837E+02	0.3717E+01	0.2142E-01	0.2806E-02	0.1617E-04	0.2119E-05	
	2	61.0	0	613	0.13403E+04	0.2831E+02	0.4043E+01	0.2112E-01	0.3017E-02	0.1576E-04	0.2251E-05	
	2	428.0	0	614	0.10858E+04	0.1992E+02	0.2592E+01	0.1835E-01	0.2388E-02	0.1690E-04	0.2199E-05	
	2	428.0	1	616	0.11512E+04	0.1993E+02	0.2722E+01	0.1731E-01	0.2364E-02	0.1504E-04	0.2054E-05	
	2	428.0	2	615	0.13560E+04	0.2920E+02	0.3714E+01	0.2154E-01	0.2739E-02	0.1588E-04	0.2020E-05	
	2	650.0	0	617	0.63500E+03	0.6261E+01	0.8311E+00	0.9859E-02	0.1309E-02	0.1352E-04	0.2061E-05	
	3	-672.0	0	619	0.44252E+03	0.3162E+01	0.5225E+00	0.7146E-02	0.1181E-02	0.1615E-04	0.2668E-05	
	3	-428.0	0	620	0.10175E+04	0.1682E+02	0.2275E+01	0.1653E-01	0.2236E-02	0.1624E-04	0.2197E-05	
	3	-428.0	1	622	0.10796E+04	0.1832E+02	0.2460E+01	0.1697E-01	0.2278E-02	0.1572E-04	0.2110E-05	
	3	-428.0	2	621	0.12704E+04	0.2137E+02	0.3376E+01	0.1682E-01	0.2638E-02	0.1324E-04	0.2092E-05	
	3	-61.0	0	623	0.11594E+04	0.2088E+02	0.3143E+01	0.1801E-01	0.2711E-02	0.1553E-04	0.2338E-05	
	3	61.0	0	624	0.11324E+04	0.2200E+02	0.3128E+01	0.1943E-01	0.2762E-02	0.1715E-04	0.2439E-05	
	3	428.0	0	625	0.89576E+03	0.1439E+02	0.1946E+01	0.1606E-01	0.2172E-02	0.1793E-04	0.2425E-05	
	3	428.0	1	627	0.93181E+03	0.1614E+02	0.2037E+01	0.1732E-01	0.2186E-02	0.1859E-04	0.2346E-05	
	3	428.0	2	626	0.11646E+04	0.2128E+02	0.2850E+01	0.1826E-01	0.2447E-02	0.1568E-04	0.2101E-05	
	3	650.0	0	628	0.49808E+03	0.4702E+01	0.6781E+00	0.9439E-02	0.1361E-02	0.1895E-04	0.2733E-05	
	4	-672.0	0	629	0.45749E+03	0.3417E+01	0.4854E+00	0.7469E-02	0.1061E-02	0.1633E-04	0.2319E-05	
	4	-428.0	0	630	0.10143E+04	0.1771E+02	0.2400E+01	0.1746E-01	0.2366E-02	0.1721E-04	0.2333E-05	
	4	-428.0	1	631	0.10743E+04	0.1778E+02	0.2432E+01	0.1655E-01	0.2264E-02	0.1541E-04	0.2107E-05	
	4	-428.0	2	632	0.12238E+04	0.2387E+02	0.3323E+01	0.1951E-01	0.2715E-02	0.1594E-04	0.2218E-05	
	4	-61.0	0	633	0.11616E+04	0.2417E+02	0.3394E+01	0.2080E-01	0.2922E-02	0.1791E-04	0.2515E-05	
	4	61.0	0	634	0.11679E+04	0.2359E+02	0.3396E+01	0.2020E-01	0.2904E-02	0.1729E-04	0.2490E-05	
	4	428.0	0	635	0.91633E+03	0.1645E+02	0.2524E+01	0.1795E-01	0.2754E-02	0.1959E-04	0.3005E-05	
	4	428.0	1	636	0.96996E+03	0.1718E+02	0.2199E+01	0.1771E-01	0.2267E-02	0.1826E-04	0.2337E-05	
	4	428.0	2	637	0.11927E+04	0.2580E+02	0.3832E+01	0.2163E-01	0.3213E-02	0.1814E-04	0.2694E-05	
	4	650.0	0	638	0.51279E+03	0.5097E+01	0.7320E+00	0.9944E-02	0.1427E-02	0.1939E-04	0.2784E-05	
A13	4	-428.0	0	639	0.98213E+03	0.1547E+02	0.2222E+01	0.1575E-01	0.2262E-02	0.1604E-04	0.2303E-05	
	4	-61.0	0	640	0.12154E+04	0.2633E+02	0.3903E+01	0.2166E-01	0.3211E-02	0.1782E-04	0.2642E-05	
	4	61.0	0	641	0.12312E+04	0.2763E+02	0.3625E+01	0.2244E-01	0.2944E-02	0.1822E-04	0.2391E-05	
	4	428.0	0	642	0.10582E+04	0.2260E+02	0.3005E+01	0.2155E-01	0.2839E-02	0.2036E-04	0.2603E-05	
A12	3	-428.0	0	643	0.97781E+03	0.1676E+02	0.2356E+01	0.1714E-01	0.2410E-02	0.1753E-04	0.2464E-05	
	3	-61.0	0	644	0.12033E+04	0.2753E+02	0.3776E+01	0.2288E-01	0.3138E-02	0.1901E-04	0.2608E-05	
	3	61.0	0	645	0.12167E+04	0.2837E+02	0.4020E+01	0.2331E-01	0.3304E-02	0.1916E-04	0.2713E-05	
	3	428.0	0	646	0.10441E+04	0.2213E+02	0.2926E+01	0.2120E-01	0.2802E-02	0.2030E-04	0.2684E-05	
A57	3	-428.0	0	651	0.10122E+04	0.1716E+02	0.2471E+01	0.4537E-01	0.1695E-01	0.2441E-02	0.1674E-04	0.2412E-05
	3	-61.0	0	649	0.11273E+04	0.2406E+02	0.3539E+01	0.2134E-01	0.3140E-02	0.1893E-04	0.2783E-05	
	3	61.0	0	648	0.11348E+04	0.2418E+02	0.3528E+01	0.2130E-01	0.3109E-02	0.1877E-04	0.2740E-05	
	3	428.0	0	647	0.98256E+03	0.1809E+02	0.2498E+01	0.1841E-01	0.2542E-02	0.1874E-04	0.2587E-05	
A31	4	-428.0	0	652	0.91034E+03	0.1379E+02	0.1956E+01	0.1515E-01	0.2149E-02	0.1664E-04	0.2360E-05	
	4	-61.0	0	653	0.11616E+04	0.2430E+02	0.3575E+01	0.2092E-01	0.3078E-02	0.1801E-04	0.2650E-05	
	4	61.0	0	654	0.11770E+04	0.2537E+02	0.3546E+01	0.2155E-01	0.3013E-02	0.1831E-04	0.2560E-05	
	4	428.0	0	655	0.10128E+04	0.1960E+02	0.2636E+01	0.1935E-01	0.2602E-02	0.1911E-04	0.2570E-05	

ASSEMBLY PLANE	Z(MM)	X	RUN NO.	CS137(CPS)	CS134(CPS)	EU154(CPS)	PR144(CPS)	134/137	154/137	134/137/137	154/137/137
A23	1 -672.0	0	656	0.50719E+03	0.3925E+01	0.5041E+00		0.7739E-02	0.9939E-03	0.1526E-04	0.1960E-05
	1 -428.0	0	657	0.12420E+04	0.2185E+02	0.3086E+01		0.1759E-01	0.2485E-02	0.1416E-04	0.2001E-05
	1 -428.0	1	658	0.11529E+04	0.2071E+02	0.2809E+01		0.1797E-01	0.2437E-02	0.1558E-04	0.2113E-05
	1 -428.0	2	659	0.14078E+04	0.2830E+02	0.4046E+01		0.2010E-01	0.2874E-02	0.1428E-04	0.2042E-05
	1 -61.0	0	660	0.13687E+04	0.3013E+02	0.4145E+01		0.2201E-01	0.3028E-02	0.1608E-04	0.2212E-05
	1 61.0	0	661	0.13872E+04	0.3218E+02	0.4224E+01		0.2320E-01	0.3045E-02	0.1672E-04	0.2195E-05
	1 428.0	0	662	0.11674E+04	0.2412E+02	0.3111E+01		0.2066E-01	0.2665E-02	0.1769E-04	0.2283E-05
	1 428.0	1	663	0.10863E+04	0.2094E+02	0.2985E+01		0.1927E-01	0.2748E-02	0.1774E-04	0.2530E-05
	1 428.0	2	664	0.13724E+04	0.3021E+02	0.4317E+01		0.2202E-01	0.3145E-02	0.1604E-04	0.2292E-05
	1 650.0	0	665	0.70304E+03	0.8074E+01	0.1023E+01		0.1149E-01	0.1455E-02	0.1634E-04	0.2069E-05
	2 -672.0	0	666	0.56408E+03	0.4397E+01	0.6068E+00		0.7795E-02	0.1076E-02	0.1382E-04	0.1907E-05
	2 -428.0	0	667	0.13490E+04	0.2561E+02	0.3434E+01		0.1898E-01	0.2545E-02	0.1407E-04	0.1887E-05
	2 -428.0	1	669	0.10703E+04	0.1861E+02	0.2688E+01		0.1739E-01	0.2511E-02	0.1624E-04	0.2346E-05
	2 -428.0	2	668	0.14028E+04	0.2820E+02	0.3936E+01		0.2010E-01	0.2806E-02	0.1433E-04	0.2000E-05
	2 -61.0	0	670	0.14623E+04	0.3309E+02	0.4859E+01		0.2263E-01	0.3323E-02	0.1547E-04	0.2273E-05
	2 61.0	0	671	0.14459E+04	0.3514E+02	0.4478E+01		0.2430E-01	0.3097E-02	0.1681E-04	0.2142E-05
	2 428.0	0	672	0.11922E+04	0.2558E+02	0.3378E+01		0.2146E-01	0.2833E-02	0.1800E-04	0.2376E-05
	2 428.0	1	674	0.12272E+04	0.2883E+02	0.3870E+01		0.2349E-01	0.3154E-02	0.1914E-04	0.2570E-05
	2 428.0	2	673	0.13528E+04	0.2914E+02	0.3985E+01		0.2154E-01	0.2946E-02	0.1592E-04	0.2178E-05
	2 650.0	0	675	0.73118E+03	0.9453E+01	0.1155E+01		0.1293E-01	0.1579E-02	0.1768E-04	0.2160E-05
	3 -672.0	0	682	0.41962E+03	0.3175E+01	0.3910E+00		0.7567E-02	0.9317E-03	0.1803E-04	0.2220E-05
	3 -428.0	0	686	0.98472E+03	0.1695E+02	0.2440E+01	0.4534E-01	0.1721E-01	0.2478E-02	0.1748E-04	0.2516E-05
	3 -428.0	1	684	0.10129E+04	0.1845E+02	0.2565E+01		0.1822E-01	0.2532E-02	0.1798E-04	0.2500E-05
	3 -428.0	2	683	0.11619E+04	0.2184E+02	0.3268E+01		0.1880E-01	0.2813E-02	0.1618E-04	0.2421E-05
	3 -61.0	0	681	0.11993E+04	0.2682E+02	0.3709E+01		0.2236E-01	0.3092E-02	0.1865E-04	0.2579E-05
	3 61.0	0	680	0.12334E+04	0.2887E+02	0.4012E+01		0.2339E-01	0.3250E-02	0.1895E-04	0.2633E-05
	3 428.0	0	677	0.10638E+04	0.23333E+02	0.3096E+01		0.2193E-01	0.2910E-02	0.2061E-04	0.2736E-05
	3 428.0	1	679	0.10143E+04	0.2212E+02	0.2751E+01		0.2181E-01	0.2712E-02	0.2150E-04	0.2674E-05
	3 428.0	2	678	0.13426E+04	0.3177E+02	0.4233E+01		0.2367E-01	0.3153E-02	0.1763E-04	0.2348E-05
	3 650.0	0	676	0.59280E+03	0.7067E+01	0.9142E+00		0.1192E-01	0.1542E-02	0.2011E-04	0.2601E-05
	4 -672.0	0	687	0.46388E+03	0.3354E+01	0.5486E+00		0.7229E-02	0.1183E-02	0.1558E-04	0.2549E-05
	4 -428.0	0	688	0.10776E+04	0.1888E+02	0.2641E+01		0.1732E-01	0.2451E-02	0.1626E-04	0.2274E-05
	4 -428.0	1	689	0.10804E+04	0.1955E+02	0.2742E+01		0.1809E-01	0.2538E-02	0.1675E-04	0.2350E-05
	4 -428.0	2	690	0.11696E+04	0.2203E+02	0.3424E+01		0.1852E-01	0.2875E-02	0.1557E-04	0.2417E-05
	4 -61.0	0	691	0.11525E+04	0.2599E+02	0.3528E+01		0.2198E-01	0.2984E-02	0.1859E-04	0.2523E-05
	4 61.0	0	692	0.11774E+04	0.2458E+02	0.3493E+01		0.2087E-01	0.2966E-02	0.1773E-04	0.2519E-05
	4 428.0	0	693	0.94657E+03	0.1903E+02	0.2736E+01		0.2006E-01	0.2885E-02	0.2115E-04	0.3041E-05
	4 428.0	1	694	0.10479E+04	0.2242E+02	0.3135E+01		0.2139E-01	0.2992E-02	0.2042E-04	0.2855E-05
	4 428.0	2	695	0.10865E+04	0.2249E+02	0.3136E+01		0.2070E-01	0.2886E-02	0.1905E-04	0.2657E-05
	4 650.0	0	696	0.51065E+03	0.5457E+01	0.7638E+00		0.1069E-01	0.1496E-02	0.2093E-04	0.2929E-05
A67	4 -428.0	0	697	0.10321E+04	0.1785E+02	0.2502E+01		0.1729E-01	0.2424E-02	0.1675E-04	0.2349E-05
	4 -61.0	0	698	0.12165E+04	0.2791E+02	0.3951E+01		0.2266E-01	0.3248E-02	0.1880E-04	0.2670E-05
	4 61.0	0	699	0.12297E+04	0.2975E+02	0.4241E+01		0.2419E-01	0.3449E-02	0.1967E-04	0.2805E-05
	4 428.0	0	700	0.10741E+04	0.2168E+02	0.3163E+01		0.2018E-01	0.2945E-02	0.1879E-04	0.2742E-05
A26	1 -672.0	0	701	0.53529E+03	0.4028E+01	0.5619E+00		0.7525E-02	0.1050E-02	0.1406E-04	0.1961E-05
	1 -428.0	0	703	0.12723E+04	0.2443E+02	0.3272E+01		0.1920E-01	0.2572E-02	0.1509E-04	0.2021E-05
	1 -428.0	1	702	0.10910E+04	0.1908E+02	0.2512E+01		0.1748E-01	0.2302E-02	0.1602E-04	0.2110E-05
	1 -428.0	2	704	0.13993E+04	0.2863E+02	0.4225E+01		0.2060E-01	0.3020E-02	0.1472E-04	0.2158E-05
	1 -61.0	0	705	0.14384E+04	0.3423E+02	0.4842E+01		0.2379E-01	0.3366E-02	0.1654E-04	0.2340E-05
	1 61.0	0	706	0.14650E+04	0.3583E+02	0.5270E+01		0.2446E-01	0.3597E-02	0.1669E-04	0.2456E-05
	1 428.0	0	707	0.12235E+04	0.2821E+02	0.3839E+01		0.2306E-01	0.3138E-02	0.1885E-04	0.2565E-05
	1 428.0	1	708	0.12808E+04	0.3087E+02	0.3898E+01		0.2410E-01	0.3043E-02	0.1882E-04	0.2376E-05
	1 428.0	2	709	0.13391E+04	0.3147E+02	0.4341E+01		0.2350E-01	0.3242E-02	0.1755E-04	0.2421E-05
	1 650.0	0	710	0.73501E+03	0.9617E+01	0.1249E+01		0.1308E-01	0.1700E-02	0.1780E-04	0.2312E-05

ASSEMBLY PLANE	Z(MM)	X	RUN NO.	CS137(CPS)	CS134(CPS)	EU154(CPS)	PR144(CPS)	134/137	154/137	134/137/137	154/137/137	
2	-672.0	0	711	0.52490E+03	0.3921E+01	0.5959E+00		0.7470E-02	0.1135E-02	0.1423E-04	0.2163E-05	
2	-428.0	0	712	0.12491E+04	0.2459E+02	0.3495E+01		0.1968E-01	0.2798E-02	0.1576E-04	0.2240E-05	
2	-428.0	1	714	0.12805E+04	0.251E+02	0.3532E+01		0.1984E-01	0.2758E-02	0.1550E-04	0.2154E-05	
2	-428.0	2	713	0.14403E+04	0.2952E+02	0.4106E+01		0.2049E-01	0.2851E-02	0.1423E-04	0.1979E-05	
2	-61.0	0	715	0.14756E+04	0.3419E+02	0.4934E+01		0.2317E-01	0.3344E-02	0.1570E-04	0.2266E-05	
2	61.0	0	716	0.14651E+04	0.3627E+02	0.4775E+01		0.2476E-01	0.3259E-02	0.1690E-04	0.2225E-05	
2	428.0	0	717	0.11430E+04	0.2116E+02	0.3822E+01		0.2376E-01	0.3344E-02	0.2079E-04	0.2926E-05	
2	428.0	1	719	0.12086E+04	0.2101E+02	0.3775E+01		0.2235E-01	0.3124E-02	0.1849E-04	0.2584E-05	
2	428.0	2	718	0.13786E+04	0.3233E+02	0.4140E+01		0.2345E-01	0.3003E-02	0.1701E-04	0.2178E-05	
2	650.0	0	720	0.71134E+03	0.8871E+01	0.1163E+01		0.1247E-01	0.1634E-02	0.1759E-04	0.2298E-05	
3	-672.0	0	727	0.46671E+03	0.3689E+01	0.4801E+00		0.7905E-02	0.1029E-02	0.1694E-04	0.2204E-05	
3	-428.0	0	731	0.10937E+04	0.1988E+02	0.2050E+01	0.5101E-01	0.1818E-01	0.2606E-02	0.1662E-04	0.2382E-05	
3	-428.0	1	729	0.94986E+03	0.1590E+02	0.2293E+01		0.1674E-01	0.2414E-02	0.1763E-04	0.2541E-05	
3	-428.0	2	728	0.12882E+04	0.2690E+02	0.3614E+01		0.2088E-01	0.2806E-02	0.1621E-04	0.2178E-05	
3	-61.0	0	726	0.12633E+04	0.2949E+02	0.3785E+01		0.2334E-01	0.2996E-02	0.1848E-04	0.2371E-05	
3	61.0	0	725	0.12843E+04	0.3111E+02	0.4293E+01		0.2423E-01	0.3342E-02	0.1886E-04	0.2603E-05	
3	428.0	0	722	0.10624E+04	0.2275E+02	0.3088E+01		0.2141E-01	0.2906E-02	0.2016E-04	0.2736E-05	
3	428.0	1	724	0.10775E+04	0.2511E+02	0.3415E+01		0.2336E-01	0.3169E-02	0.2168E-04	0.2941E-05	
3	428.0	2	723	0.12646E+04	0.2841E+02	0.3795E+01		0.2247E-01	0.3001E-02	0.1777E-04	0.2373E-05	
3	650.0	0	721	0.58746E+03	0.7101E+01	0.8938E+00		0.1209E-01	0.1522E-02	0.2058E-04	0.2590E-05	
4	-672.0	0	732	0.41242E+03	0.2837E+01	0.4658E+00		0.6879E-02	0.1129E-02	0.1668E-04	0.2738E-05	
4	-428.0	0	733	0.96897E+03	0.1707E+02	0.2568E+01		0.1761E-01	0.2650E-02	0.1810E-04	0.2739E-05	
4	-428.0	1	734	0.97039E+03	0.1775E+02	0.2701E+01		0.1829E-01	0.2784E-02	0.1885E-04	0.2869E-05	
4	-428.0	2	735	0.11568E+04	0.2138E+02	0.3127E+01		0.1849E-01	0.2703E-02	0.1598E-04	0.2337E-05	
4	-61.0	0	736	0.12074E+04	0.2809E+02	0.3865E+01		0.2326E-01	0.3201E-02	0.1927E-04	0.2651E-05	
4	61.0	0	737	0.12100E+04	0.2896E+02	0.4125E+01		0.2393E-01	0.3409E-02	0.1978E-04	0.2810E-05	
4	428.0	0	738	0.10608E+04	0.2330E+02	0.3308E+01		0.2196E-01	0.3118E-02	0.2070E-04	0.2939E-05	
4	428.0	1	739	0.11385E+04	0.2927E+02	0.3705E+01		0.2220E-01	0.3254E-02	0.1950E-04	0.2858E-05	
4	428.0	2	740	0.12121E+04	0.2892E+02	0.4101E+01		0.2386E-01	0.3383E-02	0.1968E-04	0.2791E-05	
4	650.0	0	741	0.60387E+03	0.7742E+01	0.9741E+00		0.1282E-01	0.1613E-02	0.2123E-04	0.2671E-05	
A 40	3	-428.0	0	742	0.10031E+04	0.1834E+02	0.2656E+01		0.1829E-01	0.2648E-02	0.1823E-04	0.2640E-05
3	-61.0	0	743	0.12676E+04	0.3124E+02	0.3984E+01		0.2465E-01	0.3143E-02	0.1944E-04	0.2479E-05	
3	61.0	0	744	0.12949E+04	0.3224E+02	0.4498E+01		0.2490E-01	0.3474E-02	0.1923E-04	0.2683E-05	
3	428.0	0	745	0.11646E+04	0.2619E+02	0.3914E+01		0.2249E-01	0.3275E-02	0.1931E-04	0.2812E-05	
A 1	4	-428.0	0	746	0.92529E+03	0.1474E+02	0.1892E+01		0.1593E-01	0.2045E-02	0.1722E-04	0.2210E-05
4	-61.0	0	747	0.12115E+04	0.2138E+02	0.3910E+01		0.2260E-01	0.3145E-02	0.1865E-04	0.2596E-05	
4	61.0	0	748	0.12293E+04	0.3031E+02	0.4070E+01		0.2466E-01	0.3311E-02	0.2006E-04	0.2693E-05	
4	428.0	0	749	0.10930E+04	0.2566E+02	0.3338E+01		0.2347E-01	0.3052E-02	0.2147E-04	0.2792E-05	
A 8	1	-672.0	0	750	0.57864E+03	0.5008E+01	0.7298E+00		0.8655E-02	0.1261E-02	0.1496E-04	0.2180E-05
1	-428.0	0	751	0.12536E+04	0.2381E+02	0.3370E+01		0.1900E-01	0.2688E-02	0.1515E-04	0.2145E-05	
1	-428.0	1	752	0.10843E+04	0.1906E+02	0.2559E+01		0.1758E-01	0.2361E-02	0.1622E-04	0.2177E-05	
1	-428.0	2	753	0.14032E+04	0.2955E+02	0.4166E+01		0.2106E-01	0.2969E-02	0.1501E-04	0.2116E-05	
1	-61.0	0	754	0.14599E+04	0.3564E+02	0.4805E+01		0.2441E-01	0.3291E-02	0.1672E-04	0.2254E-05	
1	61.0	0	755	0.14507E+04	0.3626E+02	0.4955E+01		0.2500E-01	0.3416E-02	0.1723E-04	0.2354E-05	
1	428.0	0	756	0.12146E+04	0.2572E+02	0.3595E+01		0.2118E-01	0.2960E-02	0.1744E-04	0.2437E-05	
1	428.0	1	757	0.12815E+04	0.3126E+02	0.3959E+01		0.2439E-01	0.3090E-02	0.1904E-04	0.2411E-05	
1	428.0	2	758	0.13204E+04	0.2988E+02	0.4098E+01		0.2263E-01	0.3103E-02	0.1714E-04	0.2350E-05	
1	650.0	0	759	0.73481E+03	0.8942E+01	0.1164E+01		0.1217E-01	0.1584E-02	0.1656E-04	0.2156E-05	
2	-672.0	0	766	0.58194E+03	0.5143E+01	0.6704E+00		0.8837E-02	0.1152E-02	0.1519E-04	0.1979E-05	
2	-428.0	0	770	0.12645E+04	0.2475E+02	0.3435E+01	0.5022E-01	0.1958E-01	0.2716E-02	0.1548E-04	0.2148E-05	
2	-428.0	1	768	0.10643E+04	0.2020E+02	0.2826E+01		0.1898E-01	0.2656E-02	0.1784E-04	0.2495E-05	
2	-428.0	2	767	0.14310E+04	0.2975E+02	0.4312E+01		0.2079E-01	0.3013E-02	0.1455E-04	0.2106E-05	
2	-61.0	0	765	0.14706E+04	0.3598E+02	0.4892E+01		0.2447E-01	0.3327E-02	0.1664E-04	0.2262E-05	
2	61.0	0	764	0.14187E+04	0.3546E+02	0.4880E+01		0.2500E-01	0.3440E-02	0.1762E-04	0.2425E-05	
2	428.0	0	761	0.11813E+04	0.2487E+02	0.3409E+01		0.2105E-01	0.2885E-02	0.1782E-04	0.2443E-05	
2	428.0	1	763	0.12569E+04	0.2867E+02	0.3782E+01		0.2281E-01	0.3009E-02	0.1815E-04	0.2394E-05	
2	428.0	2	762	0.13506E+04	0.3191E+02	0.4248E+01		0.2362E-01	0.3146E-02	0.1749E-04	0.2329E-05	
2	650.0	0	760	0.71600E+03	0.9333E+01	0.1092E+01		0.1303E-01	0.1526E-02	0.1820E-04	0.2131E-05	

ASSEMBLY PLANE	Z(MM)	X	RUN NO.	C5137(CPS)	C5134(CPS)	EU134(CPS)	PR144(CPS)	134/137	134/137	134/137/137	134/137/137
3	-672.0	0	793	0.46004E+03	0.3396E+01	0.4237E+00		0.7382E-02	0.9211E-03	0.1605E-04	0.2002E-05
3	-428.0	0	794	0.10624E+04	0.1947E+02	0.2758E+01		0.1832E-01	0.2596E-02	0.1725E-04	0.2444E-05
3	-428.0	1	796	0.92269E+03	0.1618E+02	0.2294E+01		0.1754E-01	0.2486E-02	0.1900E-04	0.2693E-05
3	-428.0	2	795	0.12994E+04	0.2258E+02	0.3665E+01		0.1969E-01	0.2821E-02	0.1915E-04	0.2171E-05
3	-61.0	0	797	0.12207E+04	0.2758E+02	0.3999E+01		0.2260E-01	0.3276E-02	0.1851E-04	0.2684E-05
3	61.0	0	798	0.12434E+04	0.2946E+02	0.4023E+01		0.2370E-01	0.3235E-02	0.1906E-04	0.2602E-05
3	428.0	0	799	0.16644E+04	0.2390E+02	0.3191E+01		0.2246E-01	0.2998E-02	0.2110E-04	0.2817E-05
3	428.0	1	801	0.10984E+04	0.2637E+02	0.3672E+01		0.2401E-01	0.3343E-02	0.2186E-04	0.3044E-05
3	428.0	2	800	0.12731E+04	0.2866E+02	0.3951E+01		0.2251E-01	0.3103E-02	0.1768E-04	0.2437E-05
3	650.0	0	802	0.59184E+03	0.7088E+01	0.9850E+00		0.1198E-01	0.1664E-02	0.2024E-04	0.2812E-05
4	-672.0	0	781	0.43246E+03	0.3044E+01	0.4468E+00		0.7040E-02	0.1033E-02	0.1628E-04	0.2389E-05
4	-428.0	0	792	0.97613E+03	0.1659E+02	0.2443E+01	0.4567E-01	0.1694E-01	0.2503E-02	0.1741E-04	0.2564E-05
4	-428.0	1	784	0.95182E+03	0.1703E+02	0.2569E+01		0.1790E-01	0.2699E-02	0.1880E-04	0.2836E-05
4	-428.0	2	785	0.11598E+04	0.2200E+02	0.3294E+01		0.1901E-01	0.2840E-02	0.1639E-04	0.2449E-05
4	-61.0	0	786	0.12347E+04	0.2864E+02	0.4102E+01		0.2320E-01	0.3322E-02	0.1879E-04	0.2691E-05
4	61.0	0	787	0.12150E+04	0.2993E+02	0.4062E+01		0.2462E-01	0.3341E-02	0.2026E-04	0.2749E-05
4	428.0	0	788	0.10682E+04	0.2373E+02	0.3119E+01		0.2222E-01	0.2920E-02	0.2080E-04	0.2734E-05
4	428.0	1	789	0.11372E+04	0.2634E+02	0.3629E+01		0.2316E-01	0.3192E-02	0.2037E-04	0.2807E-05
4	428.0	2	790	0.12803E+04	0.3081E+02	0.4194E+01		0.2406E-01	0.3276E-02	0.1880E-04	0.2599E-05
4	650.0	0	791	0.60630E+03	0.7645E+01	0.9898E+00		0.1261E-01	0.1632E-02	0.2080E-04	0.2693E-05

Appendix 2 Axial and Radial Distributions of Gamma-Ray Intensities and Intensity Ratios in the JPDR-I Fuel Assemblies

Axial and radial distributions of measured ^{137}Cs , ^{134}Cs , ^{154}Eu , $^{134}\text{Cs}/^{137}\text{Cs}$, and $^{154}\text{Eu}/^{137}\text{Cs}$ are represented in the following figures for the twelve assemblies measured at forty positions. Each assembly has five figures: Four figures of the axial distributions on four sides, and one figure of the radial distributions at the axial positions of ± 428 mm. The radial distribution is expressed by developing the four sides of an assembly into one plane which has a cut at the narrow-narrow gap corner. The abscissa in the figure on the axial distribution represents the distance from the bottom end of active fuel.

Symbols used in the figures have the following meanings.

- ; intensity of ^{137}Cs ($\times 10^{-2}$ cps).
- △ ; intensity of ^{134}Cs ($\times 0.4$ cps).
- ; intensity of ^{154}Eu ($\times 2$ cps).
- × ; intensity ratio of $^{134}\text{Cs}/^{137}\text{Cs}$ ($\times 5 \times 10^2$).
- + ; intensity ratio of $^{154}\text{Eu}/^{137}\text{Cs}$ ($\times 2.5 \times 10^3$).

Solid lines for ^{137}Cs , $^{134}\text{Cs}/^{137}\text{Cs}$, and $^{154}\text{Eu}/^{137}\text{Cs}$ represent the fitted functions discussed in Section 4.2.

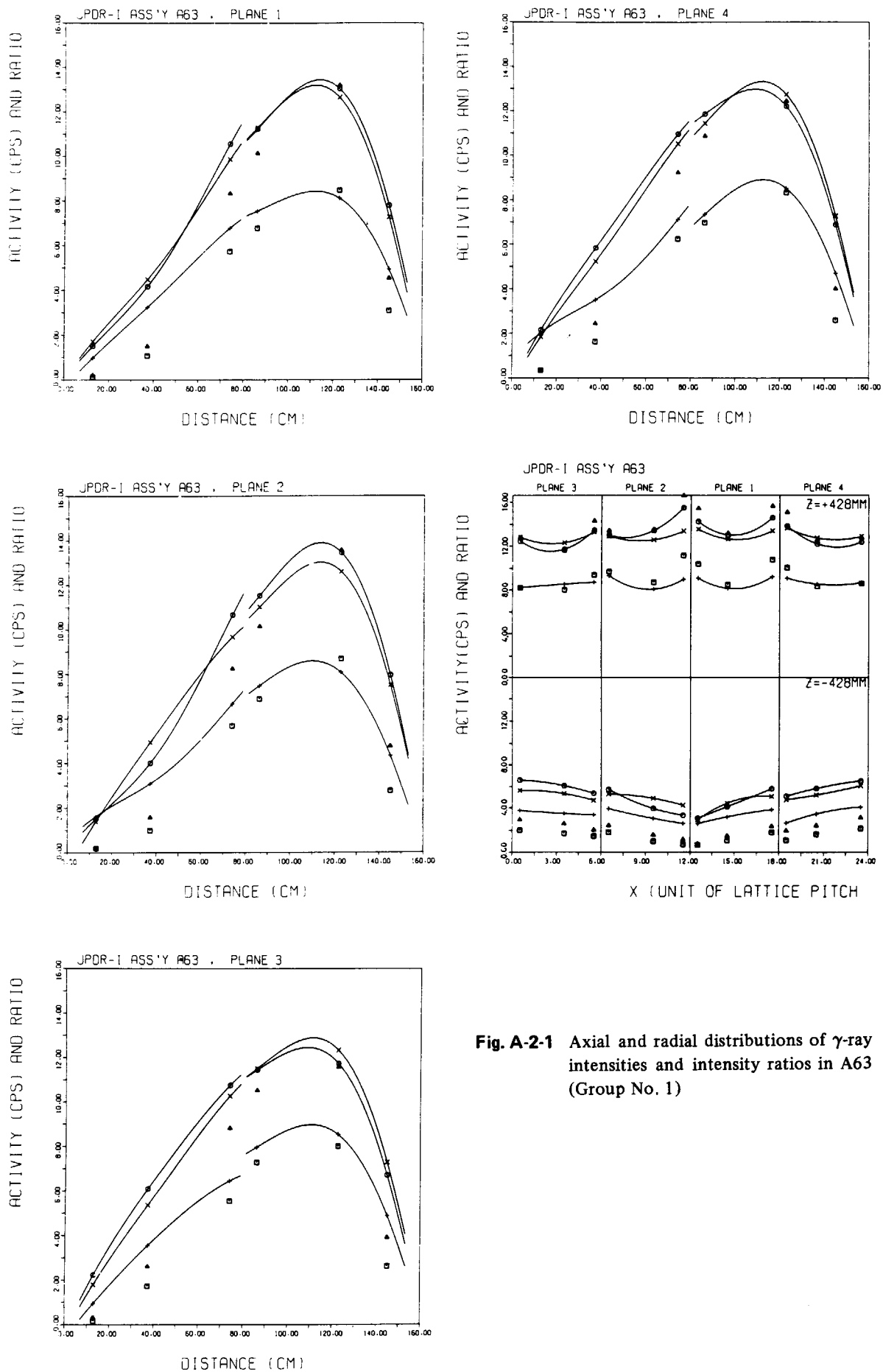


Fig. A-2-1 Axial and radial distributions of γ -ray intensities and intensity ratios in A63 (Group No. 1)

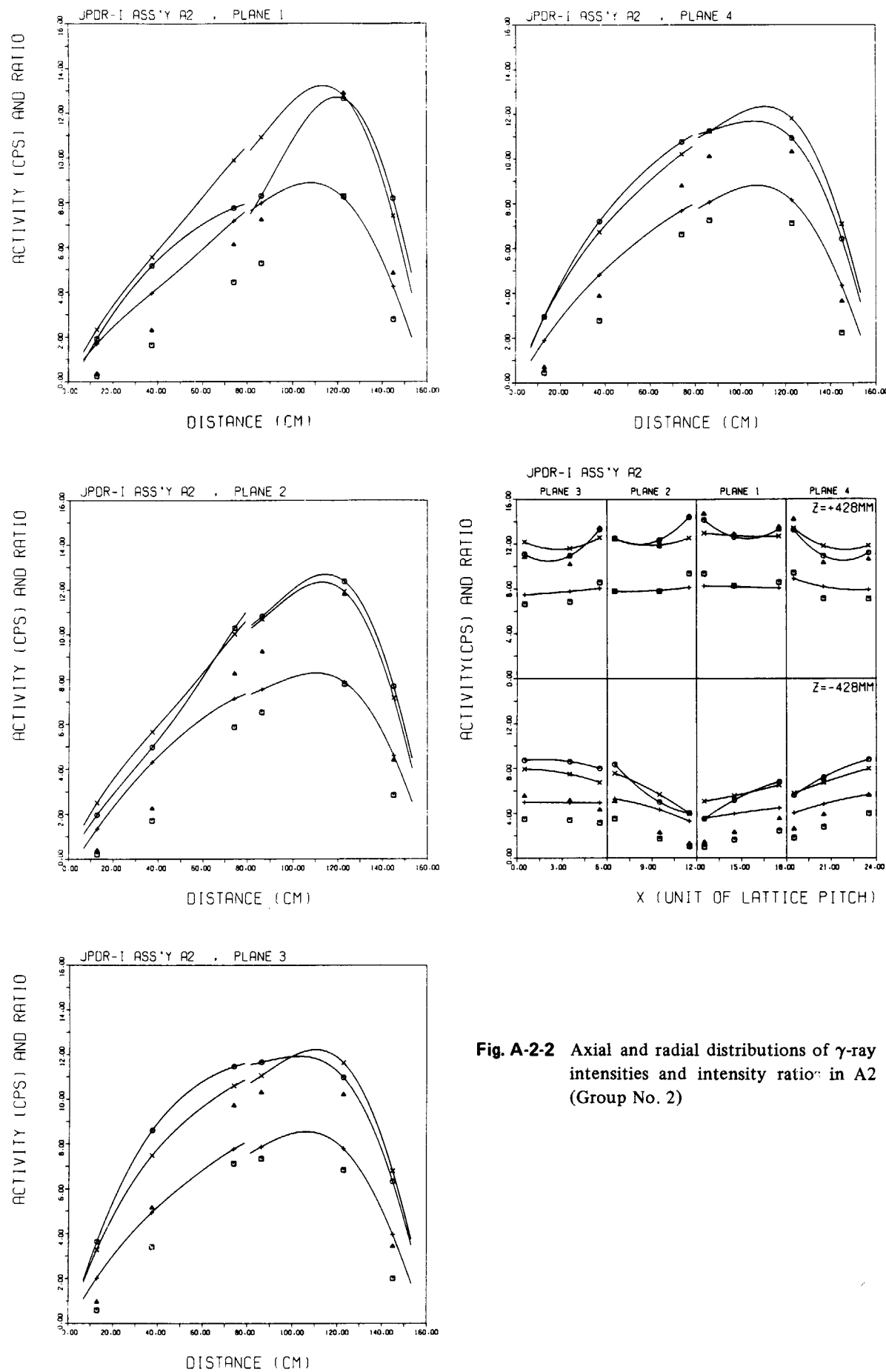


Fig. A-2-2 Axial and radial distributions of γ -ray intensities and intensity ratios in A2 (Group No. 2)

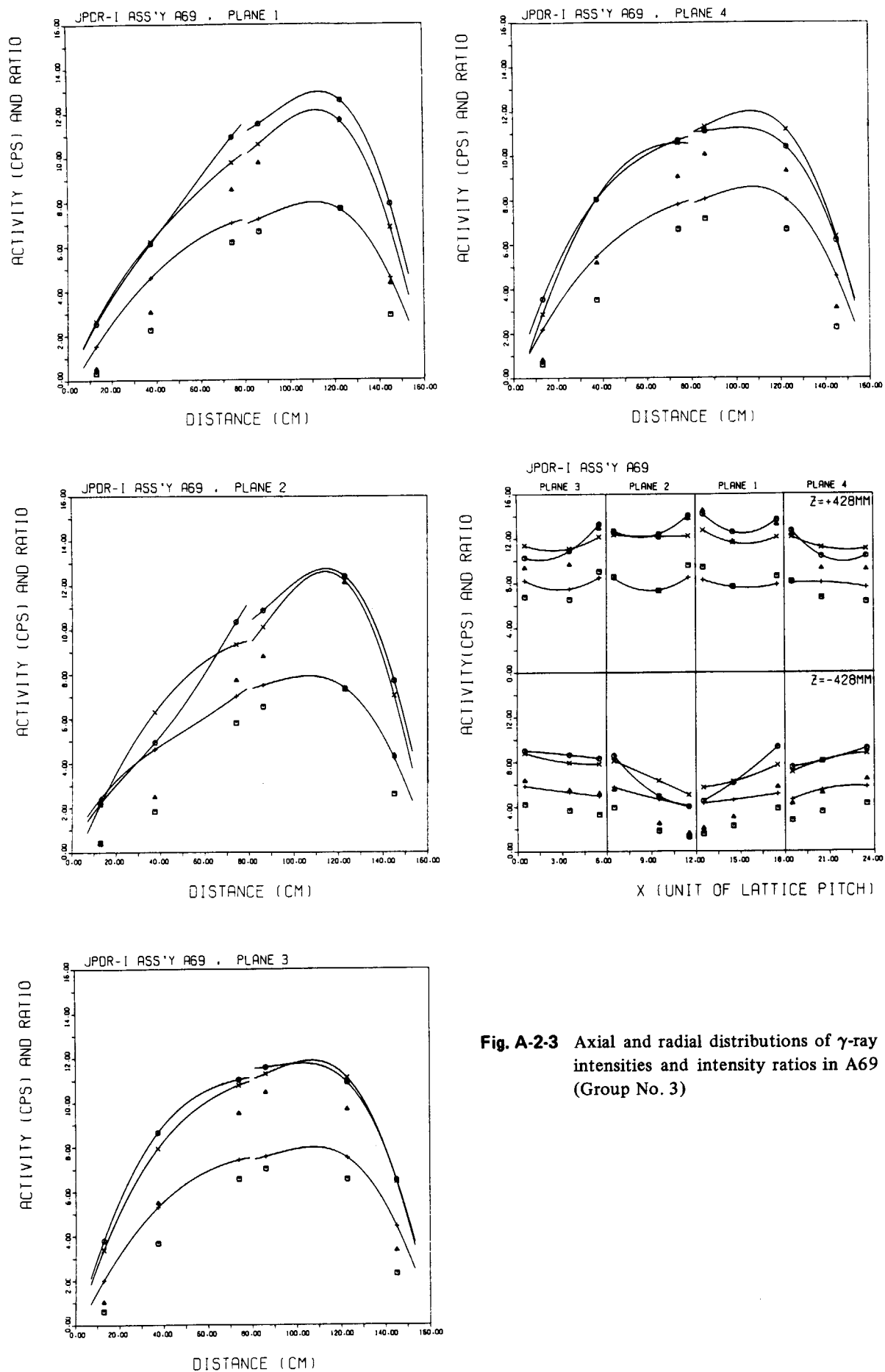


Fig. A-2-3 Axial and radial distributions of γ -ray intensities and intensity ratios in A69 (Group No. 3)

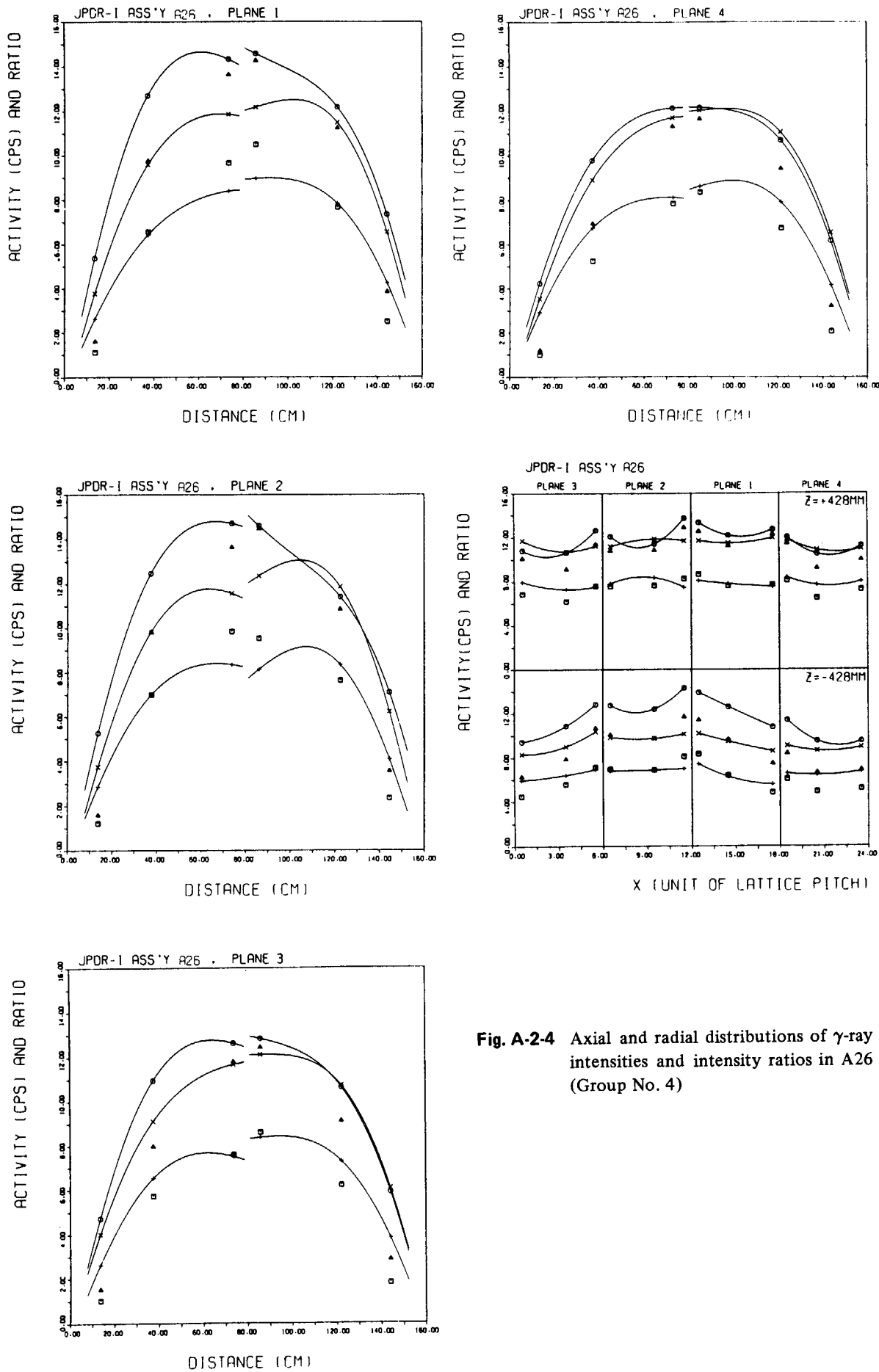


Fig. A-2-4 Axial and radial distributions of γ -ray intensities and intensity ratios in A26 (Group No. 4)

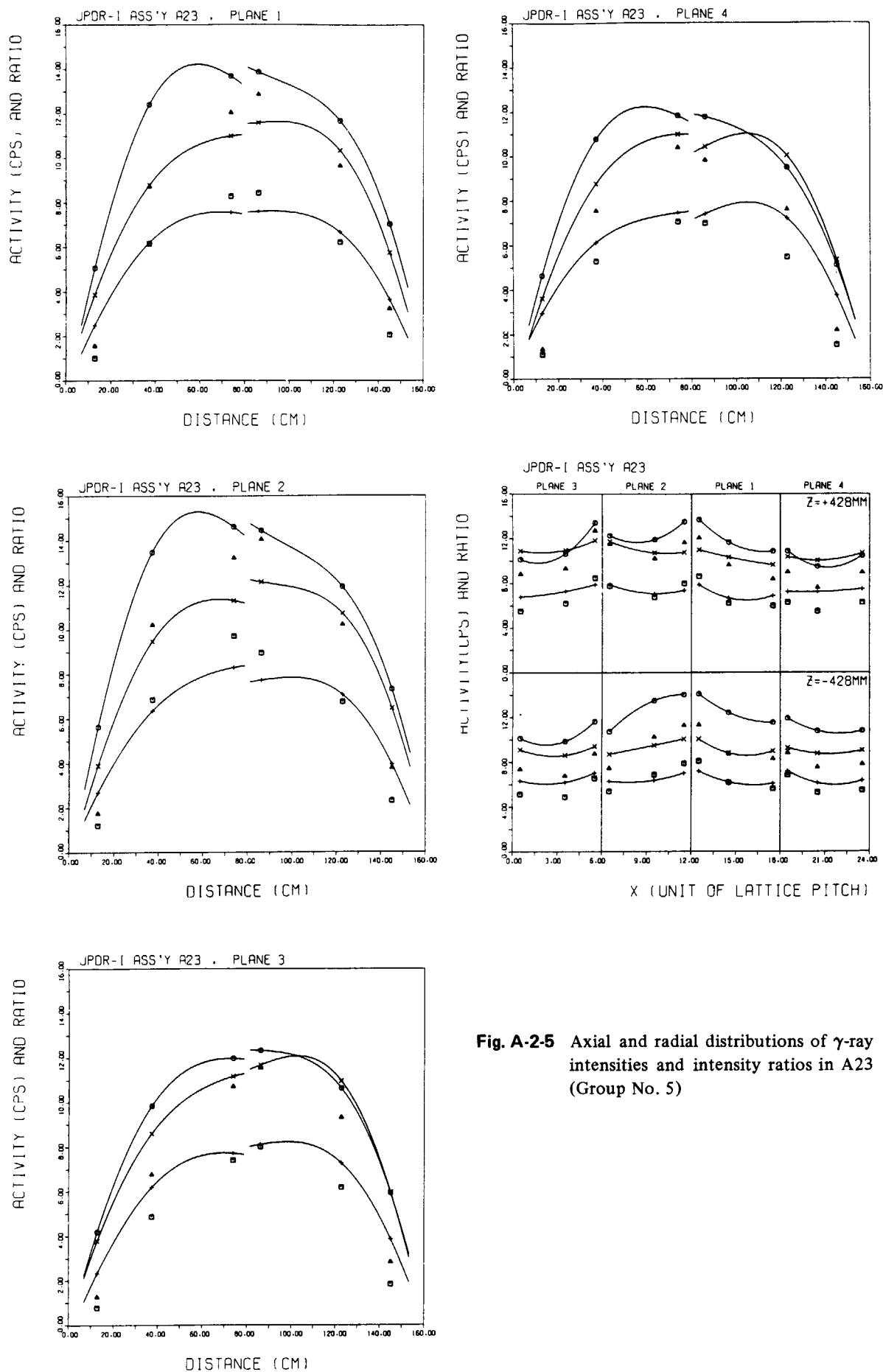


Fig. A-2-5 Axial and radial distributions of γ -ray intensities and intensity ratios in A23 (Group No. 5)

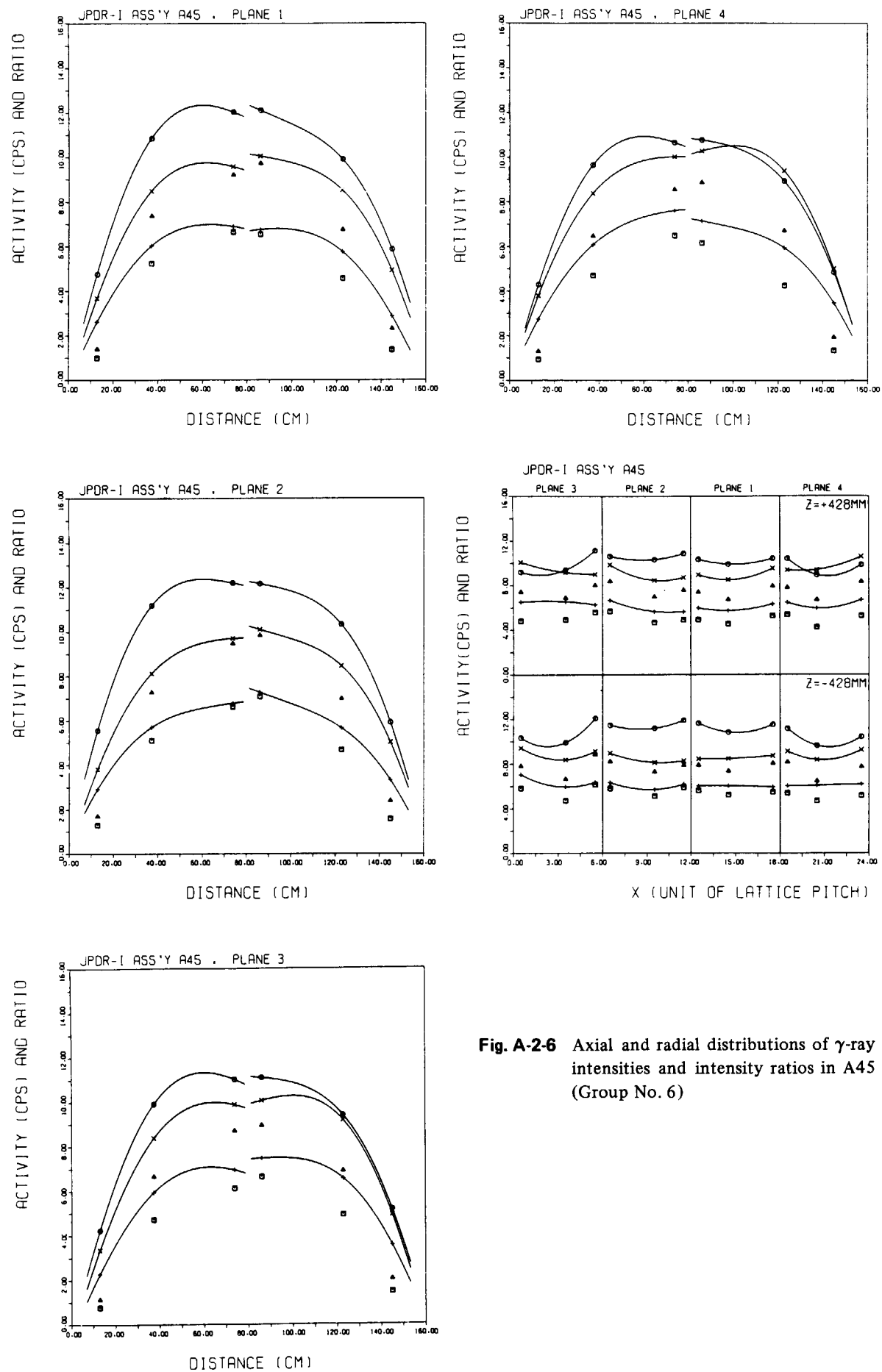


Fig. A-2-6 Axial and radial distributions of γ -ray intensities and intensity ratios in A45 (Group No. 6)

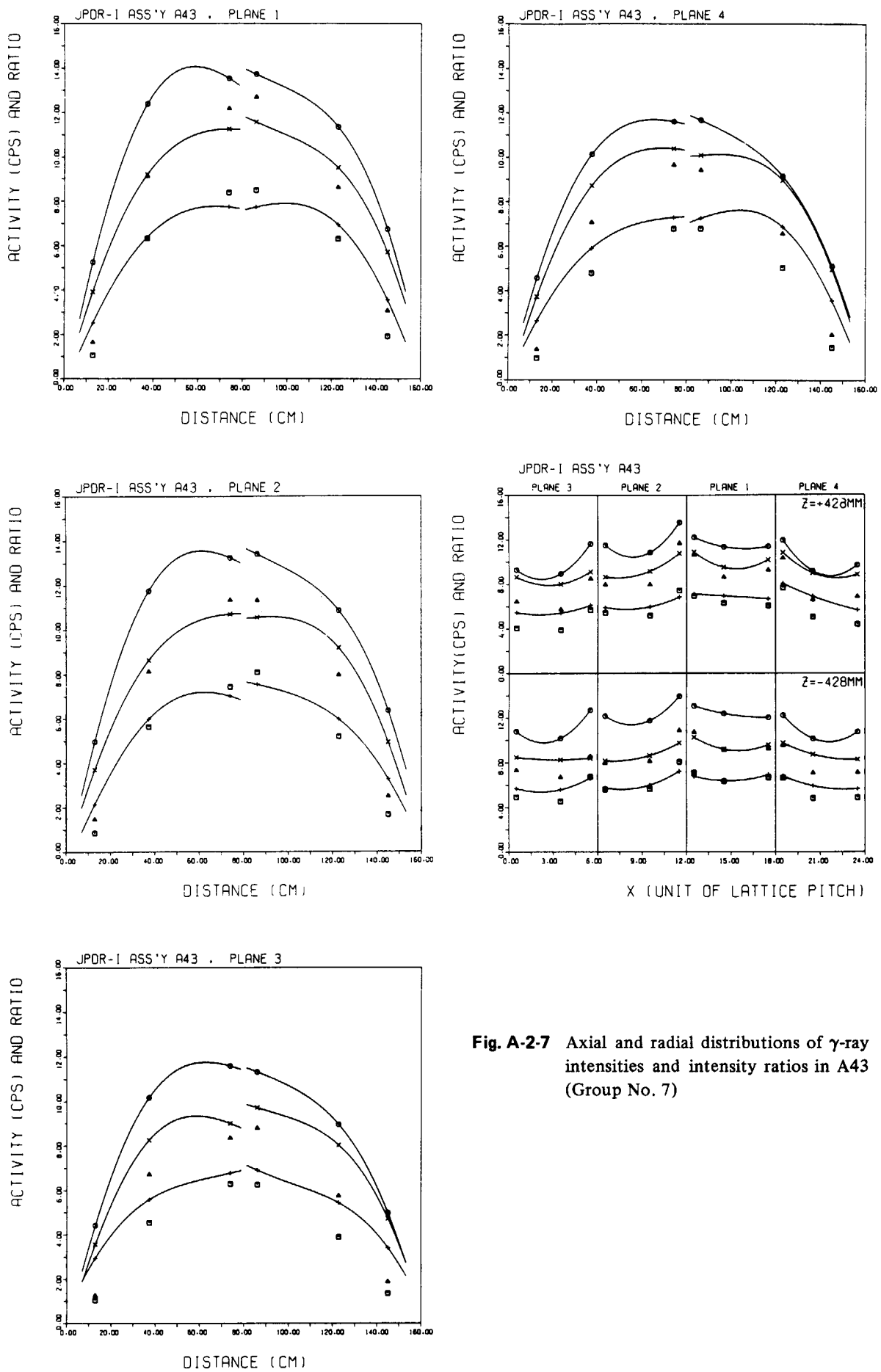


Fig. A-2-7 Axial and radial distributions of γ -ray intensities and intensity ratios in A43 (Group No. 7)

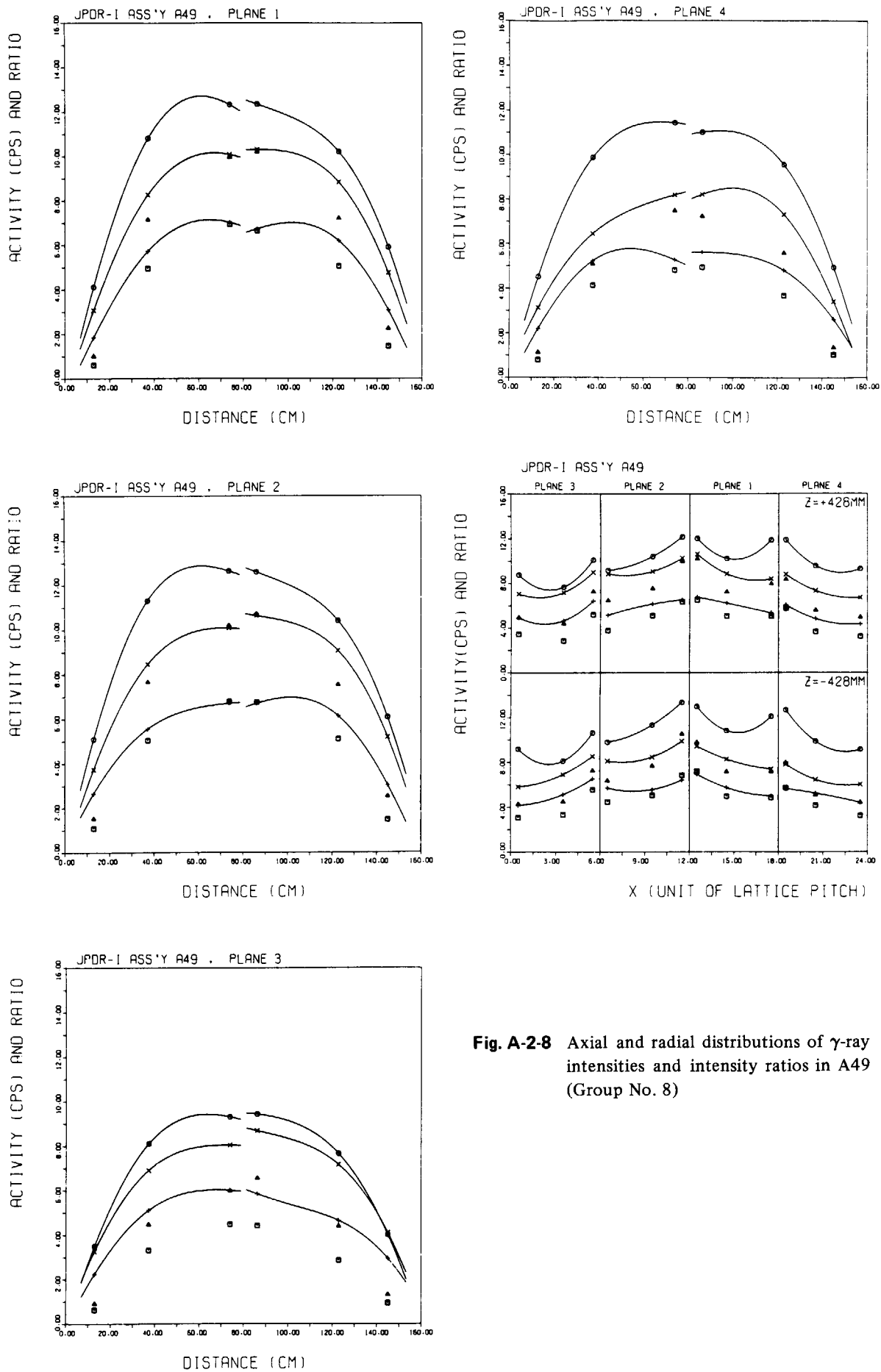


Fig. A-2-8 Axial and radial distributions of γ -ray intensities and intensity ratios in A49 (Group No. 8)

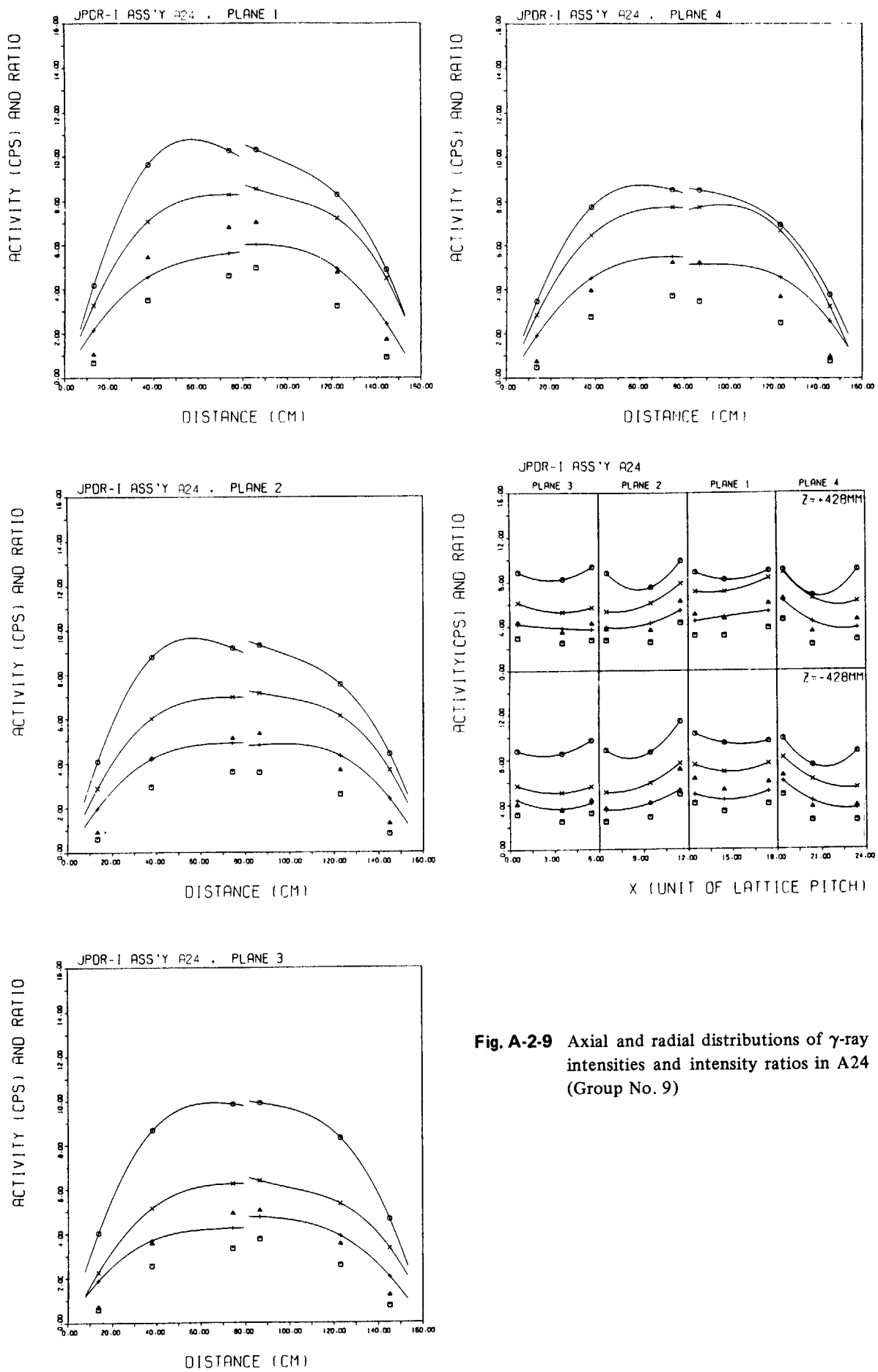


Fig. A-2-9 Axial and radial distributions of γ -ray intensities and intensity ratios in A24 (Group No. 9)

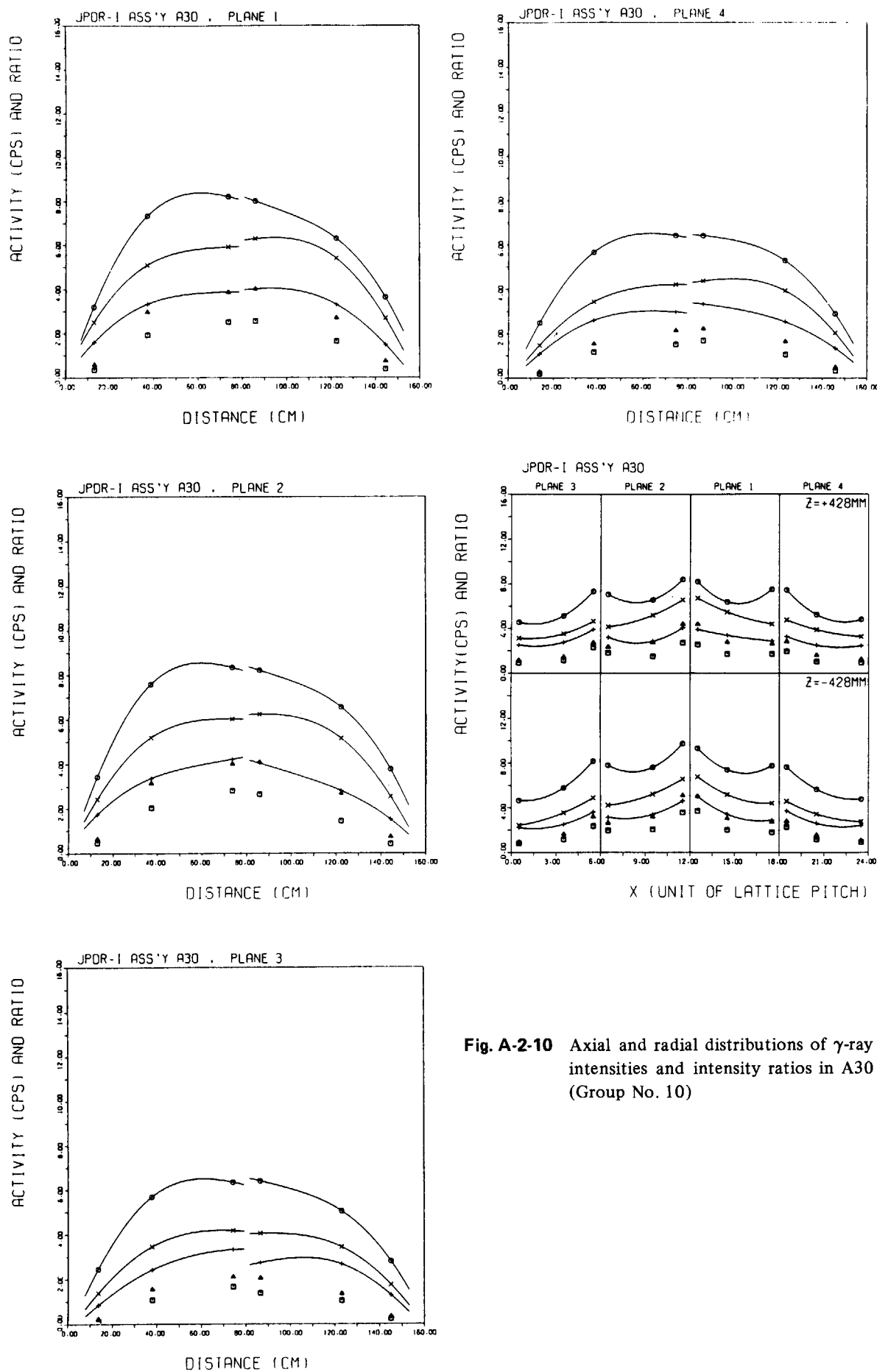


Fig. A-2-10 Axial and radial distributions of γ -ray intensities and intensity ratios in A30 (Group No. 10)

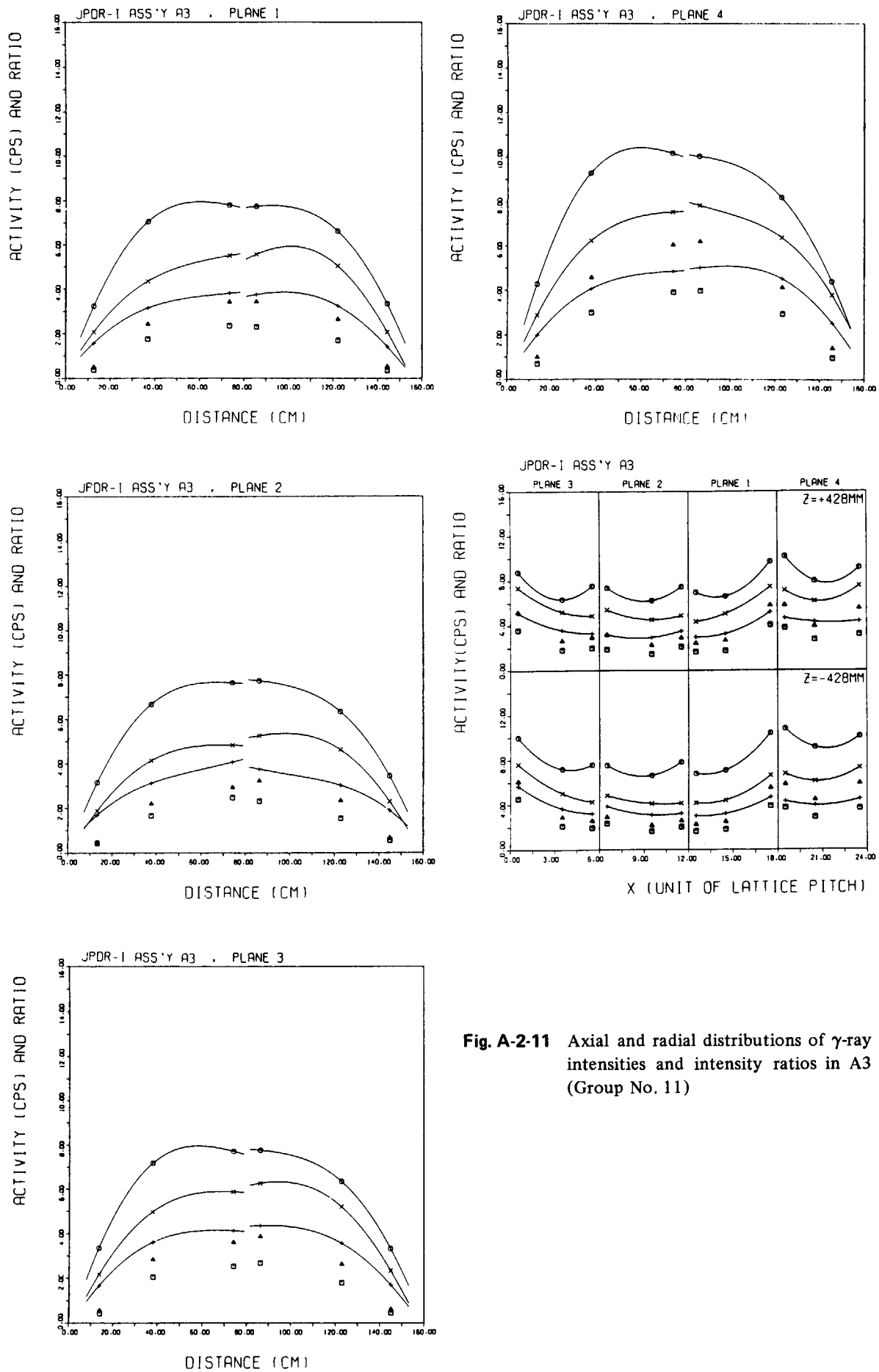


Fig. A-2-11 Axial and radial distributions of γ -ray intensities and intensity ratios in A3 (Group No. 11)

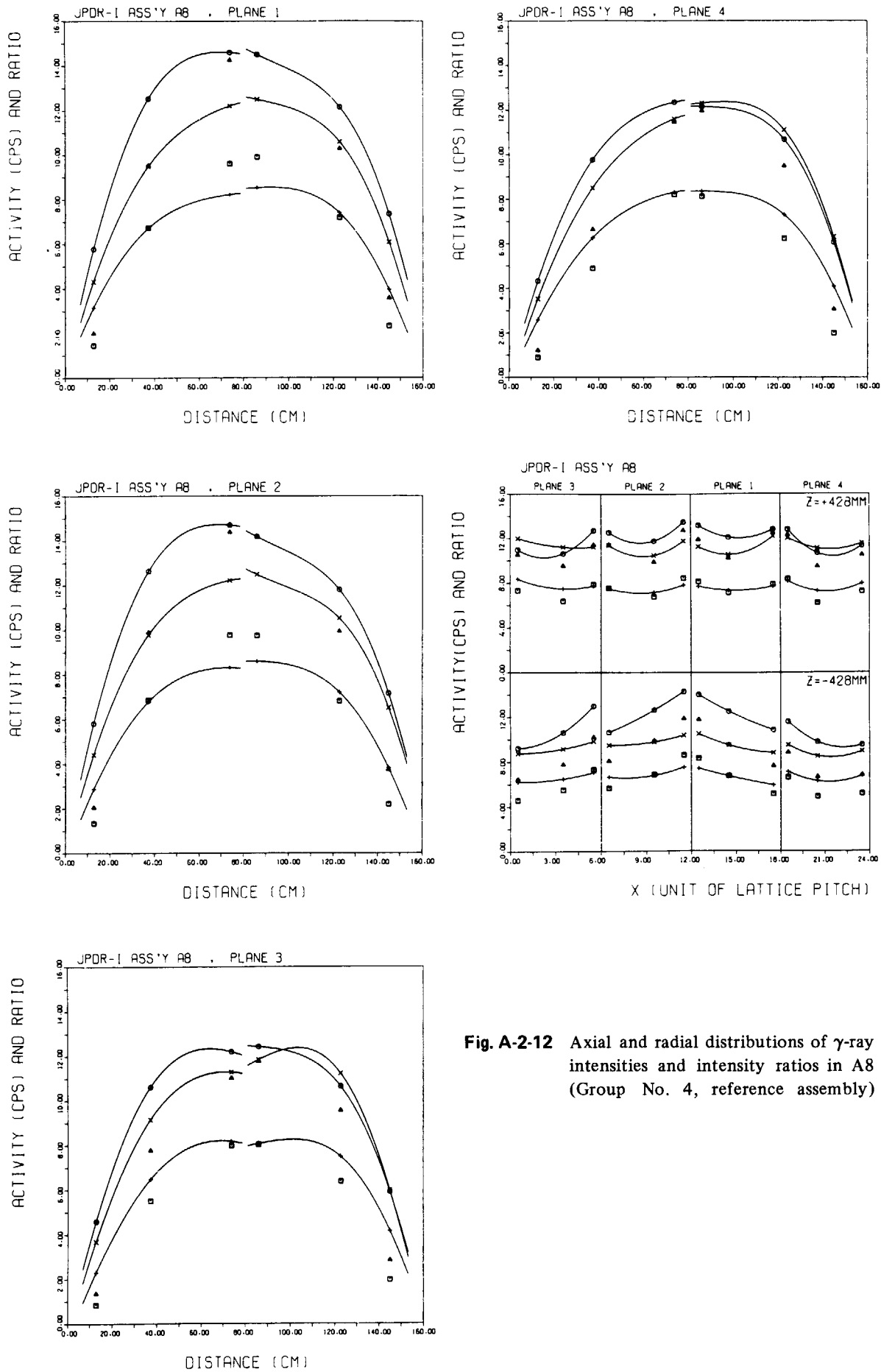


Fig. A-2-12 Axial and radial distributions of γ -ray intensities and intensity ratios in A8 (Group No. 4, reference assembly)

Appendix 3 Measurement of Penetration Rates of Gamma-Rays in a Fuel Assembly

In the non-destructive measurement of FP gamma-rays emitted from an assembly surface, there is an annoying problem that the gamma-rays from a fuel rod located at an inner position in the assembly are strongly absorbed by the other rods existing on the path of gamma-rays, and contribute much less to the measured intensity than those from an outer rod. Therefore, in the case that the radial distribution of gamma-ray source is concaved in the assembly, the measured intensity overestimates the radial average of source strength. And, in the case of convexed distribution, it results in the reverse. The radial distribution is usually concaved in a BWR assembly owing to water gaps surrounding the assembly. This is the reason of the positive value of \bar{A}_r in Eq.(13) in most cases, as discussed in Section 4.2. The variation of \bar{A}_r among assemblies for the non-destructive measurement is considered to be the main cause of systematic deviation of the measured assembly-averaged gamma-ray intensity of intensity ratio. The \bar{A}_r depends on the penetration rates of gamma-rays as seen in Eq.(13). For the purpose to verify the penetration rates calculated by Eq.(10) which were used to evaluate the \bar{A}_r , the following experiment was carried out.

Six upper-segments of the assembly A20 were used for the experiment. As shown in **Fig. A-3-1**, the fuel segments were inserted at aligned positions of a channel box having the same lattice spacing as the JPDR-I fuel assembly, and the gamma-rays were measured by using the same apparatus as those shown in **Fig. 3**. At first, the gamma-ray spectrum was measured for each segment inserted at the position-1, and intensities of $^{137}\text{Cs}(662 \text{ keV})$, $^{134}\text{Cs}(796 \text{ and } 802 \text{ keV})$ and $^{154}\text{Eu}(1275 \text{ keV})$ were determined. They were notated like S_i^{137} for the intensity of ^{137}Cs on the i -th segment. Then, the same intensities were measured in cases that the positions-1 to $-i$ were occupied by the segments numbered correspondingly to the positions, and they were notated like A_i^{137} . Necessary cares were given upon the reproducibility of

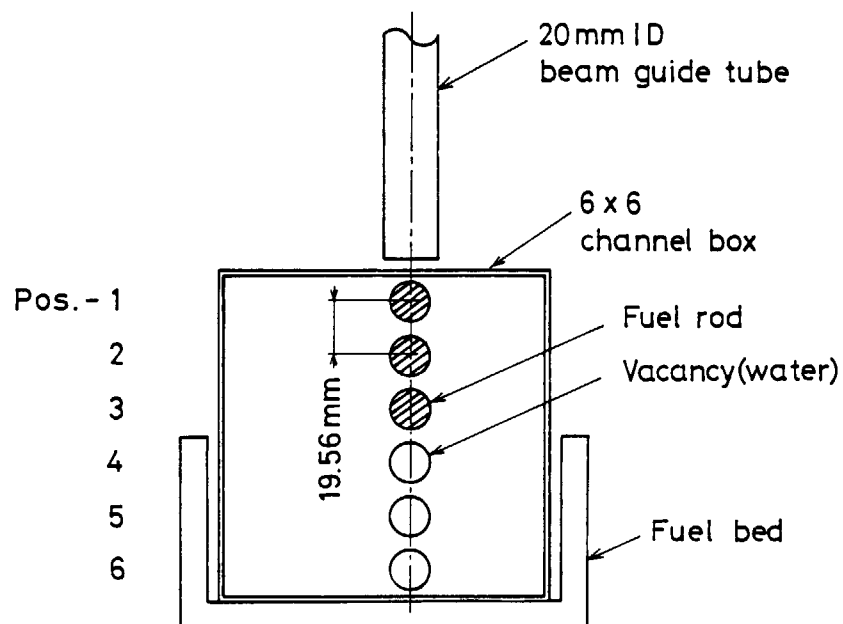


Fig. A-3-1 Cross-sectional view of experimental arrangement on penetration rate of gamma-rays in an assembly.

settings of the measurement apparatus throughout the experiment. In order to ascertain the reproducibility, each measurement was made at two axial positions: +18.4 cm and +30.6 cm from the lower end of the upper segment.

Since A_i is expressed as

$$A_i = \sum_{j=1}^i S_j r'_j, \quad (\text{A-3-1})$$

the relative penetration rate of the i -th segment located at the position- i (r'_i) is obtained by

$$r'_i = \frac{A_i - A_{i-1}}{S_i} \quad (i=1 \text{ to } 6, A_0=0). \quad (\text{A-3-2})$$

The r'_i is equal to r_i/r_1 defined by Eq.(10). The measured results of r'_i are shown in Fig. A-3-2 with the calculated ones. For the r'_i larger than about 0.03, both results agree fairly well. From this comparison, it is concluded that the simple equation (10) gives the penetration rates of gamma-rays in an assembly with a sufficient accuracy.

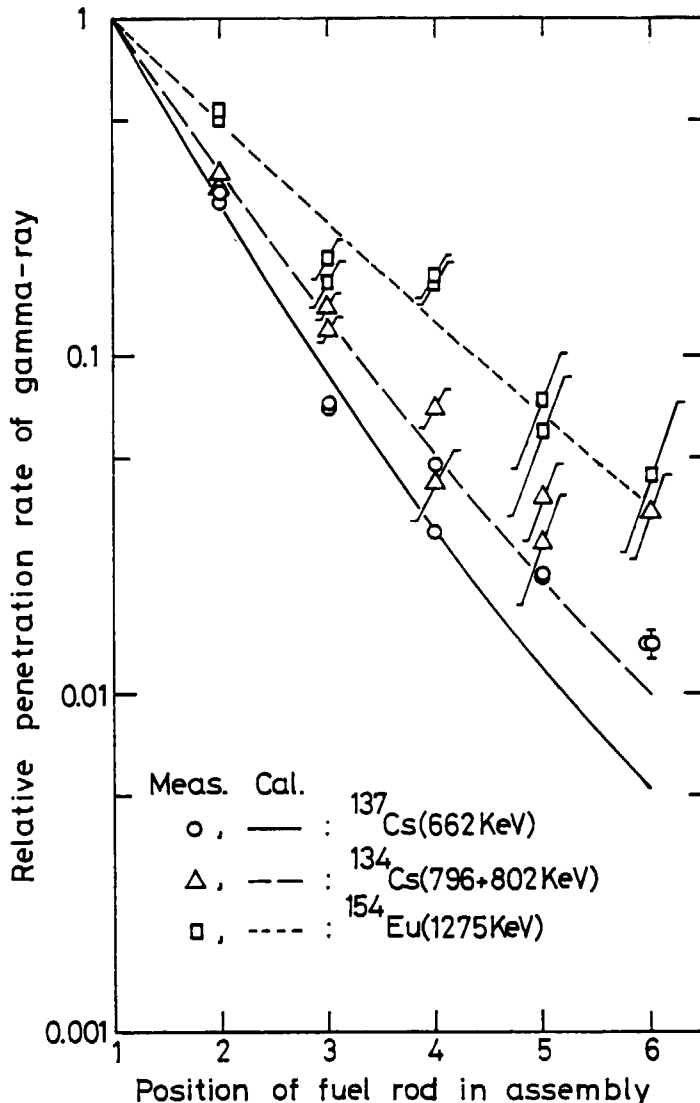


Fig. A-3-2 Measured and calculated relative penetration rates of gamma-rays in an assembly.